Energy Management of Grid-Connected Microgrids, Incorporating Battery Energy Storage and CHP Systems Using Mixed Integer Linear Programming

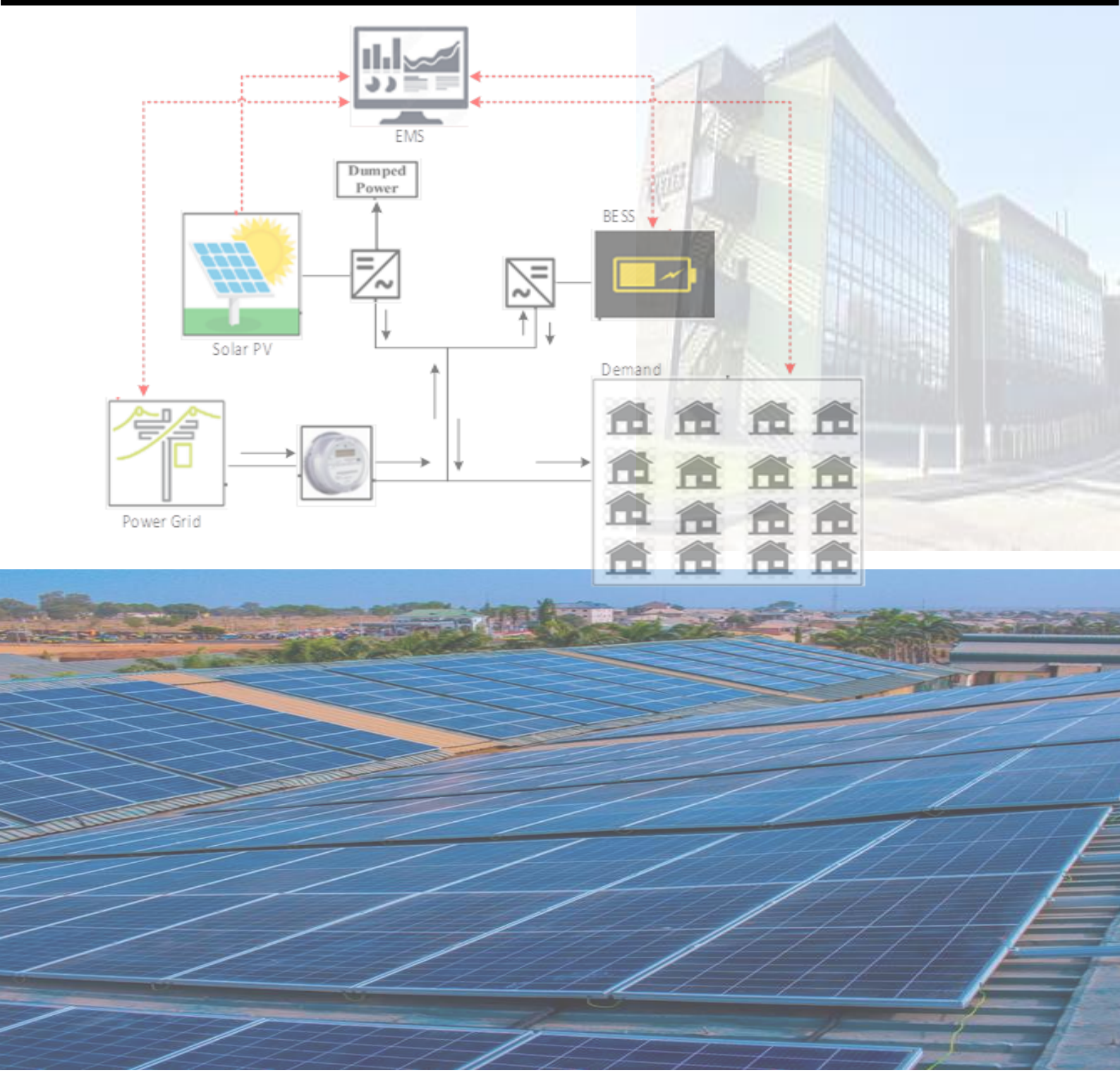

Marvin Barivure Sigalo
PhD Renewable Energy System.
Faculty of Environment, Science and Economy.
University of Exeter, Penryn Campus. Cornwall, United Kingdom.

Energy Management of Grid-Connected Microgrids, Incorporating Battery Energy Storage and CHP Systems Using Mixed Integer Linear Programming

Submitted by
Marvin Barivure Sigalo, to the University of Exeter as a thesis for the degree of Doctor of Philosophy in Renewable Energy, August 2022

I certify that all material in this thesis which is not my own work has been identified and that any material that has previously been submitted and approved for the award of a degree by this or any other University has been acknowledged.

Signature: ____  ____

Dedication

This thesis is dedicated to God Almighty

Declaration

I hereby declare that except where specific reference is made to the work of others, the contents of this dissertation are original and have not been submitted in whole or in part for consideration for any other degree or qualification in this or any other university. This dissertation is my own work and contains nothing which is the outcome of work done in collaboration with others, except as specified in the text and acknowledgements. This dissertation contains fewer than 65,000 words, including appendices, bibliography, footnotes, tables and equations, and fewer than 150 figures.

Acknowledgements

A wonderful experience at the University of Exeter is coming to an end, a period when I learned how to overcome new problems when my passion for renewable energies and a cleaner future for our planet got renewed and full of new ideas.

I would like to first express my gratitude to the eternal God of all creation, who was and who is to come, for the gift of life and the opportunity to carry out this research.

Also, I wish to express my sincere gratitude to my lovely wife: Mrs Nhuomachi Marvin-Sigalo, and my parents Prof. and Mrs Friday. B. Sigalo. It is from these people that I derive my greatest inspiration, and I thank them all for their unwavering support and encouragement.

This work would not have been possible without the Nigerian Government's financial support through a PhD grant from the PTDF (Petroleum Technology Development Fund); therefore, I gratefully acknowledge your support and thank you.

This acknowledgement will be incomplete without a worthy mention and salutation to my supervisors, Prof. Mohammad Abusara and Dr Saptarshi Das, who have ensured that this project has come to a reality and not just a fantasy. I also wish to register my profound appreciation and gratitude to Dr Ajit Pillai, Dr Essam Hussain, and Dr Hisham Mahmood for the support I received from you all and the entire College of Engineering, Mathematics and Physical Sciences staff, University of Exeter, Penryn campus. I gratefully acknowledge the support, guidance, and assistance of Richard Little and Debbie Moran for taking out timeout to proofread my thesis.

Finally, I wish to thank my brothers (Clifford Burabari and Isreal Sibari Sigalo), my inlaws (Elder and Mrs W. Wosu), other family members, friends (Chika Amadi, Elor, Enefaa Thomas, Imonitie Omo-Ojugo, Gbenga Wahab, Mr & Mrs Afolabi, Mr & Mrs Osunkeyesi, Lewis Jowah, Believe), colleagues (Ali, Miguel, Eze, Raul and Yusuf) and business associates for supporting, inspiring and motivating me during my study at the University of Exeter.

Marvin Barivure Sigalo
University of Exeter, August 2022

Abstract

In this thesis, an energy management system (EMS) is proposed for use with battery energy storage systems (BESS) in solar photovoltaic-based (PV-BESS) grid-connected microgrids and combined heat and power (CHP) applications. As a result, the battery's charge/discharge power is optimized so that the overall cost of energy consumed is minimized, considering the variation in grid tariff, renewable power generation and load demand. The system is modelled as an economic load dispatch optimization problem over a 24-hour time horizon and solved using mixed integer linear programming (MILP) for the grid-connected Microgrid and the CHP application. However, this formulation requires information about the predicted renewable energy power generation and load demand over the next 24 hours. Therefore, a long short-term memory (LSTM) neural network is proposed to achieve this. The receding horizon (RH) strategy is suggested to reduce the impact of prediction error and enable real-time implementation of the energy management system (EMS) that benefits from using actual generation and demand data in real-time.

At each time-step, the LSTM predicts the generation and load data for the next 24 h. The dispatch problem is then solved, and the real-time battery charging or discharging command for only the first hour is applied. Real data are then used to update the LSTM input, and the process is repeated. Simulation results using the Ushant Island as a case study show that the proposed online optimisation strategy outperforms the offline optimisation strategy (with no RH), reducing the operating cost by 6.12%.

The analyses of the impact of different times of use (TOU) and standard tariff in the energy management of grid-connected microgrids as it relates to the charge/discharge cycle of the BESS and the optimal operating cost of the Microgrid using the LSTM-MILP-RH approach is evaluated. Four tariffs UK tariff schemes are considered: (1) Residential TOU tariff (RTOU), (2) Economy seven tariff (E7T), (3) Economy ten tariff (E10T), and (4) Standard tariff (STD). It was found that the RTOU tariff scheme gives the lowest operating cost, followed by the E10T tariff scheme with savings of 63.5% and 55.5%, respectively, compared to the grid-only operation. However, the RTOU and E10 tariff scheme is mainly used for residential applications with the duck curve load demand structure. For community grid-connected microgrid applications except for residential-only communities, the E7T and STD, with 54.2% and 39.9%, respectively, are the most likely options offered by energy suppliers.

The use of combined heat and power (CHP) systems has recently increased due to their high combined efficiency and low emissions. Using CHP systems in behind-the-meter applications, however, can introduce some challenges. Firstly, the CHP system must operate in load-following mode to prevent power export to the grid. Secondly, if the load drops below a predefined threshold, the engine will operate at a lower temperature and hence lower efficiency, as the fuel is only half-burnt, creating significant emissions. The aforementioned issues may be solved by combining CHP with a battery energy storage system. However, the dispatch of CHP and BESS must be optimized. Offline optimization methods based on load prediction will not prevent power export to the grid due to prediction errors. Therefore, a real-time EMS using a combination of LSTM neural networks, MILP, and RH control strategy is proposed. Simulation results show that the

proposed method can prevent power export to the grid and reduce the operational cost by 8.75% compared to the offline method.

The finding shows that the BESS is a valuable asset for sustainable energy transition. However, they must be operated safely to guarantee operational cost reduction and longer life for the BESS.

Table of Contents

Dedication ii
Declaration iii
Acknowledgements iv
Abstract v
Table of Contents viii
List of Figures xii
List of Tables xv
Abbreviations xvi
Table of Symbols xvii
1. Chapter 1 1-1
Introduction 1-1
1.1 Background 1-1
1.2 The Microgrid System 1-3
1.2.1 Solar PV system 1-4
1.2.2 The Thermal Power Generator Model (Thermal Units) 1-5
1.2.3 Battery Energy Storage System 1-6
1.3 The Model of a Microgrid System with Central Controller 1-9
1.4 EMS for Microgrids: An Overview 1-10
1.4.1 BESS Function in Microgrids 1-12
1.5 Research Questions 1-13
1.5.1 Research Aims and Objectives 1-14
1.6 Thesis Contribution 1-15
1.7 Thesis Structure/Outline 1-16
2. Chapter 2 2-17
A Review of Optimal Energy Management of Microgrids with Battery Storage Systems and Renewable Energy Sources 2-17

2.1 Introduction 2-17
2.2 Energy Management Requirements for Microgrids 2-20
2.2.1 Generation and consumption balance and operational cost minimisation. 2-21
2.2.2 Compliance and implementation of the rules for connecting and disconnecting the Microgrid to the upper distribution system. .. 2-21
2.2.3 Optimal Utilisation of Existing Resources. 2-22
2.3 Energy Management Optimisation Strategies for Microgrids. 2-22
2.3.1 A Review of Multi-Agent-System Based Energy Management System 2-23
2.3.2 A Review of Energy Management Based on Metaheuristic Approach. 2-26
2.3.3 A Review of Dynamic Programming Strategy in Energy Management Systems. 2-31
2.3.4 A Review of Robust Programming and Stochastic Based Methods for Energy Management in Microgrids. 2-33
2.3.5 A Review of Reinforcement Learning Based EMS 2-36
2.3.6 A Review of Linear and Nonlinear Programming Based EMS .. 2-38
2.4 A Review of Energy Management System in CHP Applications . 2-43
2.5 Summary and Research Gap 2-47
3. Chapter 3 3-49
A Real-Time EMS for Controlling BESS in a Grid-Connected Microgrid using MILP 3-49
3.1 Introduction 3-49
3.2 Optimal Operation of Battery using MILP 3-50
3.2.1 The MILP Formulation 3-51

3.2.2 LSTM Prediction Networks 3-57

3.3 Receding Horizon Control 3-68
3.4 Simulations and Results 3-69
3.5 Summary/Discussion 3-79
4. Chapter 4 4-82
Analysis of the Impact of Time-Of-Use (TOU) and Standard Tariffs Schemes in Energy Management for Grid-Connected Microgrids with Energy Storage. 4-82
4.1 Introduction 4-82
4.2 System Model and Configuration 4-84
4.3 Operational Strategy 4-88
4.4 Results and Discussions 4-89
4.4.1 Technical Analysis Based on the Four Tariff Schemes 4-92

4.4.2 Optimal Operating Cost Analysis Based on the Four Tariff Schemes 4-102

4.5 Conclusion 4-106
5. Chapter 5 5-108
Real-Time Economic Dispatch of CHP Systems with Energy Storage for Behind-the-Meter Industrial Distributed Energy Application 5-108
5.1 Introduction 5-108
5.2 System Description 5-108
5.3 Problem Formulation 5-110
5.3.1 Economic Operation of the Hybrid CHP System using MILP ... 5-110

5.4 EMS Implementation 5-116
5.4.1 Offline Implementation 5-116

5.4.2 Online Implementation using RH 5-117

5.5 Simulation Results 5-119
5.5.1 Load Prediction using LSTM 5-121

5.5.2 EMS Implementation Results 5-123

5.6 Summary/ Discussion 5-130
6. Chapter 6 6-132
Conclusion and Future Works 6-132
6.1 Conclusion 6-132
6.2 Future Works 6-135
7. References 7-137

List of Figures

Figure 1-1: Components of the Microgrid System with Storage 1-4
Figure 1-2: Possible services provided by storage in a system with high shares of Variable Renewable Energy (VRE) 1-8
Figure 1-3: Depth of Discharge (DOD) representation of the LA and LI BESS..... 1-9
Figure 1-4: A Typical Microgrid Model with a Central Controller [50]..... 1-10
Figure 1-5: General structure of EMS in Microgrids [50] 1-12
Figure 2-1: Representation of a Microgrid with Energy Management System(EMS)2-20
Figure 2-2: Configuration of a multi-agent-based distributed system for microgrids [73] 2-24
Figure 3-1: Schematic diagram of the EMS..... **Error! Bookmark not defined.**
Figure 3-2: Grid Connected Microgrid Model with Power Flow Possibilities..... 3-51
Figure 3-3: The LSTM block diagram 3-58
Figure 3-4: Real and predicted PV data (from the LSTM prediction network for selected months of the year) 3-63
Figure 3-5: Real and predicted load demand (from the LSTM prediction network for selected months of the year) 3-67
Figure 3-6: Illustration of the RH control strategy. 3-68
Figure 3-7: EMS flow model for scenario 1 (real-time operation with the RH control strategy). 3-71
Figure 3-8: EMS flow model for scenario 2 (offline optimization using predicted data) 3-72
Figure 3-9: The microgrid dispatch for January for real-time operation of the Microgrid using RH control with the charge/discharge cycle limited to one cycle. 3-73
Figure 3-10: The microgrid dispatch for May for real-time operation of the Microgrid using RH control with the charge/discharge cycle limited to one cycle..... 3-73
Figure 3-11: The microgrid dispatch for August for real-time operation of the Microgrid using RH control with the charge/discharge cycle limited to one cycle. 3-74
Figure 3-12: The microgrid dispatch for November for real-time operation of the Microgrid using RH control with the charge/discharge cycle limited to one cycle. 3-74
Figure 3-13: Optimal cost comparison between the benchmark, online and offline optimization 3-75
Figure 3-14: The microgrid dispatch for January for real-time operation of the Microgrid using RH control with the charge/discharge cycle limited to two cycles... 3-76
Figure 3-15: The microgrid dispatch for May for real-time operation of the Microgrid using RH control with the charge/discharge cycle limited to two cycles. 3-77
Figure 3-16: The microgrid dispatch for August for real-time operation of the Microgrid using RH control with the charge/discharge cycle limited to two cycles... 3-77

Figure 3-17: The microgrid dispatch for November for real-time operation of the Microgrid using RH control with the charge/discharge cycle limited to two cycles... 3-78
Figure 3-18: Optimal cost comparison between the benchmark, online and offline optimization. 3-78
Figure 4-1: EMS Controlled Model for A Grid-Connected Microgrid with PV and BESS..... **Error! Bookmark not defined.**
Figure 4-2: Ushant Island Annual Solar PV Generation 4-85
Figure 4-3: Ushant Island annual Load Demand Distribution 4-85
Figure 4-4: Ushant Island Average Daily PV Generation for January, April, July and October 4-86
Figure 4-5: Ushant Island Average Daily Load Demand for January, April, July and October 4-86
Figure 4-6: Cost of energy under the standard (STD) and TOU tariff rates..... 4-87
Figure 4-7: Comparison of the optimal result for four tariff schemes based on an annual optimal approach (t=8760)..... 4-91
Figure 4-8: Microgrid Dispatch commands for January using the RTOU Tariff . 4-93
Figure 4-9: Microgrid Dispatch commands for April using the RTOU Tariff..... 4-93
Figure 4-10: Microgrid Dispatch commands for July using the RTOU Tariff..... 4-94
Figure 4-10: Microgrid Dispatch commands for October using the RTOU Tariff . 4-94
Figure 4-12: Microgrid Dispatch commands for January using the E7 Tariff 4-95
Figure 4-12: Microgrid Dispatch commands for April using the E7 tariff..... 4-96
Figure 4-14: Microgrid Dispatch commands for July using the E7 Tariff 4-96
Figure 4-15: Microgrid Dispatch commands for October using the E7 tariff 4-97
Figure 4-16: Microgrid Dispatch commands for January using the E10 Tariff 4-98
Figure 4-17: Microgrid Dispatch commands for April using the E10 Tariff..... 4-98
Figure 4-18: Microgrid Dispatch commands for July using the E10 Tariff 4-99
Figure 4-19: Microgrid Dispatch commands for October using the E10 tariff 4-99
Figure 4-20: Microgrid Dispatch commands for January using the STD Tariff .. 4-100
Figure 4-21: Microgrid Dispatch commands for April using the STD Tariff..... 4-101
Figure 4-22: Microgrid Dispatch commands for July using the STD Tariff..... 4-101
Figure 4-23: Microgrid Dispatch commands for October using the STD Tariff .. 4-102
Figure 4-23: Optimal Operating Cost comparison for the four Tariff schemes for Jan, Apr, Jul and May. 4-103
Figure 4-24:Daily Average Optimal Operating cost for each Tariff Scheme on a Monthly Basis for the PV-BESS Grid-Connected Operations..... 4-104
Figure 4-25: Daily Average Operating cost for Grid Operations only on a Monthly Basis. 4-104
Figure 4-27: Annual Operating Cost Comparison between Grid supply only and Grid-Connected PV-BESS Supply..... 4-105
Figure 5-1: Grid-connected CHP system with energy storage (CHP+BAT+GRID).. 5-109

Figure 5-2: Nonlinear cost function approximated by piecewise linear approximation. 5-111
Figure 5-3: LSTM-MILP flow model for real-time operation of the grid-connected CHP system (offline optimisation scheme). 5-117
Figure 5-4: Illustration of the RH control strategy. 5-118
Figure 5-5: LSTM-MILP-RH flow model for real-time operation of the grid-connected CHP system (online optimisation). 5-119
Figure 5-6: Real and predicted electrical load with RMSE 5-122
Figure 5-7: Real and Predicted Heat Demand with RMSE. 5-122
Figure 5-8: Total output electrical power and heat generated from 2×250kWe CHP units using predicted load demand data. 5-123
Figure 5-9: Total electrical power generated, the ideal real-time load demand and BESS charge/discharge command (scenario 1). 5-124
Figure 5-10: Total electrical power generated, real-time load demand and BESS charge/discharge command (Scenario 2). 5-125
Figure 5-11: Grid participation, BESS SoC, grid tariff and BESS charge/discharge command (Scenario 2). 5-125
Figure 5-12: Total electrical power generated, real-time load demand and BESS charge/discharge command (Scenario 3). 5-126
Figure 5-13: Grid participation, BESS SoC, grid tariff and BESS charge/discharge command (Scenario 3). 5-126
Figure 5-14: Total heat generated by the CHP units and heat demand (offline optimization). 5-127
Figure 5-15: Total power and heat generated from 2×250kWe CHP units vs real-time electrical load (online optimization). 5-128
Figure 5-16: Total electrical power generated, real-time load demand and BESS charge/discharge command (scenario 4). 5-128
Figure 5-17: Grid participation, BESS SoC, grid tariff and BESS charge/discharge command (scenario 4). 5-129
Figure 5-18: Total heat generated by the CHP units and heat demand (online optimization). 5-129

List of Tables

Table 3-1: Decision and binary variables of the economic dispatch problem 3-53
Table 3-2: Daily TOU electricity tariff 3-70
Table 3-3: Characteristics of the lead-acid battery package 3-70
Table 3-4: Optimal cost comparison with average % difference between the two scenarios for K=3 3-75
Table 3-5: Optimal cost comparison with average % difference between the two scenarios for K=7 3-79
Table 4-1: Parameters of the Solar PV and BESS 4-88
Table 4-2: Yearly Operational cost savings for PV-BESS grid-connected microgrid considering the Tariff schemes. 4-106
Table 5-1: MILP economic dispatch continuous and binary decision variables . 5-113
Table 5-2: CHP Power and Efficiency @ 50Hz 5-120
Table 5-3: The CHP Input-Output Curve 5-120
Table 5-4: Characteristics of the Lithium-Ion BESS Package 5-120
Table 5-5: Daily TOU Electricity Tariff / Cost of Gas 5-120
Table 5-6: Total Daily Operating cost and % Saving for all Scenarios 5-129

Abbreviations

BESS	Battery Energy Storage System
CHP	Combined Heat and Power
DOD	Depth of Discharge
E7T	Economy Seven Tariff
E10T	Economy Ten Tariff
EMS	Energy Management System
LSTM	Long Short-Term Memory
MAE	Mean Absolute Error
MAPE	Mean Absolute Percentage Error
MILP	Mixed Integer Linear Programming
PV	Photovoltaic
RES	Renewable Energy Systems
RH	Receding Horizon
RL	Reinforcement Learning
RMSE	Root Mean Square Error
RTOU	Residential Time of Use Tariff
SOC	State of Charge
STD	Standard Tariff
TOU	Time of Use

Table of Symbols

Nomenclature	Description	Nomenclature	Description
P_{chp1} , P_{chp2}	Electrical power from both CHP units 1 and 2, respectively	P_{grid}^{EL}	Power from the grid to the electrical load demand
P_{bat}^{D}	Power from the BESS to the load	P_{grid}^{bat}	Power from the grid for charging the BESS
P_{grid}	Power from the grid	H_{D}	Heat load
P_{d}^{EL}	Electrical load demand	P_{chp}^{bat}	Power from the CHP units for charging the BESS
P_{chp}^{EL}	Total electrical output power of the CHP units	P_{bat}^{CH}	Total BESS charging power
Q_{hrr}	Useful heat recovery rate	β_{soc}^{min}	Minimum state of charge of the BESS
H_{chp}^{G}	Recoverable heat from the CHP unit	β_{soc}^{max}	Maximum state of charge of the BESS
I_1, I_2 and I_3	Segments of CHP units	β_{soc}	BESS state of charge
$P_{CHP_{I1}}, P_{CHP_{I2}}$ and $P_{CHP_{I3}}$	Power segments of CHP units	φ_{EESS}	BESS nominal capacity (kWh)
S_{I1}, S_{I2} and S_{I3}	The slope of each segment of the CHP Unit	η_c , η_d	Charge and discharge efficiency of the BESS, respectively
$P_{CHP_I}^{min}$	The minimum operating condition of the CHP unit	Δt	Time-step
$P_{CHP_{Ik}}^{max}$	Maximum power of each segment of the CHP unit	γ_{bat}^{CH} , γ_{bat}^{D}	On and of state of the BESS charge and discharge, respectively.
$F_I\left(P_{CHP_I}\right)$	CHP cost function	T_{grid}	Time-of-use tariff of the grid
Z	The objective function	T_{CHP} , $T_{SU_{CHP}}$	CHP operating cost and start-up cost

List of Publications Based on this Work:

1. Sigalo, Marvin B., Ajit C. Pillai, Saptarshi Das, and Mohammad Abusara. 2021. "An Energy Management System for the Control of Battery Storage in a Grid-Connected Microgrid Using Mixed Integer Linear Programming" *Energies* 14, no. 19: 6212. https://doi.org/10.3390/en14196212

2. Ali, Khawaja H., Marvin Sigalo, Saptarshi Das, Enrico Anderlini, Asif A. Tahir, and Mohammad Abusara. 2021. "Reinforcement Learning for Energy-Storage Systems in Grid-Connected Microgrids: An Investigation of Online vs Offline Implementation" *Energies* 14, no. 18: 5688. https://doi.org/10.3390/en14185688

3. Sigalo, Marvin B., Ajit C. Pillai, Saptarshi Das, and Mohammad Abusara. 2021. "Real-Time Economic Dispatch of CHP Systems with Battery Energy Storage for Behind-The-Meter Applications" (MDPI Energies: Energy Storage application)

Chapter 1
Introduction

1.1 Background

The evolution of microgrids represents a significant step towards the transition to more sustainable power systems. Recent trends in microgrids include integrating renewable energy resources and energy storage systems. However, integrating these systems creates new challenges for microgrid operations because of their stochastic and intermittent nature. To mitigate these challenges, an energy management strategy is essential to ensure the economic and optimal performance of microgrids. Microgrid system development has become promising as it contributes a great deal to the building block of future smart grid systems. In terms of stable, efficient, and economical operation of the hybrid microgrid system, the energy storage system has become an important component with great prospects in the future power system. It plays an essential role in alleviating the problem of energy crisis, environmental degradation, market deregulation, incentive policies, growth in global demand for electricity and power shortage in remote areas [1]–[3]. The development of microgrid technology has provided the opportunity and infrastructure for improving energy consumption efficiency [4]**.** Microgrid systems are typically made up of load and distributed energy resources such as PV systems, wind turbines, biogas power plants, fuel cells and battery energy BESS [5]. A microgrid can operate in a grid-connected or an islanded mode. The microgrid system, which comprises different distributed energy resources, has become promising as it provides an integral part of the development of smart grid systems [5][6]. However, there are still many challenges in implementing and operating the Microgrid, one of which arises due to the intermittent nature of the renewable energy

sources because of the stochastic nature of the underlying metrological conditions [7]. A potential solution to this challenge is the integration of a fast-response energy storage system[8]. Energy storage is an important component with great prospects in future power systems and plays an important role in alleviating the problem of supply-demand balance in remote areas [9]. Moreover, the introduction of local renewable energy generation enhances self-consumption and offers an opportunity to reduce energy costs [10].

A typical microgrid system could be grid-connected or standalone (Islanded). It could consist of distributed generators that are dispatchable units, renewable energy resources that are none controllable or non-dispatchable devices, storage units, and controllable loads that can be managed (load shedding) when necessary [11]. In a grid connected scenario, the Microgrid can sell or buy power from the grid. Therefore, the optimization of the microgrid operation is extremely important to manage the energy resources in a cost-efficient and sustainable way [8][12][13]. A complete formulation of the optimum economic operation and scheduling problem of microgrids includes modelling the BESS system, demand side policy for controllable loads (demand side management), and power exchange with the utility grid [14].

Generally, the problem is formulated as a nonlinear problem with no known exact solution or technique [8][12][13]. Therefore, several approaches have been used by different authors and researchers to solve this problem. In this research work, we propose using the mixed integer linear programming (MILP) for optimal scheduling of the grid-connected and standalone microgrid system performed through microgrid optimisation [15], [16]. The MILP optimization approach is chosen because it presents a flexible and powerful method for solving complex problems by

making fast energy management decisions via integer decision variables and identifying the best connection between the plants and utilities. It systematically finds the best trade-off in the microgrid operation to achieve maximum resource efficiency and minimum operating cost while respecting the system's operational constraints [17].

1.2 The Microgrid System

Figure 1-1 shows the components of the microgrid system with different types of energy storage systems listed. Energy storage technology has been a critical element for hybrid renewable energy systems located in isolated areas, where connection to the electricity grid is very limited [18]–[20]. This research focuses on the techno-economic analysis of the application of battery energy storage systems in solar PV-based microgrid systems and CHP applications.

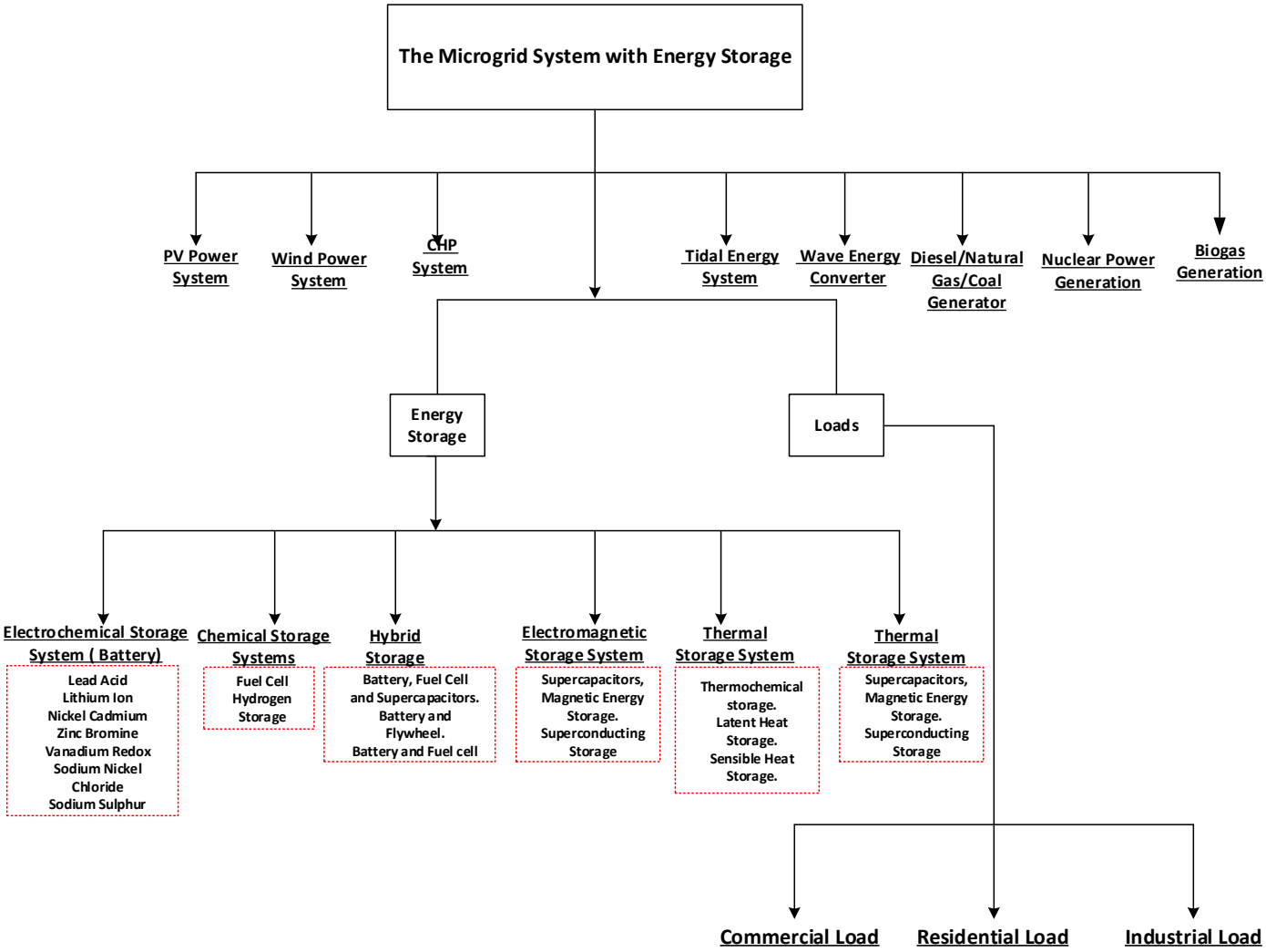

Figure 1-1: Components of the Microgrid System with Storage

1.2.1 Solar PV system

This renewable energy source depends on the power density of the solar irradiation and the ambient temperature of the photovoltaic module [18]. PV systems are not to be confused with other solar technologies, such as concentrated solar power or solar thermal, which are used for heating and cooling. PV systems transform light directly into electricity, while these other solar technologies do not [19], [21]. A solar array is limited to the collection of solar panels, which is the only visible element of the photovoltaic system. It does not contain any of the other hardware, which comprises battery banks, chargers, mounting hardware, switches, one or more solar inverters, wiring, and battery systems. Other alternative components

include a renewable energy credit revenue-grade metre, a maximum power point tracker, a GPS solar tracker, energy management software, solar concentrators, solar irradiance sensors, anemometers, or task-specific add-ons made to match a system owner's unique needs commonly referred to as the balance of system [22]. PV systems can be small-scale, as those placed on rooftops or incorporated into buildings, with capabilities ranging from a few kilowatts to large utility-scale power stations of hundreds of megawatts. Off-grid or standalone photovoltaic systems make up a very small fraction of the market compared to grid-connected PV systems, which account for the vast majority of installations in today's world [23]. PV systems have evolved from applications for a niche market into a mature technology utilised for mainstream power generation. In addition to not producing any noise or environmental pollution, PV systems do not have any moving components. Within 0.7 to 2 years of its installation, a rooftop system will have recouped the energy used in its production and throughout its 30-year operational lifetime, it will provide around 95% of net clean, renewable energy [24][25].

1.2.2 The Thermal Power Generator Model (Thermal Units)

The thermal unit model is represented by four curves: fuel input (Fuel Cost), heat rate, input/output (I/O) and incremental cost. Generator curves are generally represented as cubic or quadratic functions [26]–[29]. The fuel cost function for the CHP, diesel generator and natural gas generator are typically approximated by a quadratic function. It is mathematically expressed, as given in equation (1-1).

$$H_{TPG}\left(P_{TPG}\right) = aP_{TPG}^{2} + bP_{TPG} + C \qquad (1\text{-}1)$$

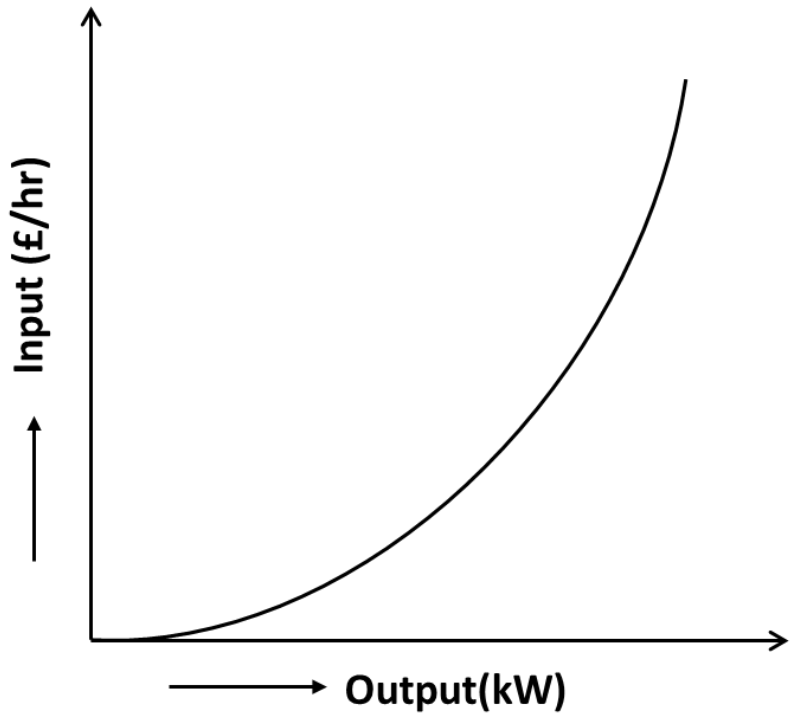

Figure 1-2:Input and Output curve of a thermal generating plant

$H_{TPG}(P_{TPG})$ is the input/output curve of the thermal unit, as shown in Figure 1-2, which is available in the manufacturer's datasheet in the form of fuel consumption, P_{TPG} is the active output power of the thermal unit in kW. The operating cost of the thermal unit can be achieved by multiplying the fuel cost C_{TPG} by the quadratic polynomial, $H_{TPG}(P_{TPG})$ as given in equation (1-2).

$$CH_{TPG}(P_{TPG}) = C_{TPG} \times (aP_{TPG}^2 + bP_{TPG} + C) \quad (1\text{-}2)$$

The thermal unit cost function parameters a[1/kW^{2}h], b[1/kWh] and c[1/h] can be obtained from the input/output measurement data taken during the heat run test when the thermal unit is operated with a different output power between its maximum and minimum operation range [12][13].

1.2.3 Battery Energy Storage System

The storage of electricity is referred to as the process of converting electrical energy from a power system into a form that can be stored and used later [30]. Then the stored energy can be used when needed by transforming it back to serve the

intended purpose [31]. BESS technologies are the best solution for the challenges associated with DG proliferation [32]. The storage of electricity is a technology that has the capability to reduce peaks, provide a balance between generation and consumption and improve the management, reliability and overall stability of the electrical system [31][33][20]. Typical BESS systems range anywhere from 2kW (5 kWh – 20 kWh) up to 50MW (MWh). They are set apart by their fast response, mobility, and flexibility to be fitted to either high-power or high-energy applications [35]. Batteries have the unique potential to provide energy storage services at all levels of the grid (generation, transmission, distribution and consumer level), while also providing several ancillary functions to their different users [36]–[38]. They have become a critical tool for increasing consumer comfort, reducing electricity bills, and earning revenue [39].

The storage device allows the consumer to store energy for a longer time and save the consumer's money by charging the storage devices during off-peak hours when the price is low and using them during peak hours [33]. This increasing importance of energy storage devices has encouraged researchers to achieve highly efficient and cost-effective storage devices [40]. However, there are many other factors associated with energy storage devices, which include energy storage capacity (MWh), power capacity (MW), device cost, and maintenance cost [34][40]–[42]. The charging and discharging process of the storage devices requires adequate control strategies to perform the reliable operation of grids even during the peak demand [43]–[45].

The BESS has become one of the core parts of the microgrid system; it is used to store surplus energy generated by the microgrid power generation system, the energy stored in the BESS is discharged to meet the load demand during low

generation and when the cost of electricity from the grid is very high (Peak Period) in grid connected systems [43]. For the healthy operation of the battery storage system, the state of charge (SOC) of the BESS should be within a certain range.

Figure 1-3 shows the possible services that can be provided by energy storage systems for microgrids with a high share of variable renewable resources[34], [46].

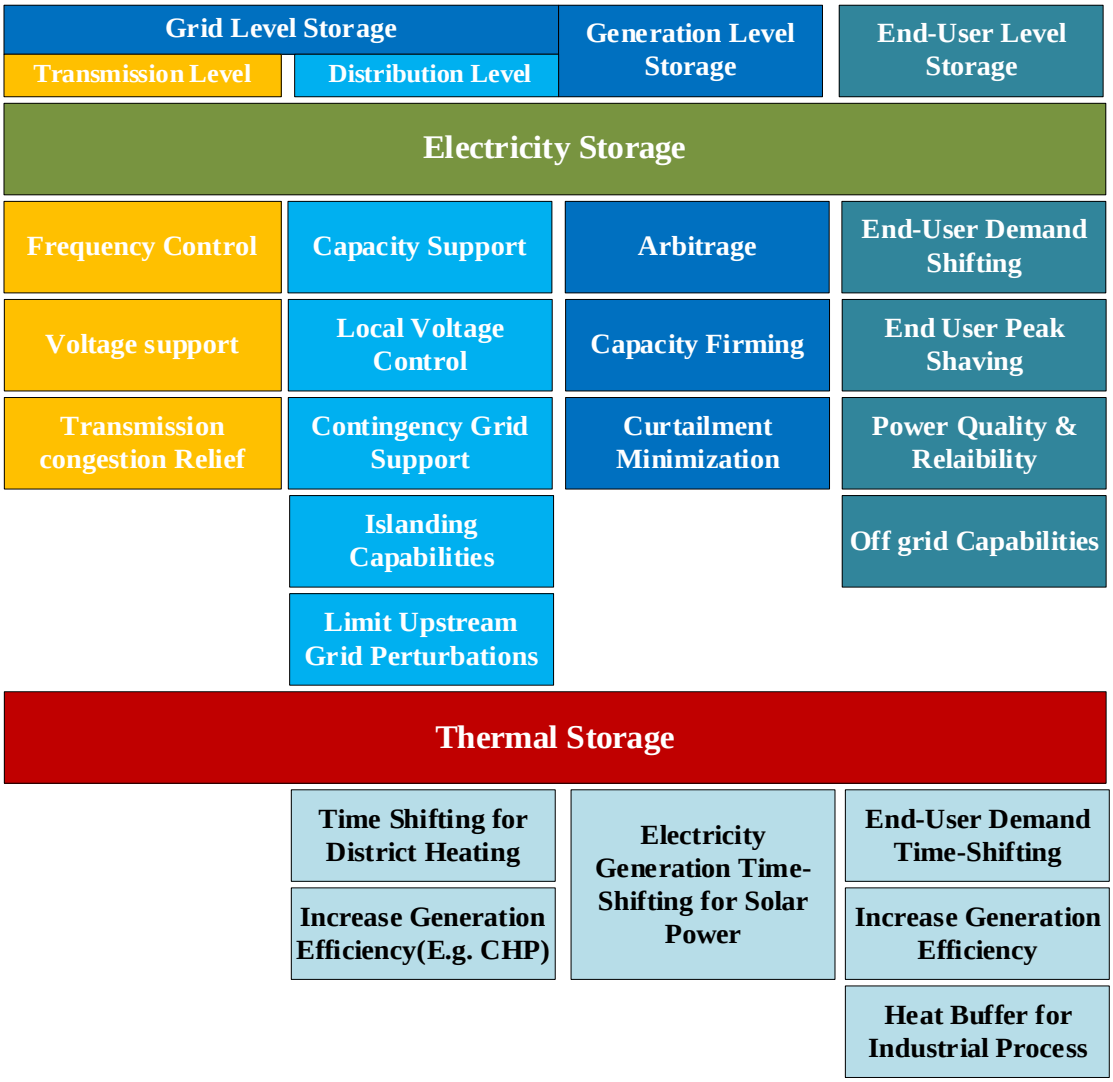

Figure 1-3: Possible services provided by storage in a system with high shares of Variable Renewable Energy [47].

In this research, we have considered the lead-acid (LA) and the lithium-ion (LI) BESS, a detailed comparison of both BESS type have not been carried out in the research; however, Figure 1-4 shows the capabilities of the two BESS types based on their depth of discharge for safe and economic operation the BESS system.

Battery technologies for energy storage devices can be differentiated on the basis of energy density, charge and discharge (round trip) efficiency, life span, and eco-friendliness of the devices. Lithium secondary batteries store 150–250 watt-hours per kilogram (kg) and can store 1.5–2 times more energy than sodium-sulphur (Na–S) batteries, 2-3 times more than redox flow batteries, and about 5 times more than lead storage batteries [48]. One important performance element of energy storage devices is their life span, and this factor has the most significant impact in reviewing economic efficiency. Another primary consideration is eco-friendliness or the extent to which the devices are environmentally harmless and recyclable. Charge and discharge efficiency is a performance scale that can be used to assess battery efficiency. Lithium secondary batteries have the highest charge and discharge efficiency, at 95%, lead-acid batteries at about 60%–70%, and redox flow batteries at about 70%–75% [48].

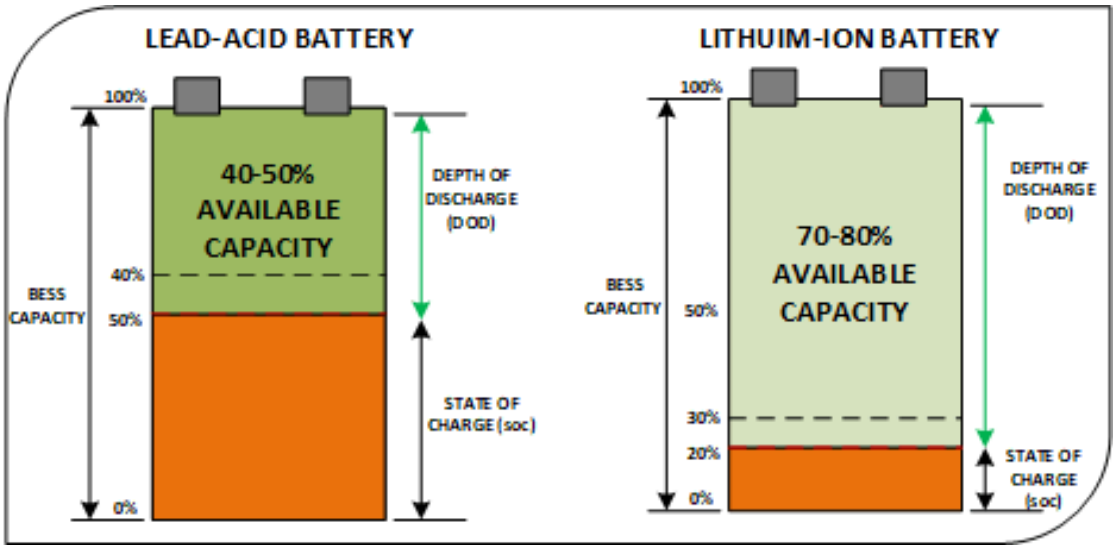

Figure 1-4: Depth of Discharge (DOD) representation of the LA and LI BESS.

1.3 The Model of a Microgrid System with Central Controller

Figure 1-5 shows a typical microgrid model with a centralised controller. Microgrids are usually accounted for as parts of distribution networks. For this research, the

grid connected microgrid model will be the basis of the problem formulation. In this case, renewable generation must always be adopted when generating since they have no generation cost compared to fossil fuel; thus, their costs are ignored in the optimization process [49]. The microgrid operation can be determined by unit commitment and economic dispatch for the grid-connected operations. At the same time, power is being sold to and bought from the grid in an economical way that minimizes the cost of operation of the Microgrid [50][51]. The unit commitment is performed from one day to one week ahead, providing the start-up and shutdown schedule for each generating unit, which can minimize the operating cost of the Microgrid.

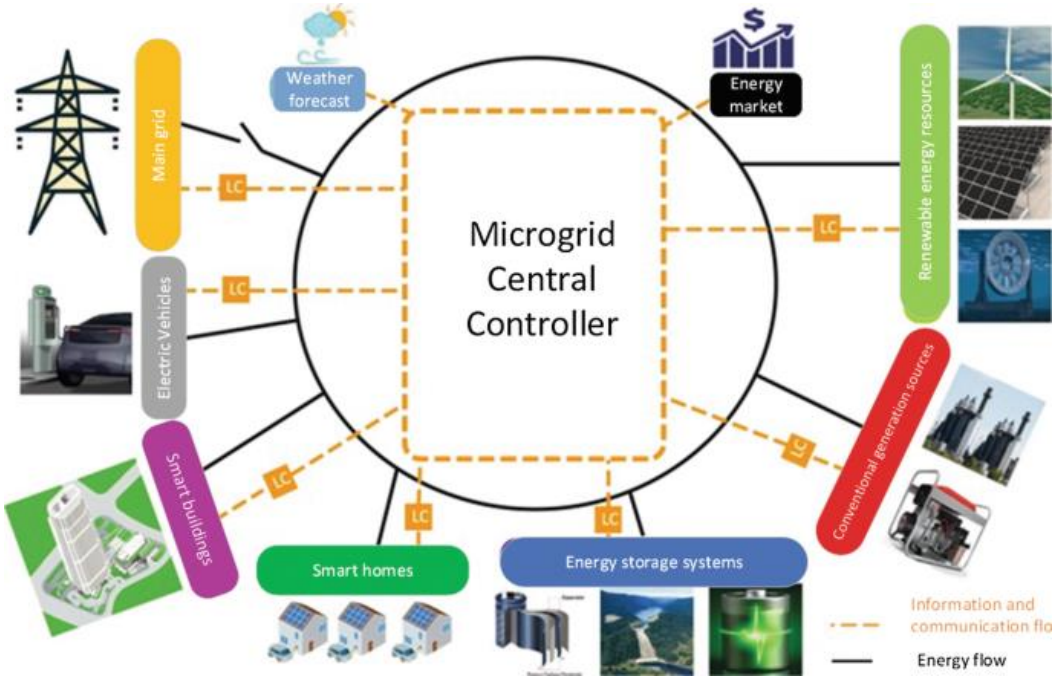

Figure 1-5: A Typical Microgrid Model with a Central Controller [52].

1.4 EMS for Microgrids: An Overview

The EMS aims to minimise the operating cost of the grid-connected system and focus more on delivering power for longer time intervals (i.e., enough energy is available) and power management (to regulate instantaneous power), considering power generation and consumption. Energy management mainly focuses on

economics, considering factors like fuel, capital, maintenance, emission profiles, lifetimes, etc. From a general perspective, the EMS can be divided into sub-layers of operation and planning, which work in different timescales, as shown in Figure 1-6 [7]. In this way, the operation schedule defines the commands for the DG units and loads within the microgrid days or hours ahead. The sub-layer of planning is related to the maintenance or replacement schedule of the units and defines constraints related to how the units should be operated. This work is focused on researching the development of EMS in the operational scheduling layer.

Furthermore, the Microgrid EMS enables different functionalities, such as monitoring the Microgrid in different conditions, analysing the system's condition in different operational states and making quick decisions in critical situations, as shown in Figure 1-6. The EMS performs control actions by being able to gather online measurement data such as the historical and forecasted data of the energy demand and generation. Some of the distributed energy resources and loads could be dispatchable and can follow the tasks set by the EMS. The architecture of the management systems should consider the variable nature of RES and the unpredictability of consumer behaviour, limited generation capacity, and power exchange with the grid that may cause energy imbalance [53].

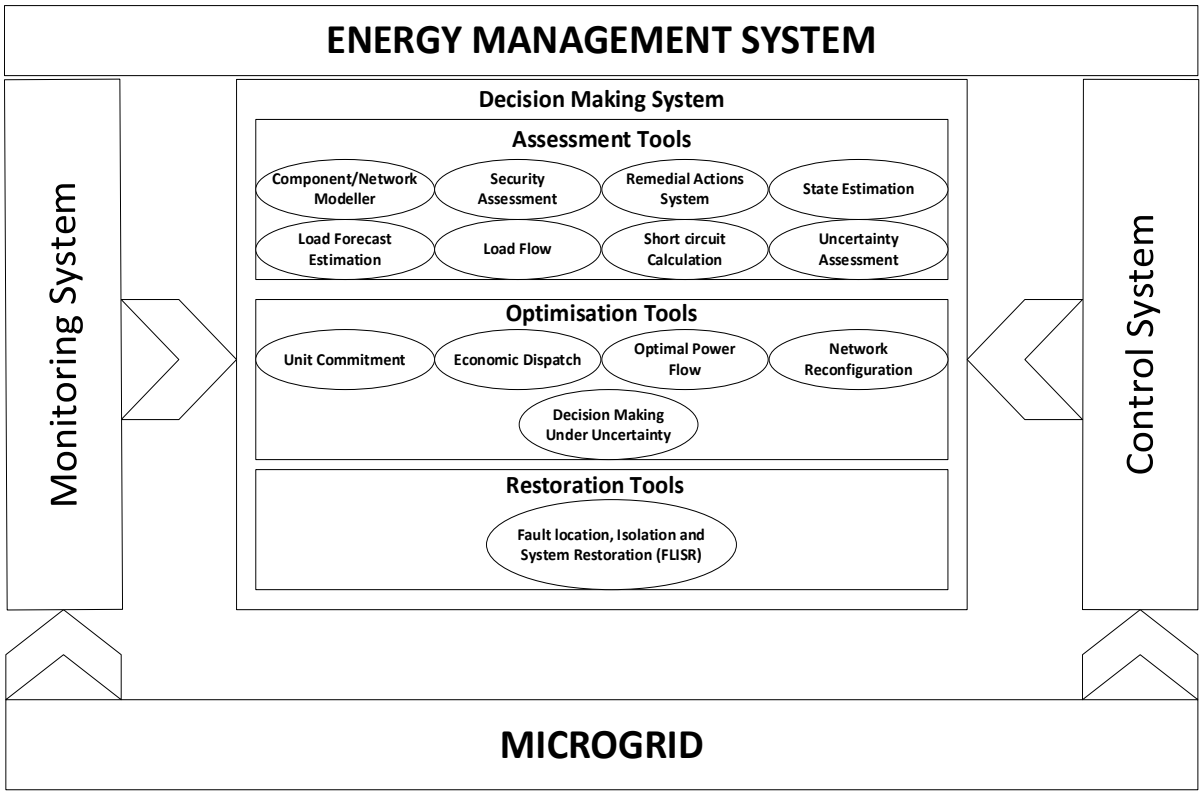

Figure 1-6: General structure of EMS in Microgrids [52]

1.4.1 BESS Function in Microgrids

Microgrids include an EMS that coordinates power exchanges between generation, load, and storage while considering demand response schemes and regulatory frameworks. The BESS is imperative to provide the system with more control and management [46], [54], [55]. Some of the benefits enabled by these technologies within a microgrid are the enhancement of management functions, such as:

1. **Energy Arbitrage Function:** This is the practice of purchasing and storing electrical energy during off-peak times and then utilizing the stored energy when the price of electricity is highest. The purpose is to minimize operation costs or earn money by storing low-cost energy during the off-peak time and selling it at a higher cost during peak demand. The difference in price between peak and off-peak demand must be big enough to compensate for the losses encountered in the storage process.

2. **Load Levelling:** The battery energy storage system can act as a load leveller when it provides load balancing services for a local grid. This involves storing power during periods of light loading on the system and delivering it during periods of high demand. During these periods of high demand, the energy storage system supplies power, reducing the load on less economical peak-generating facilities.
3. **Peak Shaving:** Energy imbalance within the power grid can be created due to the variability of renewable energy resources and variable load, such as electric vehicle (EV) systems with variable random consumptions. This variability causes a notable difference between peaks and valleys of the load profile. The peak and valleys can be eliminated through load levelling, peak shaving, and power demand management. Peak shaving is the process of reducing the amount of energy purchased from the utility company during peak demand hours. Utility companies typically have variable pricing based on demand, and the pricing during the peak demand hours is typically the highest. This pricing structure allows the utility company to increase its capacity to meet the peak demand. This additional capacity is typically older, more expensive power generation equipment. The peak pricing also acts as an encouragement to customers to reduce demand so as to drive down utility costs. The tiered pricing is what might make peak shaving an attractive option to organizations with large electrical consumption during peak times. The battery energy storage system is a solution that can assist in reducing peak demands in a grid connected microgrid system.

1.5 Research Questions

The main aim of the EMS is to manage the operation of the BESS in a grid connected Microgrid to reduce the cost of energy imported from the grid while

complying with operational constraints. The main questions that this thesis addresses are:

1. How can the EMS be implemented in real-time using predicted data of stochastically variable renewable energy sources generation and load demand?

2. How can real-time data of generation and load demand be used to reduce prediction error and improve BESS control actions?

3. How can the BESS be controlled in real-time in a grid connected Microgrid containing CHP systems in behind the meter applications? The challenge associated with this application is that the CHP has to always operate above a predefined threshold to avoid engine damage and high emission. The other challenge is that no power should be injected into the grid due to constraints imposed by the network operators.

4. How can the battery charging/discharging cycle be limited to reduce age degradation?

5. How do the different TOU and standard tariff schemes affect the optimal operation of a PV-BESS based microgrid system in terms of the optimal operating cost and limiting of the BESS charge/discharge cycle?

1.5.1 Research Aims and Objectives

This research will focus on the optimal scheduling of microgrid operations, which aims to minimise the production and operational cost of distributed energy resources and the exchange with the utility grid subject to market conditions while satisfying the predicted load demand for a certain period (e.g., a 24-hour time horizon) and

the complex operational constraints such as the energy balance and the control of battery energy storage systems based on online and offline strategies.

The research objectives of this project are listed below:

1. To study optimization techniques and architectures used in energy management systems for Microgrids with renewable energy resources and battery units.
2. To formulate the economic dispatch and unit commitment problem using a combination of long short-term memory (LSTM) predictions, receding horizon (RH) control and mixed integer linear programming (MILP).
3. To simulate the proposed energy management system in specific microgrid applications.
4. To optimize the Microgrid's performance by defining long-term daily control strategies based on online and offline strategies in real-time to satisfy all operational constraints and minimize operating costs while guaranteeing the security of supply.
5. To implement a control strategy using the LSTM-MILP-RH approach for behind the meter application with CHP systems.

1.6 Thesis Contribution

The main contribution of the thesis is the development of a novel EMS using a combination of LSTM neural networks, mixed integer linear programming (MILP), and receding horizon (RH) control strategy to control BESS in grid connected microgrids. The merits of the developed EMS are:

1. It can be implemented in real-time as it only uses previous generation and load data.
2. The RH reduces the impact of prediction error, and it outperforms offline-based EMS with no RH control.

3. The LSTM-MILP-RH approach is able to control the charge/discharge cycle of the BESS and also helps to determine the most economic TOU tariff to be used in grid-connected microgrid applications.
4. It can be implemented in behind the meter applications with CHP systems, where it reduces running costs while complying with operational constraints.
5. Using this system in behind the meter application negates the need for the battery to operate in load-following mode, resulting in suboptimal operation.

1.7 Thesis Structure/Outline

This thesis contains six chapters and is organised as follows. Chapter 2 presents the literature review of related works in the area of optimal energy management of microgrids with energy storage and background concepts of the techniques used to develop the optimisation models and solutions to EMS for microgrid applications. An EMS for controlling battery storage (with a focus on BESS charge/discharge limits) in grid connected Microgrid using LSTM, RH control and MILP is presented in Chapter 3. Chapter 4 analyses the impact of the time of use (TOU) and standard tariff schemes in energy management for grid connected microgrid systems with energy storage. A real-time economic dispatch of CHP systems with energy storage for behind-the-meter industrial distributed energy applications considering online and offline approaches is presented in chapter 5. Chapter 6 concludes the thesis by revisiting the research questions, and a general conclusion is drawn with a recommendation and future research works.

Chapter 2

A Review of Optimal Energy Management of Microgrids with Battery Storage Systems and Renewable Energy Sources

2.1 Introduction

To prevent environmental degradation, promote sustainable development and achieve net-zero targets while meeting the ever-increasing need for energy, renewable energy resources coupled with energy storage devices have emerged as a viable option [56]. The microgrid system provides various technological options that allow active consumer engagement while requiring effective management. Because of this, energy management in microgrids has evolved into a system that manages information between the customer and the distributed energy centres [57]. The distributed generation system can supply energy at the lowest possible cost through an optimisation technique. The energy management system addresses this optimisation issue by using an algebraic representation of the dispersed generators and the limitations imposed by these energy sources [58]. This review examines the numerous optimisation strategies researchers have previously used to find the most advanced solution for microgrid operations, considering various optimisation goals and the imposed constraints. Because of their intermittent nature, renewable energy resources are explored in terms of the modelling tools and methods used to manage them. Finally, this review lays the groundwork for future research in energy management for microgrids, specifically in the prediction of energy demand and renewable energy generation using deep recurrent neural networks [59].

As projected, worldwide energy consumption will increase considerably over the next few decades, going from 11.4 billion tonnes of oil in 2010 to more than 18

billion tonnes by 2030, according to forecasts made by experts. It is the developing nations that account for the majority of the demand. This growth will result in the depletion of fossil fuels such as petroleum, oil, and carbon, which will result in an increase in greenhouse gas emissions [60]. Fortunately, energy systems have developed to include small and large-scale renewable energy resources such as wind energy, PV systems, wave energy converters and tidal streams to alleviate these issues and avert global energy crises [61]. Renewable energy has grown in popularity over the last decade due to increased global energy demand and mounting environmental concerns. Renewable energy sources such as solar, wind, and tidal have zero carbon emissions and are environmentally friendly, and as a result, their penetration into the global energy market has increased at an unprecedented rate [14]. Because of the introduction of investment tax credits and the declining costs of production driven by environmental and economic policies, renewable energy resources have become an option when compared to generating electricity using traditional methods [62]. By 2040, renewable energy resources are predicted to account for around 40% of the world's total energy consumption [62]. The intermittent nature of renewable energy resources and the imbalance between energy demand and supply are significant issues to overcome [3][4]. Introducing energy storage systems will help mitigate some of these issues in the future [65]. An energy storage system is required to offer the system more control and management capabilities. When used in conjunction with a microgrid, these technologies may help to improve management functions, such as peak shaving, load levelling, and energy arbitrage, among others. Due to the rise in energy demand, the restructuring of power systems has led to energy being generated from renewable energy

resources closer to the consumer. Because of the uncertainties associated with renewable energy resources, a hybrid renewable energy system considering different energy sources with energy storage and diesel generators for standalone systems was proposed [6][7]. The Microgrid comprises a collection of loads, energy storage facilities, and small generating units that are all connected. In a broader sense, it may be defined as a medium or low-density distribution grid with dispersed generation, including renewable and conventional sources (hybrid systems) and storage devices that offer electrical energy to end consumers. Storage improves the Microgrid's stability and compensates for the intermittent nature of solar and wind power, hence increasing the dependability of the Microgrid overall [66].

Smart-grid systems, such as hybrid microgrid systems, are classified as such because of how they manage the exchange of information between consumers and dispersed generations via the use of technological solutions [8]. In the context of energy supply generation, transmission, and delivery, the EMS is defined as an information system that provides the required functionality when supported by a network to ensure energy supply generation, transmission, and delivery at the lowest possible cost [67]. Control software that allows for the system's optimal operation is required to achieve a cost-effective, sustainable, and secure service from the Microgrid. A communication system is also necessary to manage microgrids in real-time, as well as to achieve cost-effective, sustainable, and secure service from the Microgrid [6]-[10][70]. However, energy management optimisation in a microgrid is mainly carried out as an offline optimisation problem due to the difficulty of optimising the Microgrid's

performance in real-time, but it can be classified into an offline and online optimisation problem.

2.2 Energy Management Requirements for Microgrids

Due to demand growth, distribution networks face many economic, technical, and environmental challenges. To overcome these issues, distributed generation and microgrids, as shown in Figure 2-1, were developed. The arrival of microgrids has lessened so many issues regarding the operation of power systems [71]. The main feature of microgrids is the notion of their controllability which makes them different from active distribution networks, and one layer of controlling the Microgrid is the energy management process [72].

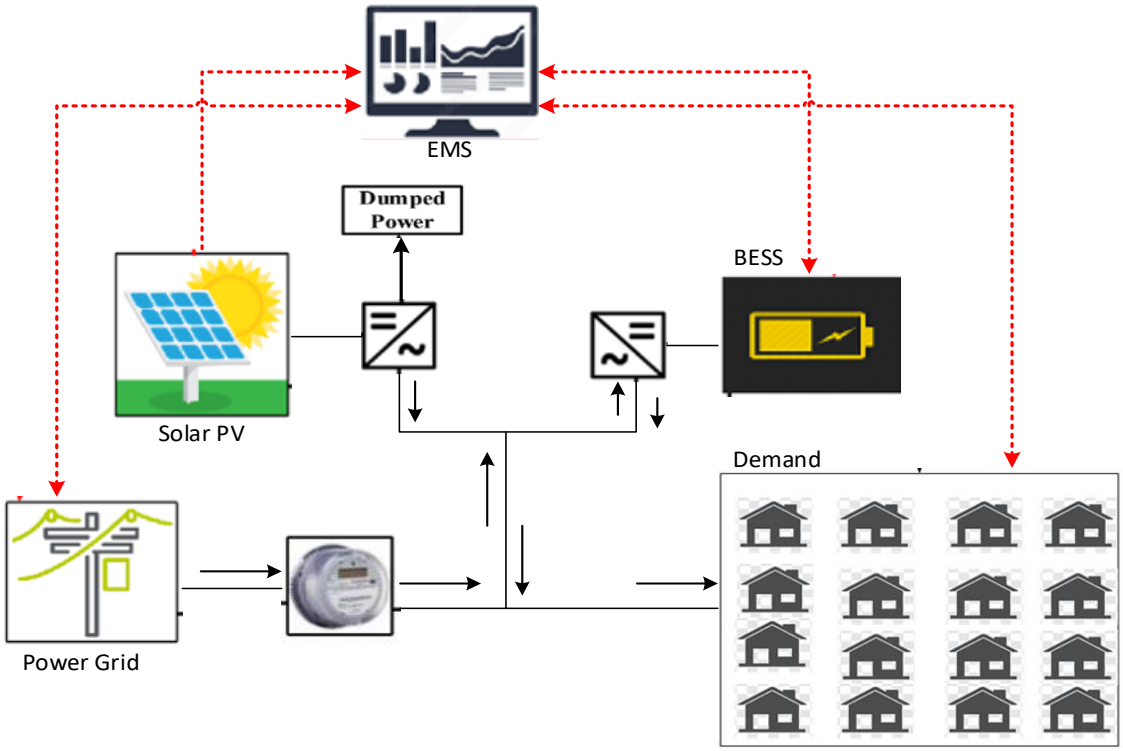

Figure 2-1: Representation of a Microgrid with an Energy Management System(EMS)

Energy management is a systematic procedure of managing energy within the Microgrid and transactions within the upper grid network to satisfy technical, environmental, and economic constraints [53]. The owner's benefits would be

maximised in the energy management process within a microgrid, optimising the production and consumption of different energy carriers. The energy management system is a microgrid's primary and most crucial part. It has the duties of gathering information, controlling various entities of the distributed energy resources (DERs) energy storage devices, and performing demand response programs where necessary, choosing the best strategies for the operation of the Microgrid according to different circumstances.

Some of the main responsibilities of the energy management system are highlighted in the subsections below:

2.2.1 Generation and consumption balance and operational cost minimisation.

Energy analyses of the microgrid systems are nearly always associated with cost; in some instances, the analyses are used solely to compare the performances of alternative packages. The cost assessment carried out by the EMS is aimed at minimising the microgrid system's operational cost by examining the cost of running the different components of the Microgrid while ensuring that the generation and consumption are balanced, guaranteeing the security of supply to the demand.

2.2.2 Compliance and implementation of the rules for connecting and disconnecting the Microgrid to the upper distribution system.

The EMS is also responsible for ensuring compliance with the rules for connecting the Microgrid to the distribution system since it acts as the control system that provides the necessary functionality, ensuring that both the generation and distribution system supply energy while satisfying the technical constraints of the Microgrid and the distribution system. In emergencies when the Microgrid has to be disconnected from the distribution network, the EMS also

plays an important role in ensuring safety. The EMS considers the needed system stability, safety, and dependability criteria to establish the most cost-effective design for power production, transmission, and distribution across the network.

2.2.3 Optimal Utilisation of Existing Resources.

The EMS achieves the operating cost minimisation via optimal utilisation of existing energy resources for both grid-connected and island. The energy EMS is a collection of computer-aided tools that are used by the operators of electric utility grids and microgrids to monitor, regulate, and maximise the efficiency of the performance of the generating or transmission system. This enables the optimal utilisation of existing energy resources.

In general, the EMS procedure can be carried out either as a short-term or a long-term task. For the short-term task, the EMS technique is focused on improving system reliability, while in the long-term, the goal is to maximise the economic benefit of the system. Literature suggests that energy management problems could be solved using deterministic or stochastic approaches and can be divided into four subcategories. Linear programming (LP), nonlinear programming (NLP), and mixed integer linear or nonlinear programming (MILP-MINLP). This chapter presents a literature review on various optimisation approaches for energy management within microgrids.

2.3 Energy Management Optimisation Strategies for Microgrids.

Many scholars have approached energy management for islanded and grid connected microgrids, as shown in Figure 2-1, through several research methods and optimisation techniques utilising advanced information technology [66][67].

The objective function for optimal operation of the hybrid microgrid system is

designed to maximise the output power of distributed generators within the Microgrid, thereby minimising the total operating cost of operating the Microgrid, minimising CO2 emissions, helping the environment, and maximising the lifetime of energy storage systems [73].

2.3.1 A Review of Multi-Agent-System Based Energy Management System

The multi-agent system (MAS) is developing as an integrated solution approach to smart grid applications, distributed artificial intelligence (DAI), communication, and data integration requirements. Dispersed and heterogeneous information may be handled locally yet used globally to coordinate distributed knowledge networks, resulting in reduced information processing time and network traffic. Parallel processes, asynchronous communication, and autonomous agent behaviours allow MAS to respond to dynamic changes in the environment, enhancing the Microgrid's dependability, responsiveness, fault tolerance, and stability. Figure 2-2 depicts a multi-agent-based optimisation technique that uses cooperation and communication among decision agents. In this context, agents make joint decisions rather than single decisions to maximise a system-wide objective [74]. Several studies have been conducted which validates the applicability of multi-agent-based EMS. A summary of some of the works is provided here.

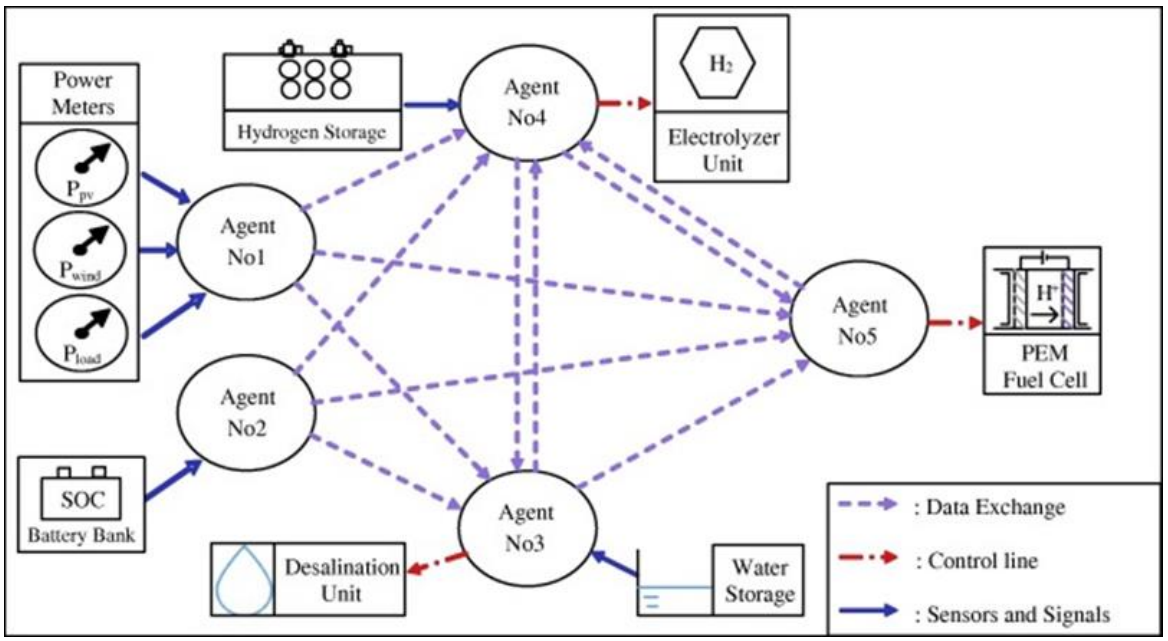

Figure 2-2: Configuration of a multi-agent-based distributed system for microgrids [75]

Mao et al. [76] Present a multi-agent-based hybrid EMS-MG with both centralised and decentralised energy control functionalities and optimisation of the economic operation of the Microgrid. A coordinated energy management framework is realised by combining autonomous control of locally distributed energy resources with coordinated energy control at a central level of the Microgrid. A novel simulation platform for energy management systems was designed based on the client-server framework and implemented in the C++ Builder environment. The simulation results show that the proposed control system effectively manages and optimises microgrid operation.

Raju et al. [77] studied the energy management of grid outage in a microgrid with two PV generators, two wind turbine generators and a local load. A multi-agent management system based on the differential evolution algorithm in JADE was used to minimise the generation costs from the intermittent nature of the solar resource and randomness of load. They claimed that the framework allowed the intelligent consumer to search for all possible logical sequences and select the

optimal management action for grid outage management to increase operational efficiency. The summary of the review of multi-agent-based EMS is presented in Table 2-1.

Table 2-1: A summarised review of multi-agent system (MAS) based EMS

Ref No.	Method	Power Sources	Connection	Summary
[78]	MAS	PV, WT, BT	Grid/Islanded Connection	Experimental results show the ability of the proposed multi-agent T-Cell-based RT-EMS to maintain the stability and smooth operation of the MG with modularity and fault tolerance features implemented through the MAS JADE platform.
[79]	MAS-RL	PV, WT, BT	Grid/Islanded Connection	A multi-agent-based EMS is developed to manage the objectives of the system. Reinforced learning is imbibed with MAS to improve the decision-making capability by learning using the sets for participation in energy trade marketing.
[80]	MAS	PV, WT, FC, BT	Grid/Islanded Connection	This paper proposes a communication rule for sharing the local information of the agents and getting access to the global information was based on an average consensus algorithm (ACA), and a restoration decisions strategy based on the discovered global information was developed.
[81]	MAS	PV, DE, BT	Islanded Connection	This paper proposes a MAS-based intelligent energy management system to operate a hybrid microgrid in islanding mode while effectively minimizing the peak demand of the system using the V2G and LED savings
[82]	MAS	PV, WT, MT, FC, BT, DE	Islanded Connection	MAS-based agent optimization is developed to optimize the operation of the distribution system with DG in energy scheduling and generation. EMS is performed for the system by considering the constraints, such as generation cost and emission of carbon.
[83]	MAS-CNN	PV, WT, DE, BT	Grid/Islanded Connection	MAS-based energy management is proposed for the generation management of the PV, wind, and load. Balancing is maintained using the CNN (convolution neural network)-based load

forecasting technique for the load demand.

PV—Photovoltaic; WT—Wind Turbine; MT—Micro Turbine; DE—Diesel; BT—Battery; FC—Fuel Cell; G—Grid; I—Islanded.

Multi-agent strategies for the optimization of microgrids have been investigated by the authors listed above, who have shown that the method may be used to efficiently manage, optimise, and improve the operational efficiency of hybrid microgrids. However, the authors have not considered the impact of the strategy on the controllable components like the BESS of the microgrid system, which creates a gap that will be addressed in this research work.

2.3.2 A Review of Energy Management Based on Metaheuristic Approach.

A metaheuristic is a higher-level procedure to find, generate, or select a heuristic (partial search algorithm) that may provide a sufficiently good solution to an optimization problem, especially with incomplete or imperfect information or limited computation capacity. The metaheuristic approach may be divided into two variations: metaheuristic, with single-solution based (local search) and metaheuristic, with population-based (global search). Some examples of metaheuristic methods based on population are Ant Colony Optimization (ACO), Genetic Algorithm (GA), Particle Swarm Optimization (PSO), and Crow Search Algorithm (CSA). Some prior research work using metaheuristic approaches in energy management systems for microgrids is discussed in several current studies. Papari et al. [84] Investigated the energy management of a microgrid connected to a utility grid using the crow search algorithm (CSA). The CSA is a metaheuristic optimisation method that mimics the behaviour of a crow when it comes to storing and hiding food. To build a robust approach for a DC microgrids energy management, a powerful optimizer that relies on the crow search

algorithm (CSA) is developed to obtain the optimal solution. A two-stage modification approach is illustrated to avoid being trapped in the local minima of the optimization algorithm and to enhance the search capability of CSA. The feasibility and performance of the proposed method in DC MG applications are evaluated in three different scenarios using a notional test system. The results are compared with other optimization algorithms and corroborate the advantage of the CSA technique.

Luna et al. [85] demonstrated an EMS that functions in real-time. The perfect, imperfect, and exact predictions were examined in three scenarios. The utilised optimisation model was tested in both connected and isolated microgrids with large imbalances between generation and load. An adaptable online microgrid EMS has been designed and experimentally tested in order to deal with the variability and uncertainty feature of microgrid systems with RESs. A quantitative evaluation framework has been proposed and used in the case study, demonstrating the effectiveness of the proposal over a selected benchmark strategy and establishing the gaps with ideal boundaries of the best and worst possible solutions.

Wasilewski [86] presented a metaheuristic optimisation technique for microgrid optimisation. The evolutionary and particle swarm algorithms are among the techniques used. These solutions accommodate the fact that the problem's deterministic assumptions significantly constrain the methodology used. However, the risk of relying on renewable energy sources due to uncertainties is acknowledged. The main objectives for a given problem are set, and then a detailed mathematical model of a stated optimisation problem is described. The objective function and a set of constraints have been presented in detail, and two

independent meta-heuristics - the evolutionary algorithm and particle swarm optimisation - have been proposed and substantiated as exemplary methods of solving the formulated optimisation problem.

An economic dispatch and battery degradation model has been proposed in [87]. In this case, genetic algorithms were employed to determine energy supply choices via the usage of a diesel generator. In the study, the researchers discovered that increasing the battery life reduces the operating expenses of microgrids. Microgrids with a diesel generator and PV system were used to test this strategy, and it was found to be successful.

Marzband et al. [88] demonstrated how the artificial bee colony (ABC) algorithm might be used to design an energy management system for an isolated microgrid. Due to the intermittent nature of solar energy supplies and wind energy output, a technique based on probability distributions is necessary to analyse the economic dispatch of producing units within a microgrid. The expenditures were reduced by 30% as a consequence of the study. Neural networks and Markov chains are used to manage the non-dispatchable generation and the unpredictability of the load.

Kuitaba et al. [89] introduced a novel technique for optimising an interconnected microgrid that blends an expert system based on 'Fuzzy Logic' with a metaheuristic algorithm known as 'Grey Wolf' optimisation to achieve greater efficiency. This strategy involves minimising both the costs of the generating units and the emission produced by fossil fuel sources as much as possible. Microgrid expenses are reduced by using this technology, which considers the appropriate capacity of batteries and reduces the usage of fossil fuels.

Das et al. [90] Investigated the effects of incorporating internal combustion engines and gas turbines into a standalone hybrid microgrid equipped with solar panels. A multi-objective genetic algorithm was used to optimise this system based on energy costs and overall efficiency. To monitor the load, both electric and thermal technologies were used. When paired with heating and cooling, all of the systems under consideration met the electrical requirements.

Abedini et al. [91] presented a particle swarm optimisation method with Gaussian mutation to optimise an energy management system for standalone hybrid microgrids that included solar, wind, and diesel generators. The system's capital and fuel expenses are minimised using the gusain mutation method.

The following are some examples of metaheuristic algorithms: particle swarm optimization (PSO), genetic algorithm (GA), modified PSO (MOPSO), non-dominated sorting genetic algorithm II (NSGA-II), enhanced velocity differential evolutionary PSO (EVDEPSO), priority PSO, multi-voxel pattern analysis (MVPA), grey wolf optimization (GWO), artificial bee colony (ABC), crow search algorithm (CSA). The metaheuristic procedures utilised in EMS are critically examined with the connection type in Table 2-2 below.

Table 2-2: A summarised review of metaheuristic methods in EMS

Ref No.	Method	Power Sources	Connection	Summary
[92]	NSGA-II	PV, WT, BT	Grid/Islanded Connection	A multi-objective optimization problem is proposed to maximize the economy. Intelligent power marketing is adapted to improve the economic dispatch of the Microgrid.
[93]	NSGA-II	PV, WT, BT	Islanded Connection	This paper establishes an integral objective function considering the demand response and user satisfaction constraints, which has an effect on the economy and operation of the system with the DR strategy.
[94]	GWO	PV, WT	Grid Connection	An EMS application of the V2G economic dispatch problem is

				optimized in the MG while converting the multi-objective problem to a single objective using the judgment matrix methodology
[95]	EVDEPSO	PV, BT	Grid Connection	A day-ahead planning schedule is determined to improve the energy market trading while managing the resources available. Includes the electric vehicles participating in the energy market, G2V and V2G.
[96]	CSA	PV, FC, DE, HY	Grid/Islanded Connection	The Pareto front is considered to investigate the operating cost, solar power uncertainty, carbon emission, and the cost of the parameters. Hydrogen fuel is considered to reduce operating costs
[97]	PSO	PV, MT, BT, TES	Grid/Islanded Connection	An optimal energy planning is proposed for the recently modelled energy hub. An efficient microgrid structure is discussed along with technical and economic prospects with optimization.
[98]	PSO	PV, WT, DE	Grid/Islanded Connection	Minimizing the operating costs while maximizing the utility benefit using the CVCPSO algorithm, which yielded the Pareto-optimal set for each objective, and the fuzzy-clustering technique was adopted to find the best compromise solution.

PV—Photovoltaic; WT—Wind Turbine; MT—Micro Turbine; DE—Diesel; FC—Fuel Cell; HY—Hydro; TES—Thermal energy storage; G—Grid; I—Islanded.

Researchers have taken a comprehensive look at energy management systems for the optimal operation of hybrid microgrids using the metaheuristic approach. They have investigated both renewable and non-renewable sources using various methods that fall within the metaheuristic optimisation approach and have achieved good results such as reducing the use of fossil fuels, optimising systems based on energy cost and overall efficiency, minimising the operating costs of the systems, and reducing their carbon footprints. The authors, on the other hand, have not taken into consideration the impact of the energy management strategy on the state of health of the battery storage system, nor have they considered

how increasing the battery life by controlling the battery charge/discharge cycle affects the operating costs of the system. This gap is addressed in this thesis

2.3.3 A Review of Dynamic Programming Strategy in Energy Management Systems.

Dynamic programming is a method that divides the optimisation problems into sub-problems and stores the solution for later use, eliminating the need to calculate the result again. The optimum substructure property describes how sub-problems can improve the overall solution. If a solution exists, dynamic programming is likely to discover it. Rouholamini and Mohammadian [99] proposed an EMS for a grid-connected hybrid generating system with a PV generator, wind turbine, fuel cell, and electrolyser that requires effective energy management. Based on the simulation findings, this system exchanges power with the local grid, utilising real-time energy pricing across a 24-hour time horizon/period. The energy management was optimised using the internal search method based on dynamic programming.

Luu et al. [100]. Presented a dynamic programming strategy and methodology based on rules applied to a standalone microgrid with diesel and photovoltaic generators and a battery energy storage system. The power balance between generation, consumption, and the capacity of each distributed generator, determines the restrictions. To reduce operating and emission expenses, dynamic programming is implemented. The constraint is imposed by the power balance between supply and demand and the operational capability of each distributed generator.

In [82], dynamic programming and mixed-integer nonlinear programming optimization techniques were utilised to design an EMS for a microgrid. The Microgrid is connected to the grid, and decisions are made based on the Bellman

equation. Power flow and battery storage are considered constraints when offline data is required. It is feasible to use the technology in a large number of microgrids at the same time.

Marabet et al. [102] proposed an energy management system for a lab-scaled hybrid microgrid powered by wind, solar, and battery energy. The data acquisition and control systems runs in real-time. The energy management system follows a set of rules and optimises the microgrid operation by managing and monitoring power production, load, and storage aspects.

Wu et al. [103] proposed that a dynamic programming approach was used for the administration and control of standalone microgrids. The deep learning system is real-time, allowing intra-day scheduling to determine a control plan for microgrid optimisation while relaying data from local controllers to the centralised management framework.

Almada et al. [104] proposed a centralised system for the energy management of microgrids either in the standalone or interconnected modes. The fuel cell only works in the standalone mode if the battery is less than 80%, and a 60% threshold is required in the interconnected mode to ensure reliable behaviour.

Choudar et al. [105] presented a battery state-of-charge and ultra-capacitor-based energy management model. Normal operating mode, photovoltaic restriction mode, recuperating, and standalone modes are the four states or operating modes of optimum microgrids management. A summarised review of dynamic programming-based EMS is presented in Table 2-3.

Table 2-3: A summarised review of dynamic program (DP) based EMS

Ref No.	Method	Power Sources	Connection	Summary
[106]	DP	DE, BT	Islanded Connection	The operating cost of traditional grids is optimised using an EMS model, which takes the penalty cost

				into account. Pontryagin's Principle may be used to minimise the amount of time spent computing.
[107]	DP	WT, DE, BT, G	Grid/Islanded Connection	Short-term forecasting is used to anticipate wind speed and determine real-time pricing, resulting in a reduction in the overall cost of operations by scheduling the available units.
[108]	DP	WT, BT	Grid Connection	Optimization of the MG is proposed considering the cost function of the unit commitment and economic dispatch operations and daily energy scheduling.

PV—Photovoltaic; WT—Wind Turbine; MT—Micro Turbine; DE—Diesel; BT—Battery; G—Grid..

The authors, on the other hand, have not taken into consideration the impact of the energy management strategy on the state of health of the battery storage system, nor have they considered how increasing the battery life by controlling the battery charge/discharge cycle and how it affects the operating costs of the system.

2.3.4 A Review of Robust Programming and Stochastic Based Methods for Energy Management in Microgrids.

One of the recently developed approaches for operating and planning distributed energy systems is the two-stage stochastic programming (SP) model, a framework for modelling optimization problems involving uncertainty. It has been demonstrated to be efficient and flexible when dealing with uncertainty in microgrids. In addition, Monte Carlo Simulation (MCS) generates stochastic variable scenarios for two-stage stochastic programming. The risk cost is enormously reduced by considering all the possible realisations.

Lujano et al. [109] created a load management strategy for hybrid systems, including wind turbines, battery banks, and diesel generators. The wind speed was predicted using the autoregressive moving average (ARMA). According to the findings, the load management method increased wind power utilisation by

moving controlled loads to wind power peaks, thereby boosting the charge in the battery bank.

Rezai and Kalantar [110] proposed a frequency deviation-minimising stochastic energy management system for a freestanding microgrid. The Microgrid's operating costs include conventional and distributed power and reserves and incentives for renewable energy production. To show the resilience of the suggested technique, the outputs of the traditional generators were also examined for different scenarios. Xiang et al. [111] proposed an optimisation model for an interconnected microgrid based on Taguchi orthogonal matrices. The uncertainty in renewable energy and load demand was estimated using an interval based on error prediction. Battistelli et al. [112] proposed a remote hybrid AC/DC microgrid energy management system that ensures economic dispatch, notwithstanding the risks associated with renewable energy sources. Load control (thermic and electric cars) is calculated based on demand, considering the generators' limitations, controlled loads, and battery capacity.

Lu et al. [113] presented a dynamic pricing approach for achieving the best operational results. This technique was used on a system made up of multiple microgrids to assess the risk of large-scale renewable energy integration. At two levels, an optimisation strategy was devised: On the top level, the pricing mechanism ensured the market operator's energy operation, while on the lower level, the microgrid transactions were formed.

Hu et al. [114] proposed a two-stage optimisation algorithm for an interconnected microgrid. In the first step, a conventional generator is employed, while the second stage uses hourly marketing to guarantee that conventional and distributed generations are dispatched economically using the Lyapunov

optimisation approach. This combination allows for the control of uncertainty in renewable energy.

Liu et al. [115] proposed an energy management system for linked microgrids considering renewable energy sources and load uncertainties. The energy management challenge may be broken down into two sub-problems: First, system safety is ensured by scheduling within established energy limits. Then, frequency control is provided by evaluating the real-time energy capacity deviation limit for frequency regulation. It was discovered that the strategy offered was more cost-effective.

Su et al. [116] developed a model for the optimal programming of linked microgrids that reduces the operational expenses of traditional generators, battery deterioration, and commercial fees associated with electricity sourced from the utility grid. There are two steps to this concept. The first step includes optimising the microgrids, and the second stage requires analysing the power output to compute the Microgrid's energy losses in real-time. Zachar and Daoutidis [117] proposed a hierarchical control system for regulating and supervising the loads and dispatchable energy inside a microgrid has been. On a small scale, stochastic optimization was employed to reduce mistakes in forecasting renewable energy, which proved beneficial. The implementation of deterministic optimization on a large scale was accomplished quickly to update the optimum dispatch circumstances.

Shen et al. [118] presented a stochastic energy management model for an interconnected microgrid. The uncertainty level is managed using Latin hypercube sampling based on the Monte Carlo method, generating various

scenarios for the distributed resources, load, and electricity price. Sensitivity analysis determines the expected price's standard deviation and reliability level.

Farzin et al. [119] proposed an energy management system for a microgrid at a remote location. During the analysis, it was assumed that islanding events were a normal probability distribution of breakdowns in the electrical grid. The goal was to keep the microgrid's operational expenses as low as possible. The costs include expenditures connected with the operation of the microturbines, wind turbines, batteries, and the disconnection of the power grid.

Kuztnesova et al. [120] Proposed a robust optimisation approach using agent-based modelling and developed a decentralised energy management system for a network of linked machines. This study examined the cost of power imbalances caused by renewable energy and the unpredictability of load power demand to assess the Microgrid's overall performance. However, the effect of the constraints on the physical microgrid components, such as the batteries, has not been explained, creating a gap to be addressed in this thesis.

2.3.5 A Review of Reinforcement Learning Based EMS

Reinforcement Learning (RL) is a type of machine learning in which an agent interacts with its environment and learns what actions to perform based on the state of the environment [121]. The agent learns via trial and error and is rewarded for performing desired behaviours. The environment is represented as a Markov decision process. RL algorithms have been around since the 1960s and 1970s. Over the years, these algorithms have been used to solve a broad range of issues, from traffic light control to watershed management [122]. The combination of RL algorithms with deep neural networks has considerably boosted the efficacy of RL approaches, allowing them to be used in computer

vision applications such as self-driving automobiles. Recent important accomplishments in RL have resulted in extensive study into RL and its applications.

RL has recently been used in a number of complex building energy management areas. RL has been used for tasks such as HVAC control, water heater control, electric vehicle charging, lighting control and appliance scheduling. Using RL to solve these issues has the benefit that the algorithm itself learns what the appropriate control strategy is. When implementing more traditional rule-based approaches, the designer must handcraft the thresholds that the system will adhere to. This simple strategy is not necessarily able to minimize energy consumption to the extent that RL can. Several factors increase the complexity of applying RL to these problems, such as identifying what state information is needed, conflicting objectives and simulator design. There are primarily two categories of online RL algorithms, which are known as off-policy and on-policy. In off-policy approaches, such as Q-learning, an approximation of the action-valued function is calculated irrespective of the policy that is currently being followed. On the other hand, when using an on-policy method, such as the state action reward state action (SARSA), the action-valued function is constantly updated in accordance with the determined policy, which makes it more challenging to converge [123].

Recent studies have suggested RL as a viable solution because of its capacity to build an optimum policy online [124]. RL has the potential to help BESS operate more efficiently. The main advantage of RL over traditional methods is that it does not need any model of the environment, and it can learn the optimum policy in real-time. Yoldas et al. [80] used the mixed integer non-linear programming

technique guided by a Q-learning algorithm to simultaneously decrease the daily energy cost and emission of harmful gases. Performance comparisons were made using only conventional Q-learning. The result showed an approximately 1.2% reduction in the daily operational costs associated with the proposed technique over conventional Q-learning approaches.

In Mbuwir et al. [123], the authors suggested using batch reinforcement learning, often known as offline RL, to address the optimization issue associated with the microgrid to develop a more cost-effective solution. The objective was to locate or statistically learn the pattern of the optimal control policy from the training data (the load and PV profiles from the previous year) in the form of multiple smaller batches (sets) and then to deploy this policy on the present environment in real-time. Comparing the batch RL method to the MILP strategy revealed that the batch RL method is 19% less effective than the MILP strategy.

2.3.6 A Review of Linear and Nonlinear Programming Based EMS

Linear programming is an optimization method for linear constraints and linear objectives. An objective function identifies the quantity to be optimised, and the purpose of linear programming is to determine the variable values that maximise or minimise the objective function. It is the goal of a linear optimization method to identify a position where this function has the least (or greatest) value, while Non-linear optimization refers to the method of solving an optimization issue in which some of the constraints or the objective function are nonlinear in nature. An optimization problem is one in which the extrema (maxima, minima, or stationary points) of an objective function over a set of unknown real variables must be calculated conditionally on the satisfaction of a system of equalities and inequalities, which are collectively referred to as constraints, are satisfied.

Mathematical optimization is a sub-field of mathematics concerned with the solution of problems that are not linear in nature.

Extensive research has been reported previously on managing microgrids using linear and nonlinear programming, much of which has focused on mathematical formulations and is usually tested under offline scenarios. However, due to the stochastic nature of the RESs, offline optimization may fail to achieve the optimal result as the uncertainties of the RESs are not considered in real-time. In [126], a linear mathematical model is suggested to balance the microgrid's generation and load by minimising the system's total operating cost over 24 hours. To demonstrate the performance of their approach, a tiered power management system composed of an advisory and a real-time layer was introduced. The advisory layer provided long-term directives to the real-time layer by solving the RH problem offline using the predicted PV and load data. However, this approach was not implemented in real-time using real data; long-term directives from the advisory layer were passed to the real-time layer. In [50], the economic dispatch problem for total operation and cost minimization in a DC microgrid has been formulated and solved with a heuristic method. However, this approach does not enhance the design of the EMS architecture so that it can be easily implemented on a physical system. A smart energy management system is defined in [127] as an architecture that sequentially connects functional modules such as power forecasting, energy storage management and an optimization module for a day ahead optimal operation of the microgrid. But this system may produce a bottleneck in the flow of data for real-time operations. These reported works do not deal with the uncertainty of the RESs generation nor the consumption in real-time. To overcome these challenges, an online strategy such as the one

proposed in [128][129] can be implemented where energy management systems are designed and implemented by considering the microgrid's current status but without considering future power generation or load demand. In [130], an optimal energy/power control method is presented for the operation of energy storage in grid-connected microgrids, considering forecast electricity usage and renewable energy generation. However, prediction errors due to long-term predictions were not considered. In [131], a rolling horizon-based energy management strategy is defined for a specific case study. The strategy consists of two stages; a deterministic management model is first formulated and then followed by a rolling horizon control strategy.

Chaouachi et al. [132] Proposed a multiobjective, intelligent energy management system for a microgrid to reduce operating costs and environmental effects. One of the most recent works is developing an artificial neural network that can anticipate solar and wind power production 24 and 1 hour in advance, respectively, as well as load demand. An expert system based on ‘fuzzy logic’ was used to schedule the batteries in the multiobjective intelligent energy management system, which consists of multiobjective linear programming and battery scheduling.

Delgado and Domínguez-Navarro [133] proposed a linear programming-based system for microgrid energy management that allowed for the most efficient running of either generators or controllable and non-controllable loads, depending on the situation. With the optimum dispatch of generators (diesel) while also fulfilling the operational and economic restrictions imposed by purchasing and selling energy corresponding to each component (generators, storage systems, and loads).

Correa et al. [134] proposed an EMS based on a virtual power plant to reduce energy use. The microgrid under investigation is equipped with solar panels and energy storage devices, and it operates in an integrated fashion. They are programmed/modelled using linear programming approaches to reduce operational expenses to the absolute minimum. Natural resources, such as hydro power, are included in an energy model, such as the Colombian model, and are the primary renewable energy source.

Cardoso et al. [135] analysed a novel model for monitoring a Microgrid's battery capacity decline. Stochastic mixed-integer linear programming was used to address the battery capacity decline, which considers a number of parameters such as loads and different sources of energy production, costs, limitations, grid topology, and local energy fees.

Sukumar et al. [136] developed a hybrid strategy for managing Microgrid energy; the hybrid strategy was accomplished by mixing utility grid electricity with fuel cell power. The problem was addressed using linear optimisation techniques, while the utility grid's on/off states were solved using MILP. To establish the most appropriate size for an energy storage system, a particle swarm optimization (PSO) approach was applied.

In [137], the energy management system of a hybrid AC/DC microgrid in an isolated hamlet that uses a solar-powered plant was investigated using mixed integer nonlinear programming. The suggested optimisation approach reduced the daily running expenses to a bare minimum, which was the goal.

Umeozor and Trifkovic [138], studied the energy management of a Microgrid using MILP by parameterising the uncertainty in solar and wind energy production, which was then used to design the microgrid. The optimization is

accomplished at two different levels following the selection of a parametrisation scheme; operational choices are made considering the variance in market prices and the configuration of storage systems.

Among other considerations, Behzadi and Niasati [139] analysed a hybrid system which included a photovoltaic system, battery, and fuel cells. Transient system simulation tool (TRNSYS) software was used to conduct the performance analysis. Manual calculations, the HOMER programme, or the genetic algorithm in the hybrid optimisation by genetic algorithm software (iHOGA) were used to establish the size. This hybrid system explored three energy management techniques for energy dispatch. Each system's extra energy was assessed, and a choice was made to make hydrogen, charge the battery, or do both. A summarised review of linear and non-linear programming-based EMS with the type of connections is presented in Table 2-4.

Table 2-4: A summarised review of linear and none-linear programming-based EMS

Ref No.	Method	Power Sources	Connection	Summary
[140]	MILP	PV, BT	Grid Connected	A three-phase EMS model with load shedding is suggested, with outage limits taken into consideration.
[141]	MILP-LP	PV, BT, FC	Grid Connected	A mixed-mode EMS system is presented, consisting of an ON/OFF mode and a continuous run mode.
[142]	MILP	PV, WT, DE, MT, FC, BT	Grid/Islanded	An optimization model for an EMS was used to determine the capital cost, fuel cost, energy cost, and penalty for emissions while also accounting for other factors. Energy sources and storage are taken into account in economic dispatch for the purpose of techno-economic analysis.
[143]	MILP	PV, WT, BT	Islanded Connection	Reduced costs are achieved by decreasing the ESS in conjunction with beneficial demand response (DR) determination.
[144]	MILP	PV, BT, DE	Grid/Islanded	Utilizing a piecewise linear function, EMS proposed a method for

				minimizing fuel costs while optimising the size of diesel generators and batteries.
[5]	MINLP	PV, WT, MT, FC, BT	Islanded Connection	EMS is developed for a three-phase system in order to reduce the amount of fuel used, as well as the cost of starting and shutdown.
[129]	MINLP	PV, BT	Grid/Islanded	The stable operation of a hybrid MG with clean water supply while minimizing the total daily operating expenses is the objective.
[145]	NLP	PV, FW, MT, FC, BT	Grid/Islanded	The MG management application determines energy market operational cost and its profit
[106]	NLP	PV, FC, BT	Grid/Islanded	Optimization of the cost-beneficial charge-discharge schedule of the battery while taking into consideration the customers' load changing events.

PV—Photovoltaic; WT—Wind Turbine; MT—Micro Turbine; DE—Diesel; FC—Fuel Cell; G—Grid; I—Islanded.

2.4 A Review of Energy Management System in CHP Applications

Due to the increased global need for energy and growing concerns about the accelerating impacts of greenhouse gasses, efficient and sustainable energy production is increasingly in focus. The trend toward lowering greenhouse gas emissions has led to an increasing emphasis on boosting energy efficiency. Consequently, distributed generation is being supported, mainly with the use of CHP systems. A CHP system simultaneously creates electricity and usable heat from a single fuel source. Many compact internal combustion engine-based CHP units can supply quick balancing energy and simultaneous heat for heat loads, such as residential, industrial, and commercial buildings [146] [147]. CHP is a technology that offers excellent primary energy savings and, consequently, lowers CO_2 emissions; this technology was identified as one of the options for attaining the primary energy-saving targets of the European Union [148]. The cost advantages gained by CHP units are a function of energy savings (power

produced that would otherwise have been imported from the grid) and heat savings (heat generated that would otherwise have been supplied by on-site gas-fired boilers). In assessing the economic feasibility of CHP units, the installation, maintenance, and fuel costs must also be considered.

The maintenance and fuel input expenses make up the CHP units' operational costs. Typically, the output from a CHP unit is roughly 40% electricity and 60% heat, with electrical efficiencies ranging from 35% to 45% and 85-90% total efficiency. A typical CHP system will convert about 90% of the fuel into energy [149]. Therefore, it is vital to verify whether the CHP sizing is based on electrical or thermal demand.

A CHP system benefits from a decrease in fuel consumption of about 35% over the use of traditional energy delivery mechanisms like diesel generators [150]. However, CHP systems would typically still suffer losses if the demand was lower than the supply. The balance between user demand and supply has been a long-standing difficulty in the context of energy management. The ever-changing demand makes it challenging to match supply to demand. It is recognised that energy storage may assist in meeting shortfalls between supply and demand. While existing CHP systems may be equipped with thermal storage, they are seldom fitted with electrical storage, although the electrical storage might also provide distinct advantages [151]. The addition of these energy storage facilities will not only improve the flexibility of a CHP system and its overall efficiency but will enable uncoupling between energy production and demand, allowing excess energy production to be stored and used when extra energy is required. The excess electricity could also be sold to the grid when the BESS is full if this option is allowed by the network operator [152]. For the CHP to work effectively, it is

advised not to operate below 50% of its capacity. This is because running uninterruptedly in low load mode may lead to increased gas consumption and subsequently to a significant accumulation of carbonised oil; or oil residue in the engine and the suction and exhaust system [153]. Such residue would impair the engine's efficiency and reliability, and as a result, maintenance expenses are likely to increase. In addition, while an engine is working in low load mode, it operates at a lower temperature and, therefore, lower efficiencies as the fuel is only half-burnt, creating white smoke with significant hydrocarbon emissions [153] [154].

Given these constraints in operating a grid-connected CHP system, numerical optimisation can be deployed to optimise their operation. Several studies have explored optimising the operation of a grid-connected CHP system, and different methods have been proposed. Because heat cannot be transported over long distances, the primary constraint is that the local heat demand must be met at all times. The economic dispatch of the system then tries to minimise the production costs (i.e. fuel costs) of the CHP units [155] [156]. Maleki *et al.* in [157] designed a grid connected CHP system to sell the excess energy produced by the CHP unit to the grid using the Feed-in Tariff (FIT). This approach is mostly dependent on the energy market agreements, which are not always in the best interest of the microgrid owner or operator. Xie *et al.* [158] present a nonlinear dynamic model of a grid connected CHP system that can effectively simulate the thermoelectric interactions and examine the impact of the CHP on the power grid based on the mass balance and energy balance equations. This study is particularly beneficial for designing new control strategies for CHP systems to maximise their efficiency and stability for the grid. In [137], an energy

management strategy for the joint operation of CHP and PV prosumers inside a grid-connected microgrid; is presented using a game theory approach. An optimisation model based on the Stackelberg game is designed, where the microgrid operator acts as the leader and PV prosumers are the followers. The properties of the game are studied, and it is proved that the game possesses a unique Stackelberg equilibrium. The heuristic algorithm based on differential evolution is proposed; the MGO can allow each prosumer can adopt nonlinear constrained programming to reach the Stackelberg equilibrium. The model's effectiveness is verified in determining MGO's prices and optimising net load characteristics.

Technical solutions for the economic dispatch of CHPs are still in the early stages of development, with the most recent advances concentrating on system design, thermal analysis, and prime mover optimisation [160][161]. There are few studies that analyse the economic dispatch of CHP systems with battery energy storage in terms of the link between the electrical load and the heat demand. Nazari-Heris *et al.* [160] present a study on the short-term scheduling of grid-connected industrial heat and power microgrid; containing a fuel cell (FC), CHP, boiler, battery storage system, and a heat buffer tank. The authors solve a multi-objective microgrid dispatch problem by minimising cost and emissions, considering demand response programs and uncertainties. A probabilistic framework based on a scenario method, considered for load demand and price signals, is employed to overcome the uncertainties in the microgrid's optimal energy management for optimal grid-connected system's optimal scheduling. Because of the temporal characteristics of energy storage, the economic analysis of this technology is always challenging to solve. How a storage unit is operated

in a one-time step affects how it can be used in the future. Optimal storage operation is a difficult choice due to the unpredictability of future situations. Different techniques may be used to solve the economic dispatch problem of CHP units with energy storage [161][162].

2.5 Summary and Research Gap

This review chapter provides a thorough evaluation of the most current analyses of the many energy management techniques proposed for the microgrid, which include classical, heuristic, and intelligent algorithms, as well as their pros and cons. It consists of a brief introduction to the architecture of microgrids, as well as different classifications within the components of the microgrid, communication technologies that are used, and auxiliary services required in microgrids. It examines the most critical applications in energy management, such as forecasting, demand response, data processing, and the control framework, among others. Furthermore, this review provides an overview of research topics in which the scope of study and the contribution of research to energy management are still in their nascent stage.

The topics covered in this chapter include optimization techniques for energy management systems in the operation of microgrids, which provides a comprehensive evaluation of the latest advances in numerous areas. Researchers looked at the effects of new technologies on the existing infrastructure, technological solutions to allow the integration of new, and the control of new technologies in particular. A survey of the available research work on central and distributed energy management using varied microgrid EMS techniques was also reviewed. The literature review also revealed several papers that have considered the control of microgrids in combination with one or more

components using multi-agent-based optimization approaches, metaheuristic methods, programming-based methods, stochastic-based methods, linear and non-linear-based and reinforcement learning approaches. Based on the surveyed literature, the following research gaps have been identified.

1. The use of the LSTM-MILP-RH approach considering online and offline implementation for real-time operation of the PV-BESS based grid-connected microgrid has not been reported in literature to solve economic dispatch problems in grid-connected microgrids.
2. The control of the BESS in such a way the charge/discharge cycle can be limited to reduce age degradation using MILP has also not been explored in literature
3. The real-time control of the BESS in a grid-connected microgrid comprising CHP units for behind-the-metre applications has not been reported. The difficulty of this application is that the CHP must constantly run over a certain threshold to prevent engine damage and excessive emissions. As a result of limits imposed by network operators, no electricity should be injected into the grid.
4. Lack of analysis of the impact of the TOU and standard tariff schemes affects the optimal operation of a PV-BESS based microgrid system in terms of the optimal operating cost and limiting of the BESS charge/discharge cycle and utilisation of the BESS system.

Chapter 3

A Real-Time EMS for Controlling BESS in a Grid-Connected Microgrid using MILP

3.1 Introduction

This chapter presents an EMS for battery storage systems in grid-connected microgrids. The battery charge/discharge power minimises the overall energy consumption cost, considering the variation in grid tariff, renewable power generation and load demand. The system is modelled as an economic load dispatch optimization problem over a 24-hours horizon and solved using MILP. This formulation, therefore, requires knowledge of the expected renewable energy power production and load demand over the next 24 hours. An LSTM neural network is proposed to achieve this. The RH strategy is suggested to reduce the impact of prediction error and enable real-time implementation of the EMS that benefits from using actual generation and demand data on the day. At each hour, the LSTM predicts generation and load data for the next 24 hours, the dispatch problem is then solved, and the battery charge/discharge command for only the first hour is applied in real-time. Real data is then used to update the LSTM input, and the process is repeated.

To evaluate the proposed approach, the daily operating cost is compared against a reference benchmark. The proposed MILP-LSTM optimization framework is executed in two different scenarios:

- Online Optimization - Execution every hour in real-time using a receding horizon of 24 hours.
- Offline Optimization – Execution once a day using a single set of LSTM predicted data with no RH strategy.

Simulations have been carried out for different operating conditions covering a period of 12 months.

3.2 Optimal Operation of Battery using MILP

A schematic of the grid-tied microgrid under study is shown in **Error! Reference source not found.**. The main components of the hybrid system are the PV, BESS and local load. The power flow within the microgrid is illustrated in Figure 3-2. The grid connection is represented in the first node, and the imported power from the grid is used to charge the BESS in the third node and directly supply the load demand in the fourth node. The second node is the PV supply source, which can also be used to charge the BESS and supply the load demand. The energy demand at all times is met by a combination of power from the PV, BESS and the grid, as described in equation (3-1):

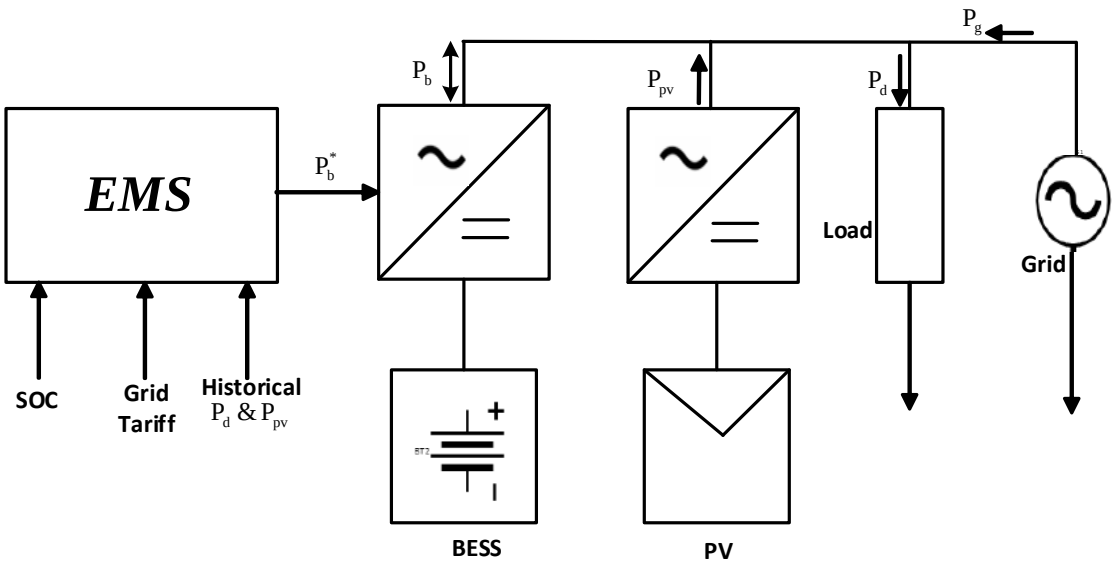

Figure 3-1: Schematic Diagram of the Microgrid System with an EMS

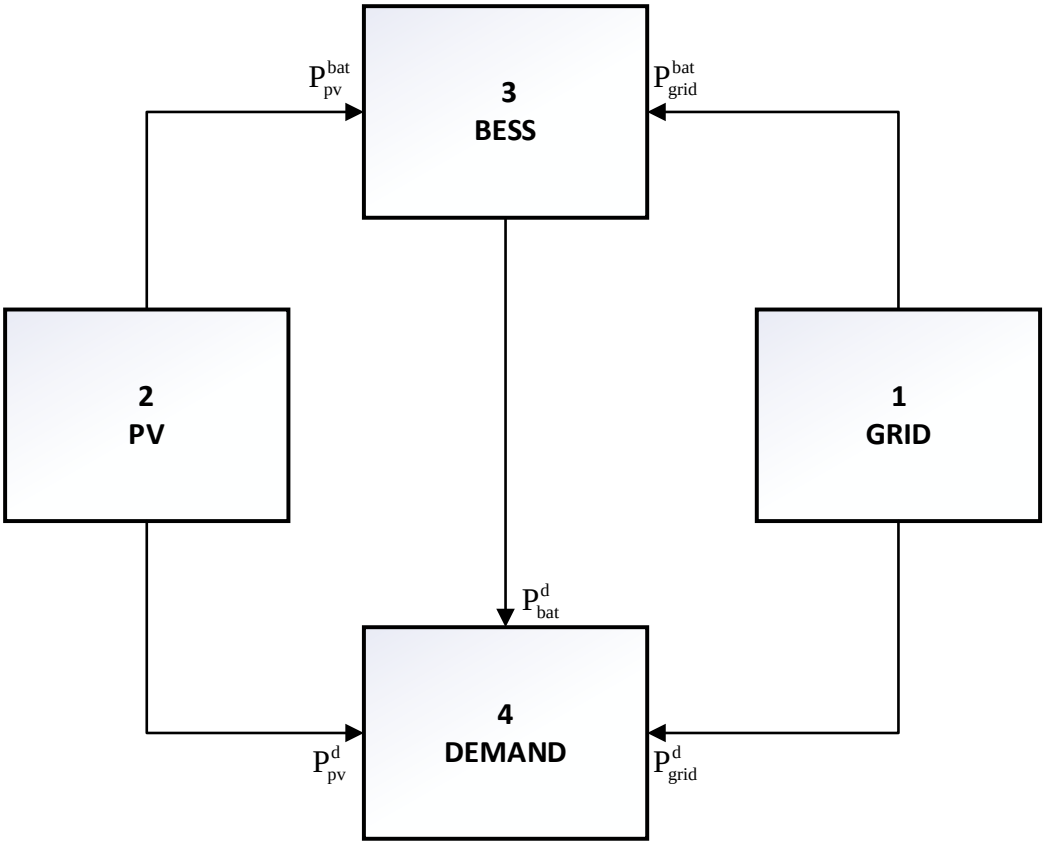

Figure 3-2: Grid Connected Microgrid Model with Power Flow Possibilities.

$$P_d(t) = P_{pv}(t) + P_g(t) + P_b^d(t) - P_b^{ch}(t), \quad (3\text{-}1)$$

The PV generation should supply the energy demand. When it is insufficient, additional power is imported from the BESS and/or the grid depending on the SoC and the grid tariff. It assumed that this is a grid-tied system and power cannot be exported to the grid, which means in the case of a surplus generation, when the BESS is fully charged, the surplus generation is dumped.

3.2.1 The MILP Formulation

The MILP is formulated to solve the economic dispatch problem to find the minimum operational cost while satisfying the load demand and respecting imposed constraints. The MILP economic dispatch problem solution results in the optimal power flow through each connection for each time step in the optimization horizon [163]. The MILP formulation is carried out in MATLAB (MATrix

LABoratory), a proprietary multi-paradigm programing language and numeric computing environment developed by MathWorks, which allows data implementation of algorithms. Figure 3-3 shows the flow chart used for the implementation of the MILP algorithm in MATLAB environment

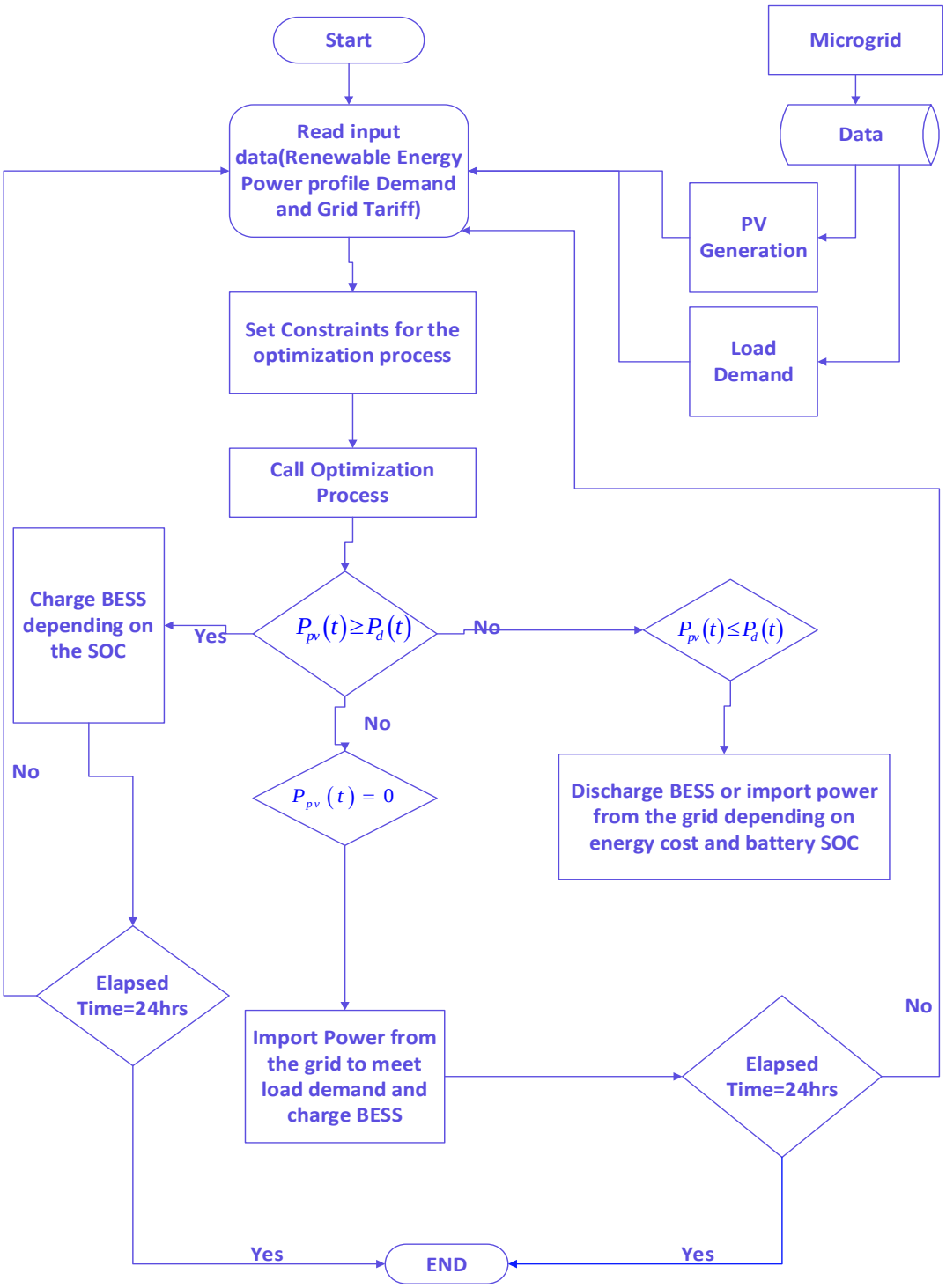

Figure 3-3: Flow Chart for the EMS implementation using MILP

To formulate the microgrid scheduling problem base on the flow chart in Figure 3-3, the cost function associated with the MILP and the constraints are defined in equation (3-2) as:

$$\begin{aligned} &\min Z = \sum_{t=0}^{T}\sum_{i=1}^{N} C(P_{gr}(i,t)), \\ &\text{subjected to:} \\ &\sum_{t=0}^{N} P_{gr}(i,t) = P_d(t) \in \vartheta(i), \end{aligned} \tag{3-2}$$

where Z is the objective function, N is the number of generators in the power system, $C(P_{gr}(i,t))$ is the cost of the generated power by P_{gr} and $\vartheta(i)$ represents the set of constraints for P_{gr}. The selected optimal solution is implemented on the system equations, and the system response, such as the BESS state of charge and charge/discharge power is measured [50]. The decision variables for the economic dispatch problem are presented in Table 3-1.

Table 3-1: Decision and binary variables of the economic dispatch problem

Decision variable	Variable Type	Description
$P_{grid}^{d}(t)$	Continuous	Power from the Grid to the Load
$P_{grid}^{bat}(t)$	Continuous	Power from the Grid to the BESS
$P_{pv}^{d}(t)$	Continuous	Power from PV to the Load
$P_{pv}^{bat}(t)$	Continuous	Power from PV to BESS
$y_{bat}^{ch}(t)$	Binary	On/off state of the BESS charge
$y_{bat}^{d}(t)$	Binary	On/off state of the BESS discharge
$\alpha(t)$	Binary	Variable for the charging state of the BESS

The charge/discharge powers from the BESS are calculated in the decision variables, while the state of charge is considered as the system state. For each time step, the total energy of the microgrid system is defined as $P_{gr}(t)\times\Delta t$. It is important that the optimization process does not schedule BESS charge and

discharge simultaneously. Therefore, an inequality constraint is formulated as an integer in equation (3-3).

$$y_{bat}^{ch}(t)+y_{bat}^{d}(t)\le 1, \tag{3-3}$$

$$\left.\begin{aligned} P_{bat}^{d}(t) &\le P_{bat}^{d\,max}\times y_{bat}^{d}(t) \\ P_{bat}^{ch}(t) &\le P_{bat}^{ch\,max}\times y_{bat}^{ch}(t) \end{aligned}\right\}, \tag{3-4}$$

The power imported from the grid is formulated as:

$$P_{grid}(t)\le P_{grid}^{max}. \tag{3-5}$$

The grid and PV powers can charge the BESS and feed the load at any time. The flow in the network considers the storage capabilities of the BESS and the possible curtailment of the PV or dumbing of excess PV generation when the BESS is fully charged. This is represented by the node balance constraints given in as:

$$P_{grid}(t)=P_{grid}^{d}(t)+P_{grid}^{bat}(t), \tag{3-6}$$

$$P_{pv}(t)\ge P_{pv}^{d}(t)+P_{pv}^{b}(t), \tag{3-7}$$

$$P_{bat}^{ch}(t)=P_{grid}^{bat}(t)+P_{pv}^{bat}(t), \tag{3-8}$$

$$P_{bat}^{d}(t)=P_{d}(t)-P_{pv}^{d}(t)-P_{grid}^{d}(t), \tag{3-9}$$

Whenever the PV system produces power greater than the load demand, the excess power is utilized in charging the BESS, depending on the SoC. The inequalities in equation (3-10) show that the power from the grid and the PV can only be positive parameters, represented as:

$$\left.\begin{aligned} P_{grid}(t)\ge 0,\ P_{pv}(t)\ge 0 \\ P_{pv}^{bat}(t)\ge 0,\ P_{grid}^{bat}(t)\ge 0 \end{aligned}\right\}, \tag{3-10}$$

The SoC of the BESS must be kept within safety limit that is defined based on the minimum and maximum SoC of the BESS given in equation (3-11).

$$\beta_{soc}^{min} \le \beta_{soc}(t) \le \beta_{soc}^{max}, \quad (3\text{-}11)$$

To enforce (3-11) further constraints are developed in (3-12) and (3-13) relating the SoC to the capacity of the BESS, and the power flows to and from the battery as:

$$\delta_c \beta_{soc}(t) + P_{bat}^{ch}(t)\eta_c \Delta t - P_{bat}^{d}(t)\eta_d \Delta t \le \delta_c \quad (3\text{-}12)$$

$$\delta_C \beta_{soc}(1) = \delta_{ESB} \quad (3\text{-}13)$$

where, η_d and η_c are the charge/discharge efficiencies of the BESS, respectively. Considering (3-12) and (3-13) the SoC difference equation can be written as:

$$\beta_{soc}(t+1) = \beta_{soc}(t) - \phi P_{bat}^{d}(t) \times \eta_d(t) + \phi P_{bat}^{ch}(t) \times \eta_c(t) \quad (3\text{-}14)$$

where, ϕ is the coefficient that converts the BESS charge/discharge power to the charging unit in percentage.

The important factor here is the SoC which is modelled based on equations (3-11) and (3-12). In this study, we consider that the BESS consists of a lead-acid battery, and hence it should be charged fully after a full discharge cycle. This is to prevent the fast rate collapse of the battery voltage during discharge events. The BESS is charged and discharged subjected to maximum charging/discharging rates P_{bch}^{max} and P_{bd}^{max}. The BESS discharge rate will also not exceed the demand due to constraints in equation (3-1). To limit the charge/discharge cycle of the BESS using a predetermined constant K, additional binary integer variables and constraints are introduced based on the BESS technology. First, we define α to be a binary integer variable that

represents the charging state of the BESS. The value of α is 0 when $P_{bat} \geq 0$ (i.e., the BESS is charging) and α is 1 when $P_{bat} \leq 0$ (i.e. the BESS is discharging). We then define an additional binary integer variable at each time-step: The binary integer variable is equal to 0 if $\alpha(t)$ and $\alpha(t-1)$ are the same and 1 if they are different, thereby representing a change in the state of the BESS. The constraints for the implementation of the limits on the charge/discharge cycle of BESS can be summarised as (3-15)–(3-19), given by:

$$\lambda(t) \leq \alpha(t) + \alpha(t-1), \quad (3\text{-}15)$$

$$\lambda(t) \geq \alpha(t) - \alpha(t-1), \quad (3\text{-}16)$$

$$\lambda(t) \geq \alpha(t-1) - \alpha(t), \quad (3\text{-}17)$$

$$\lambda(t) \leq 2 - \alpha(t) - \alpha(t-1), \quad (3\text{-}18)$$

$$\sum_{t=1}^{T} \lambda(t) \leq K, \quad (3\text{-}19)$$

The cost of energy for each time step C_{PTS} can be calculated within the constraints using equation (3-20):

$$C_{PTS} = \left(P_{grid}(t)\Delta t\right) \times T_{grig}(t), \quad (3\text{-}20)$$

where, $P_{grid} = P_{grid}^{d} + P_{grid}^{bat}$ and it is the power utilized from the grid based on the optimal schedule of the microgrid using the RH control strategy, as explained in section 3.3. Since the main objective of this research is to minimize operational cost, ensure the safe operation of the BESS and promote self-consumption, the objective function is formulated as an economic dispatch problem in equation (3-21) as:

$$\min Z = \sum_{t=1}^{T} P_{grid}(t) \times T_{grid}(t), \quad (3\text{-}21)$$

subject to (3-1), (3-3) – (3-19) as constraints.

3.2.2 LSTM Prediction Networks

In this section, LSTM-based deep learning is used for predicting the load demand and the PV generation for the future, considering one year of historical data from the Ushant Island in France[164]. LSTM networks are a type of recurrent neural network with modules typically referred to as cells rather than neurons and contain a series of gates. Each LSTM cell has a form of longer-term memory in the form of a cell state that is updated through time [165]. The LSTM model is trained with root-mean-squared error (RMSE) loss function, Adam optimizer and 300max epoch with a single gradient threshold. RMSE indicates the deviation between the predicted and measured values, and it measures the forecasting error [166]. The PV generation and load demand are predicted for the last day of each month of the year, considering the days before as the trained historical data. Before training or testing a neural network, the training and testing data must go through a series of pre-processing steps. Normalization was applied here as the pre-processing method, which reduces the effect of different scaling of the collected data, including interpolating any missing data points and organizing the data (historical PV generation and load demand) in a chronological form.

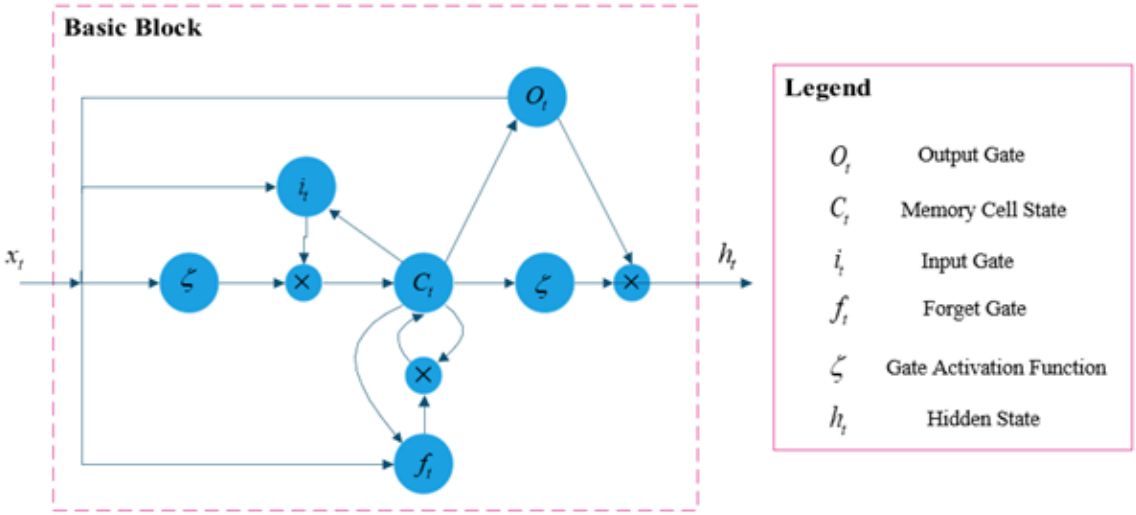

Figure 3-4: The LSTM block diagram

Figure 3-4: shows the architecture of the LSTM network with the input gate, output gate, forget gate, gate activation function, memory cell state C_t and the hidden state h_t. The input gate controls the extent to which a new value flows into the cell and receives the input sequence in which the activation units are used to trigger the gates at each time step. The input gate, output gate, and forget gate are used to manage the reading or updating of the memory cell. The LSTM operation can be expressed mathematically as follows:

$$\left.\begin{aligned} f_t &= \sigma_g\left(W_{fX_t} + W_{fh_{t-1}} + W_{fc_t} + b_f\right) \\ i_t &= \sigma_g\left(W_{iX_t} + W_{ih_{t-1}} + W_{ic_t} + b_i\right) \\ o_t &= \sigma_g\left(W_{oX_t} + W_{oh_{t-1}} + W_{oc_t} + b_o\right) \\ c_t &= f_{tc_{t-1}} + i_t tanh\left(W_{cX_t} + W_{ch_{t-1}} + W_{oc_t} + bc\right) \\ h_t &= o_t tanh\left(c_t\right) \end{aligned}\right\}. \quad (3\text{-}22)$$

where W are weights of the LSTM model that can be learned in the training stage and σ_g is the activation function.

A suitable metric for evaluating the performance of the LSTM is the root mean square error (RMSE), the RMSE indicates the deviation between the predicted value and the actual measured value, and it is a measure of the forecasting error

[1]. The lower the value of the RMSE, the better the performance. The RMSE is calculated using the following equation:

$$\mathrm{RMSE} = \sqrt{\sum_{k=1}^{K} \frac{\left(P_v - A_v\right)^2}{K}} \tag{3-23}$$

where P_v and A_v are the predicted value and the actual value, respectively, and K is the number of time slots.

Various performance indices are used to quantify and evaluate the error between the desired and the predicted value, which are the mean absolute error (MAE), and the mean absolute percentage error (MAPE). These performance indices are computed using the following equations respectively [2].

$$\mathrm{MAE} = \sum_{k=1}^{K} \frac{\left(P_v - A_v\right)^2}{K} \tag{3-24}$$

$$\mathrm{MAPE} = \sum_{k=1}^{K} \frac{\left(P_v - A_v\right)}{K} \tag{3-25}$$

The normalized data is then used as an input to the LSTM network. The initial predicted PV output power and load demand for the last day of January, May, August, and November representing the year's four seasons, are shown in Figures 3-6, respectively, with the RMSE indicating the accuracy of the predictions. To forecast the values of future time steps of the sequence, the training sequence with values shifted by one-time step is specified as the response. This means that at each time step of the input sequence, the LSTM network learns to predict the value of the next time step. To predict the next timestep, the previous prediction is used as an input to the function [167]. The result of the prediction is presented in Figures 3-5a-3-5d for the PV generation and Figures 3-6a-3-6d for the load demand. It is worth noting that the prediction

is repeated in every time-step using the receding horizon control strategy. Therefore Figures 3-5 and 3-6 represent the initial prediction.

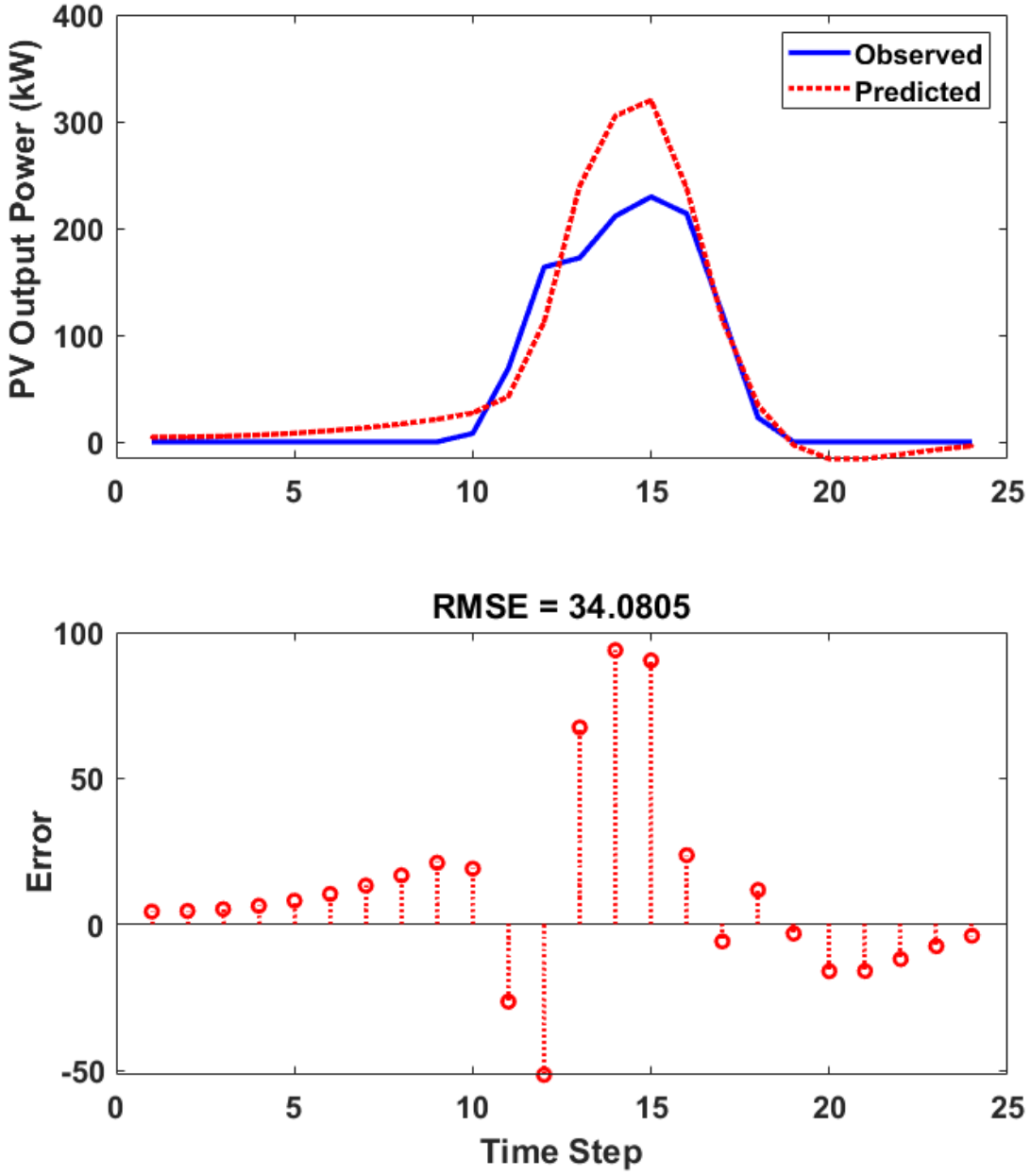

Figure 3-5a: Real and predicted Ushant Island PV data (from the LSTM prediction network for January)

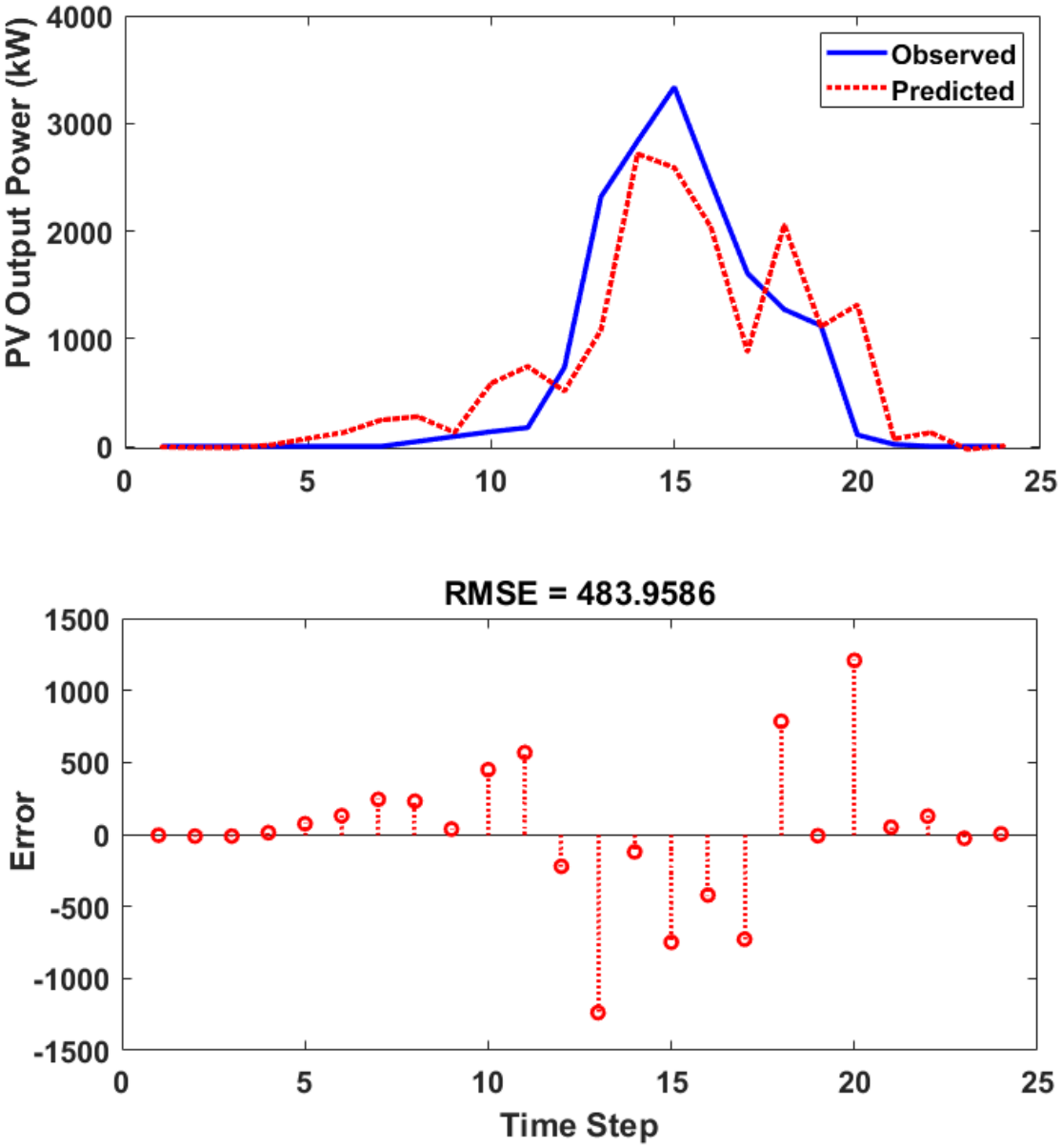

Figure 3-5b: Real and predicted Ushant Island PV data (from the LSTM prediction network for May)

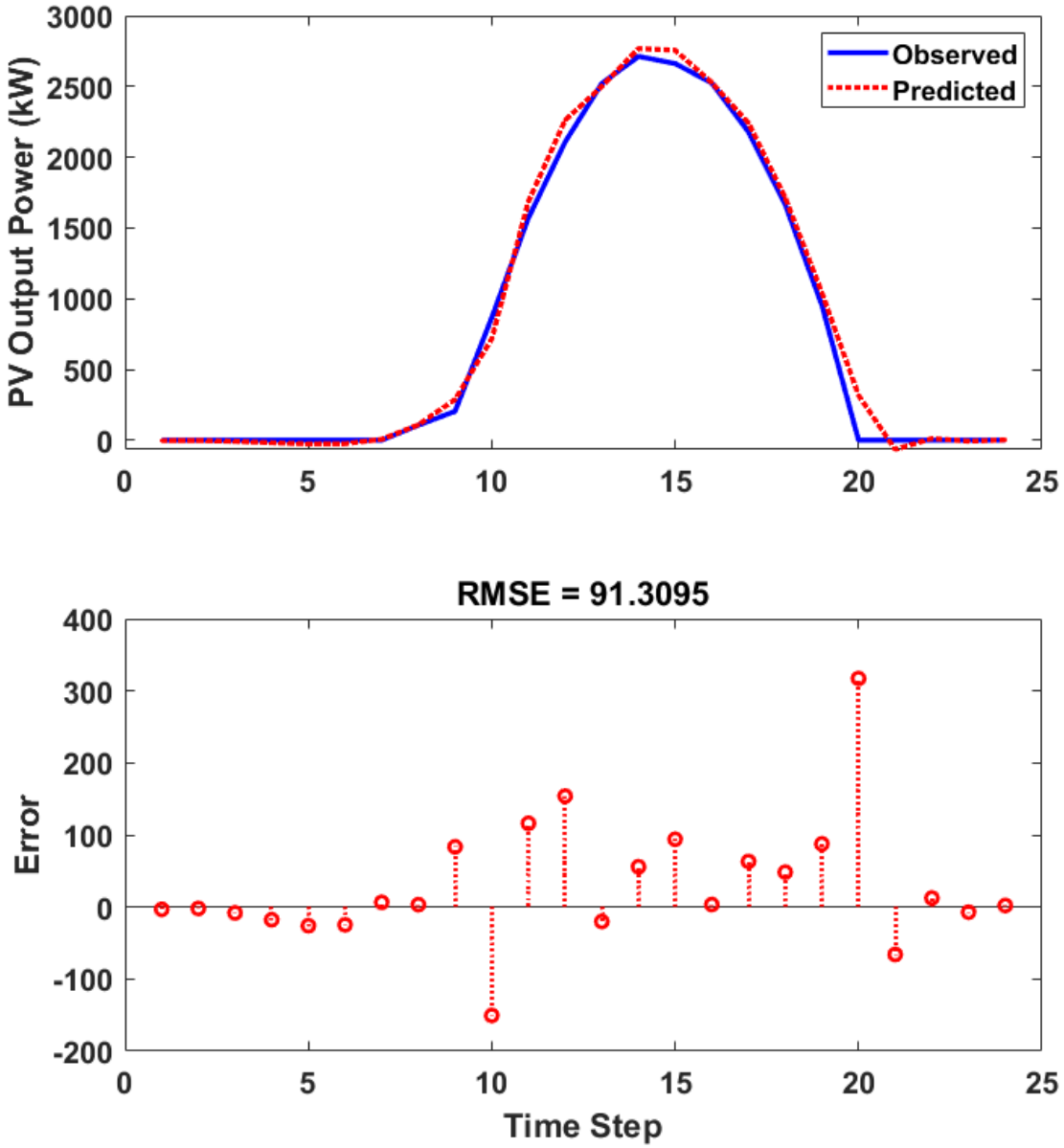

Figure 3-5c: Real and predicted Ushant Island PV data (from the LSTM prediction network for August)

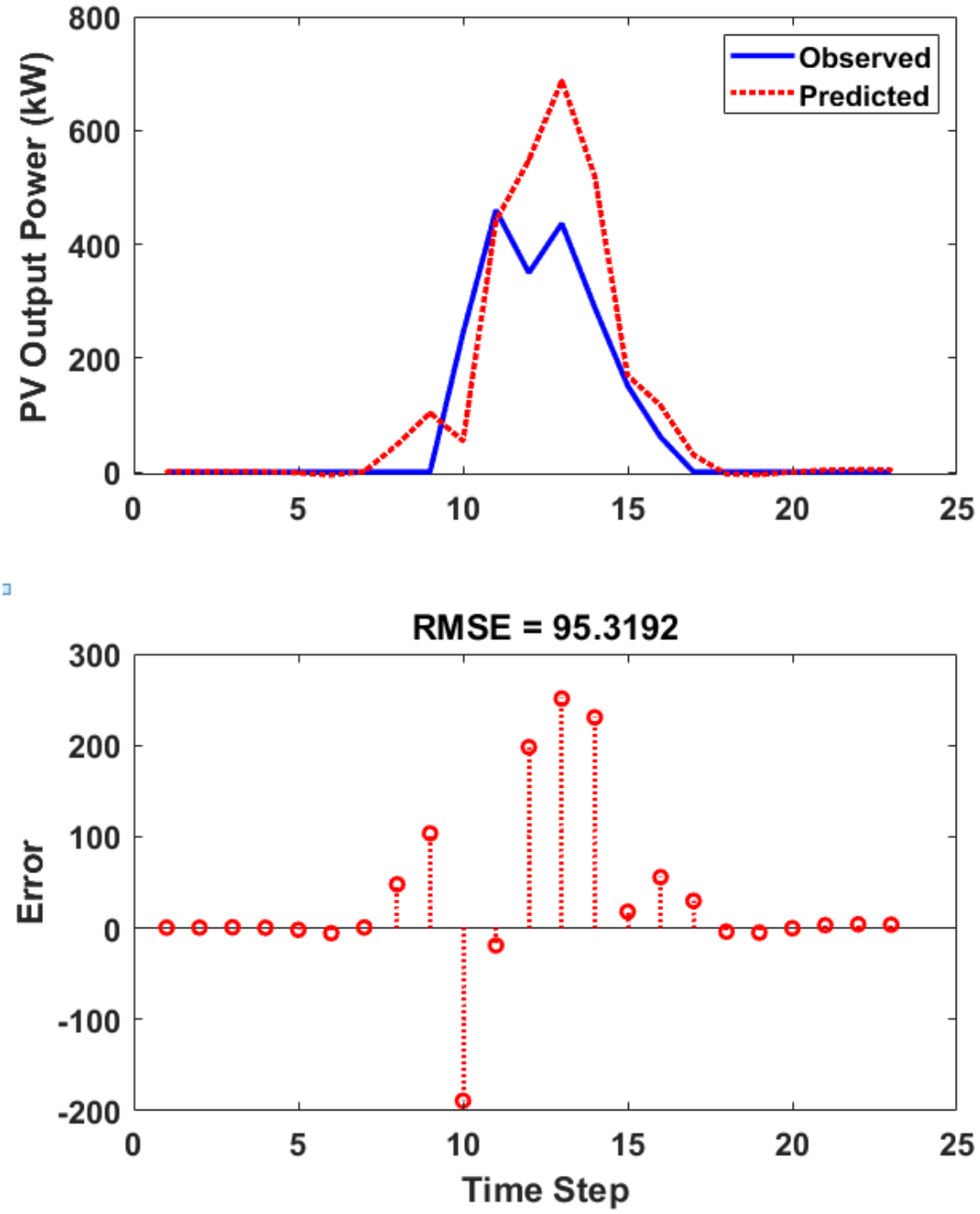

NOVEMBER

Figure 3-5d: Real and predicted Ushant Island PV data (from the LSTM prediction network for November)

The figures above represent the real and predicted PV generation for the four seasons of the year, with the RMSE select as the suitable metric for evaluating the predictor's performance. In this case, since the data are for different months of the year using the same predictor, the comparison of the value of the RMSE

for the different months will not be necessary as it is of no advantage. The value of the RMSE is always nonnegative, and it indicates the accuracy of the prediction. As a result of the intermittent nature of the solar PV generation, the RMSE will vary for different months of the year.

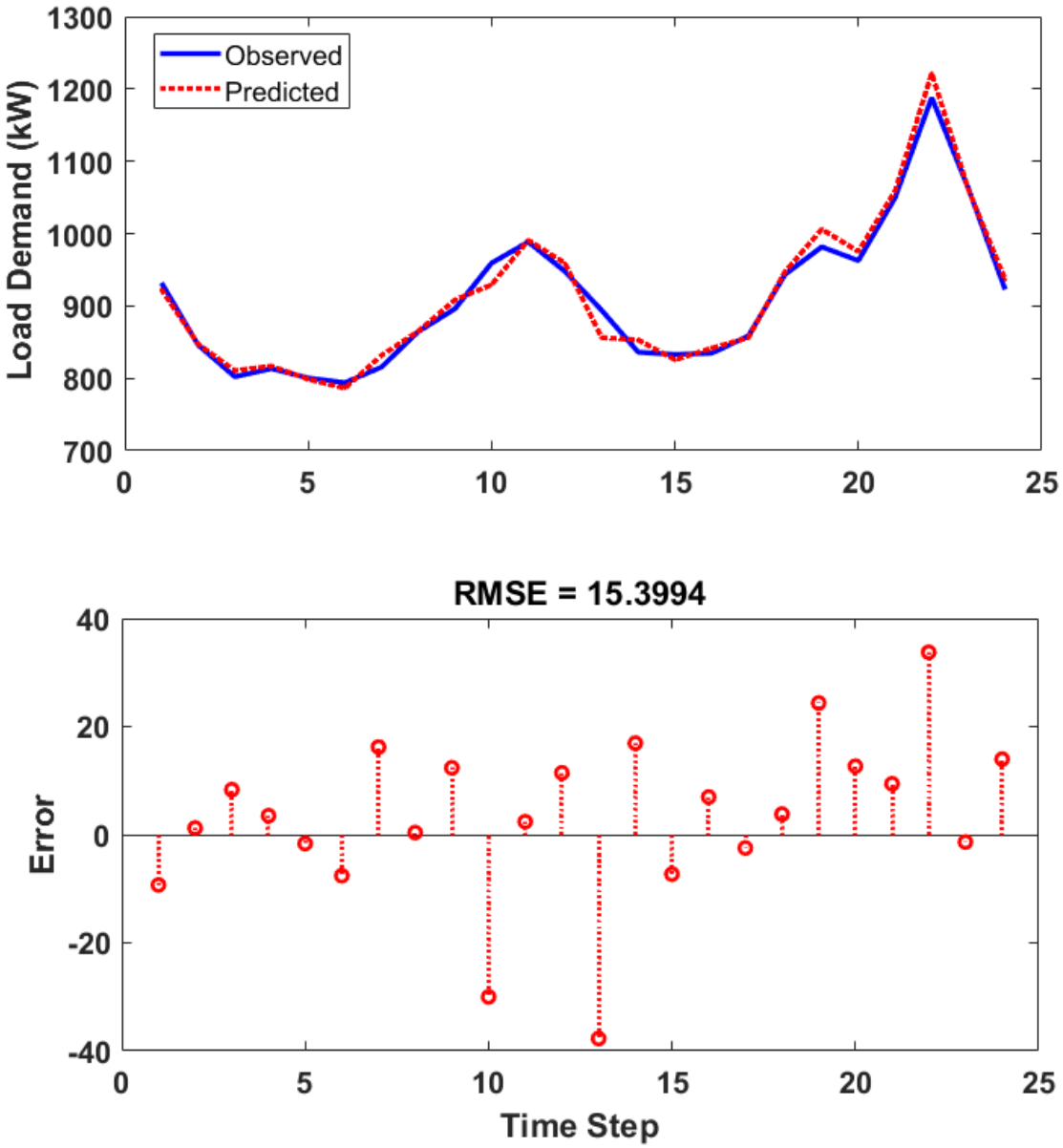

Figure 3-6a: Real and predicted load demand (from the LSTM prediction network for January)

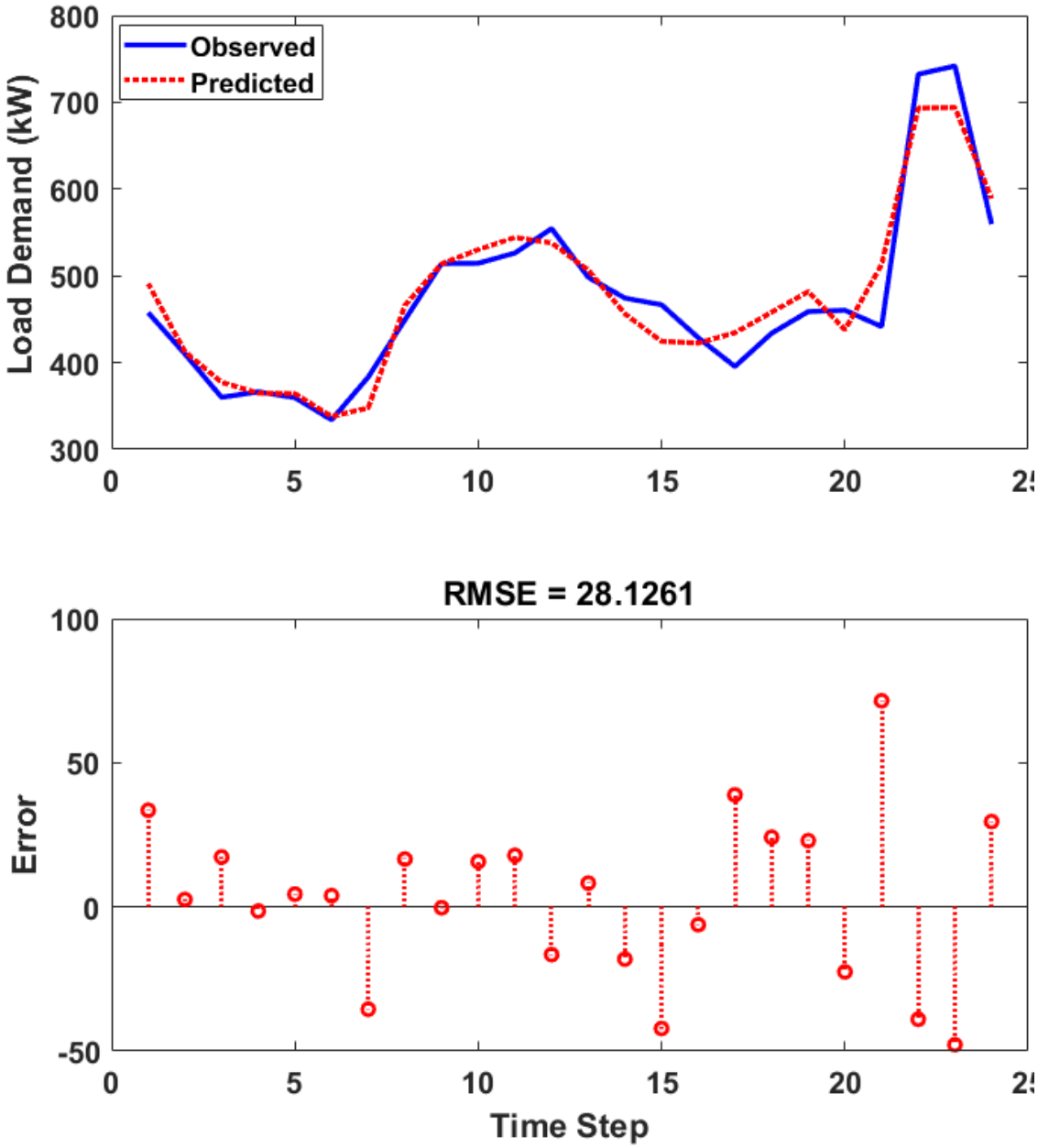

Figure 3-6b: Real and predicted Ushant Island load demand (from the LSTM prediction network for May)

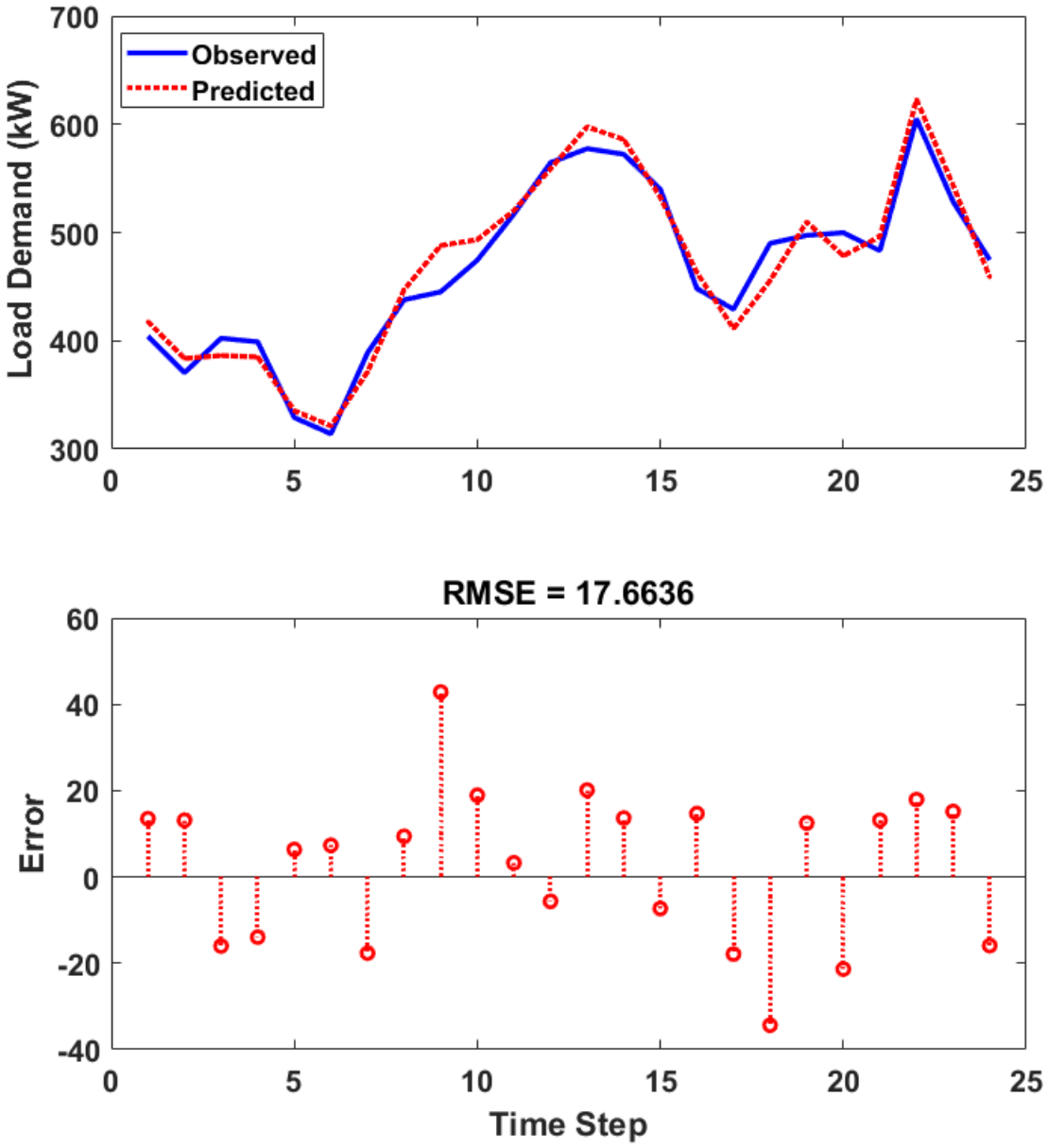

Figure 3-6c: Real and predicted Ushant Island load demand (from the LSTM prediction network for August)

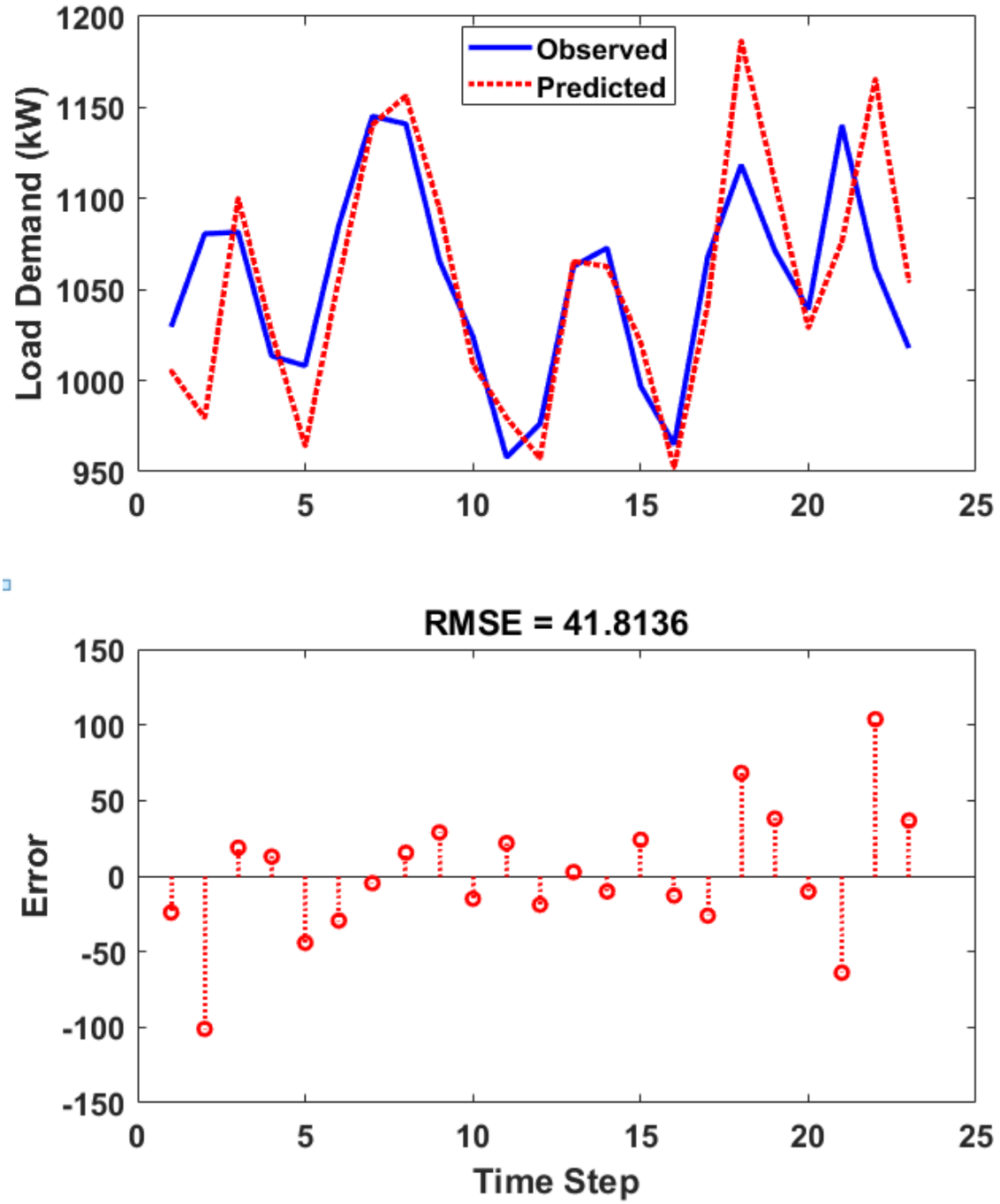

Figure 3-6d: Real and predicted Ushant Island load demand (from the LSTM prediction network for November)

Because of the certainty of the load demand, the prediction is easier and more accurate to predict when compared to the PV generation. The values of the RSME are relatively lower for Figures 3-6a-3-6d when compared to Figures 3-5a-3-5d.

3.3 Receding Horizon Control

The RH strategy is a concept adopted from the model predictive control (MPC), which solves the RH control by using online model-based optimization to determine the current control action [168]. It is a general-purpose control scheme that involves repeatedly solving a constrained optimization problem, using predictions of future generation and demand over a moving time horizon to choose the control action. The RH control handles constraints, such as limits on control variables, directly and naturally, and generates precisely calculated control actions, respecting the constraints.

The basic RH policy is very simple. At time *t*, we consider an interval extending *T* steps into the future: *t*, *t* + 1, . . ., *t* + *T* as shown in Figure *3-7*. We then carry out several steps. This method can effectively correct errors in predicting renewable energy generation and load in future iterations for power system scheduling problems with high dependency on the forecasted values of renewable energy productions and demand [169]. At each hour, the economic dispatch of the battery is obtained using 24 hours data of predicted future renewable energy production and demand using the LSTM network, as explained in section 3.2.2. The optimisation outputs are 24 hours of dispatch commands as summarized using the matrix in equation (3-26).

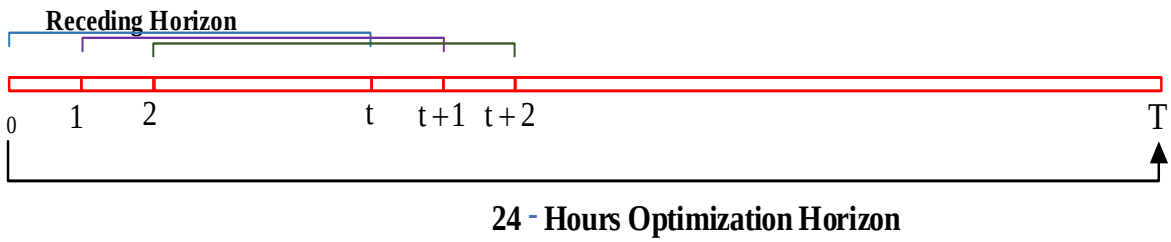

Figure 3-7: Illustration of the RH control strategy.

$$\begin{bmatrix} P^{d}_{grid}(1) & P^{d}_{grid}(2) & P^{d}_{grid}(3) & \cdots P^{d}_{grid}(T) \\ P^{bat}_{grid}(1) & P^{bat}_{grid}(2) & P^{bat}_{grid}(3) & \cdots P^{bat}_{grid}(T) \\ P^{d}_{pv}(1) & P^{d}_{pv}(2) & P^{d}_{pv}(3) & \cdots P^{d}_{pv}(T) \\ P^{bat}_{pv}(1) & P^{bat}_{pv}(2) & P^{bat}_{pv}(3) & \cdots P^{bat}_{pv}(T) \end{bmatrix} \quad (3\text{-}26)$$

Here, only the dispatch commands for the next hour (the first column of the matrix is implemented in real-time, and the rest are discarded).

The generation and demand input data to the LSTM is updated to include that of the generation and demand at the current hour t. The LSTM is then used to predict data for the next 24 hours, and the process is repeated in real-time for each time step. If the time step Δt is one hour, the algorithm is repeated $T/\Delta t$ times, representing the number of time steps ω for 24 hours of the day. The RH final solution is the optimal schedule of the renewable energy source and the grid power for supplying the load and charging the BESS.

The RH control strategy allows for the improvement of the forecasting errors for each iteration of the economic dispatch problem since the feasibility of economic dispatch and optimality depends on the accuracy of prediction of the renewable generation in power systems [50].

3.4 Simulations and Results

To solve the optimization problem, a case study is developed considering data from the Ushant Island project in France under the intelligent community energy (ICE) program to test the proposed approach for the real-time operation of the microgrid energy sources. The proposed energy management system simulation was performed in MATLAB. **Error! Reference source not found.** illustrates the Ushant Island model with the following parameters 3-MW PV system, Grid

connection and 2400-kWh BESS capacity. The daily ToU electricity tariff rate is shown in Table 3-2. The characteristics of the BESS, such as the capacity, the SoC limits or bounds and the Initial SoC, are shown in Table 3-3.

Table 3-2: Daily TOU electricity tariff

Off-peak time	22:00-5:00	0.05 £/kWh
Mid-peak time	12.00-17.00	0.08 £/kWh
Peak time	6.00 -11.00 18.00-21.00	0.17£/kWh

Table 3-3: Characteristics of the lead-acid battery package

Rated Depth of Discharge (DOD) %	50
Maximum charging power (kW)	300
Battery charge efficiency (%)	95
Battery discharge efficiency (%)	95
Maximum State of Charge (%)	100
Nominal Battery Capacity @ 100% SoC (kWh)	2400

To evaluate the proposed real-time energy management of the Microgrid, the simulation was carried out considering two scenarios. For the first scenario, as seen in the EMS flow model in Figure 3-8, the optimization is performed in real-time considering the RH technique using the real-time and predicted data simultaneously, with the real-time data used to update the input of the LSTM. The optimal daily operating cost for the 24-hour horizon is recorded, while in the second scenario, it considers a day ahead offline optimisation using predicted data only, the BESS command is applied online with actual data, and the optimal daily operating cost is recorded.

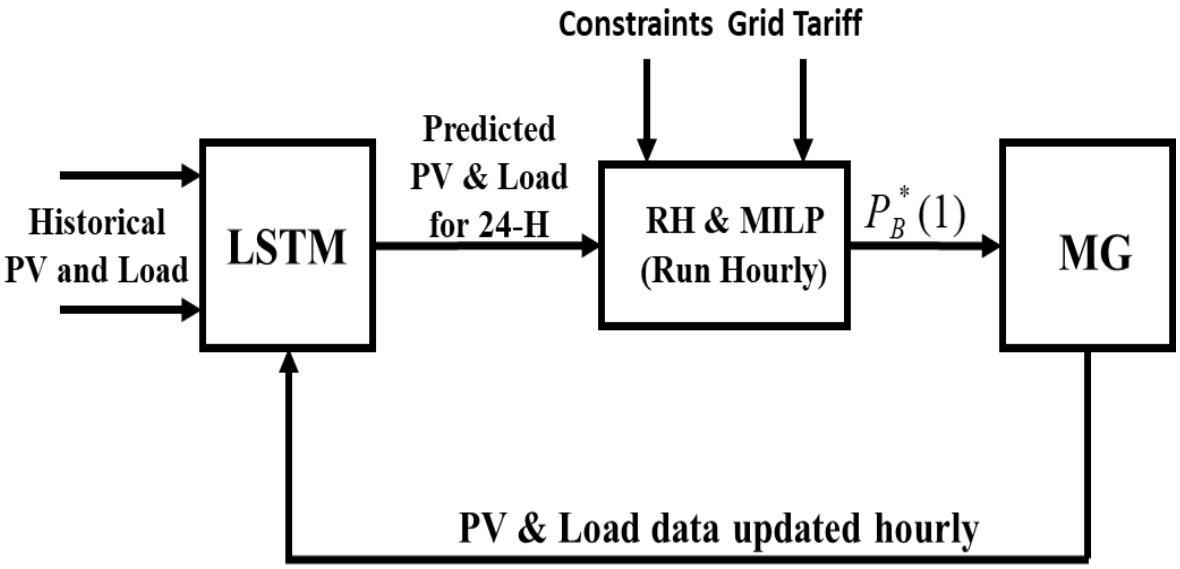

Figure 3-8: EMS flow model for scenario 1 (real-time operation with the RH control strategy).

The available historical data is utilized on a monthly basis by predicting the PV generation and load demand of the last day of every month. The BESS operation starts from its minimum SoC of 50% with a maximum charge/discharge power of 300 kW.

A day-ahead schedule based on an offline optimization is performed with the predicted PV power and load demand for the second scenario using the MILP optimization approach. The MILP module, as shown on the EMS flow model in **Error! Reference source not found.**, calculates the setpoints for the dispatchable resources 24 hours ahead based on predicted resources. The grid and the BESS are the dispatchable energy resources, meaning the power output can be controlled. At the same time, the PV system and the load demand are varying resources or non-dispatchable resources. The BESS command obtained from the offline day ahead optimization is implemented in real-time on real data, as shown in **Error! Reference source not found.**. The daily operating cost for the 24-hour horizon is calculated. To evaluate the effectiveness of the proposed

approach, the simulations were performed for the last day of every month, the monthly historical data was trained using the LSTM network, and the last day of the month was predicted. Both scenarios are tested every month, and the daily optimal operating cost is compared against a benchmark in which the forecasted data is the same as the actual data. This is a non-practical situation, but it will help us evaluate the effectiveness of the two scenarios.

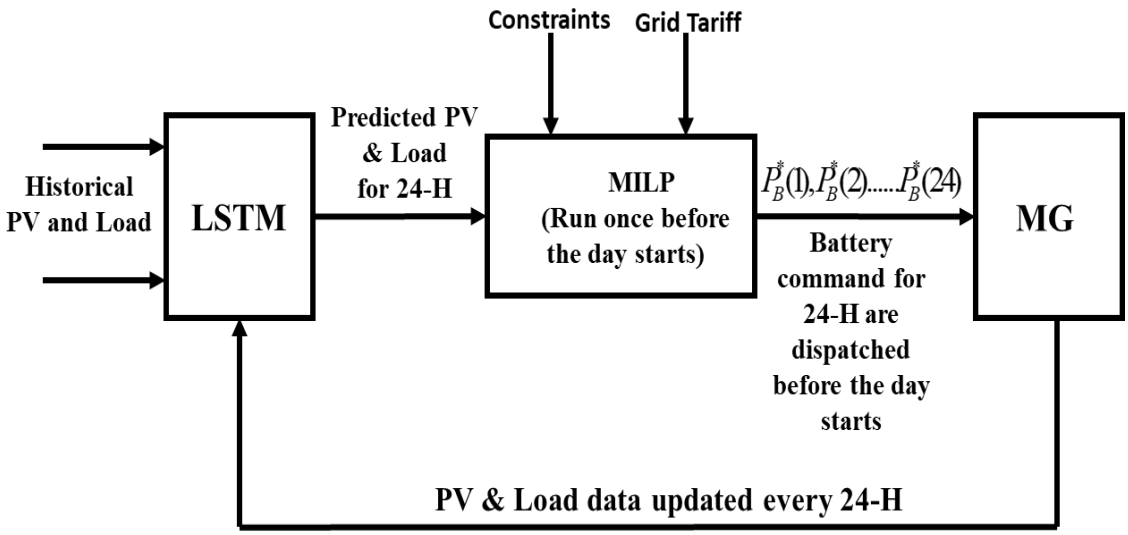

Figure 3-9: EMS flow model for scenario 2 (offline optimization using predicted data)

The results of the simulations for the microgrid dispatch limiting the BESS charge/discharge cycle to one every 24 hours for the value of K in equation (3-27) equal to three (3) for January, May, August and November, representing the four seasons of the year with background colours representing the TOU tariff regions are shown in Figure 3-10 - Figure 3-14 and Table 3-4. The results show that the operating cost of the proposed real-time strategy outperforms the offline optimisation strategy by 6.12%. Figure 3-14 shows the optimal cost comparison between the offline and online approaches with reference to the benchmark. The detail of the total percentage difference between the two scenarios and how close they are to the benchmark are shown in Table 3-4.

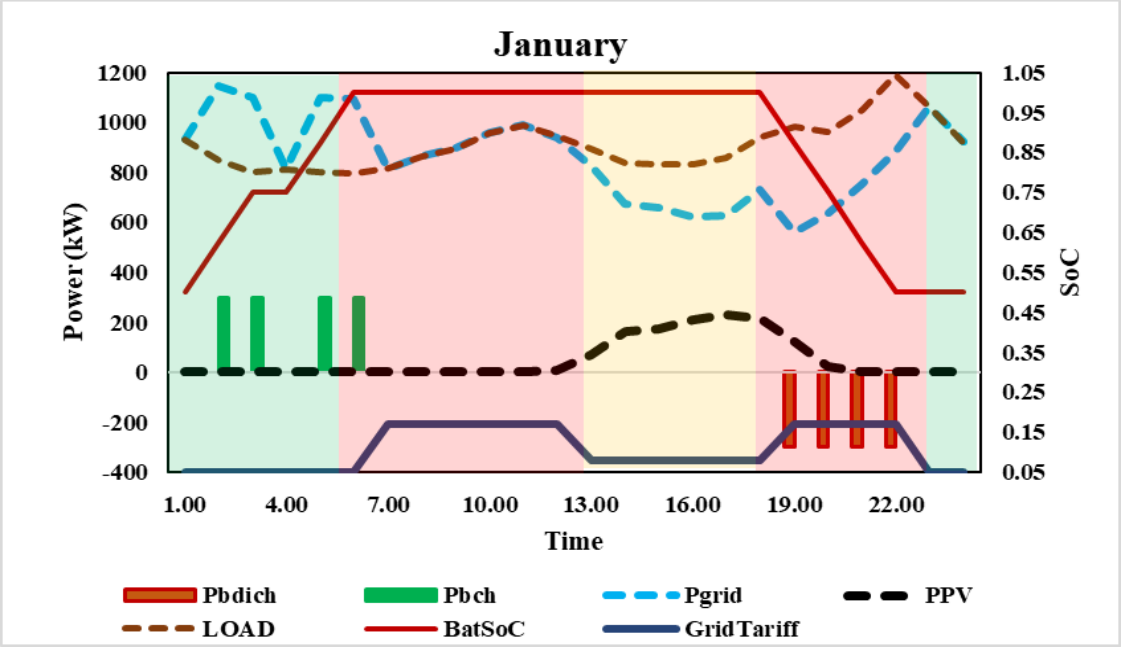

Figure 3-10: The microgrid dispatch for January for real-time operation of the Microgrid using RH control with the charge/discharge cycle limited to one cycle.

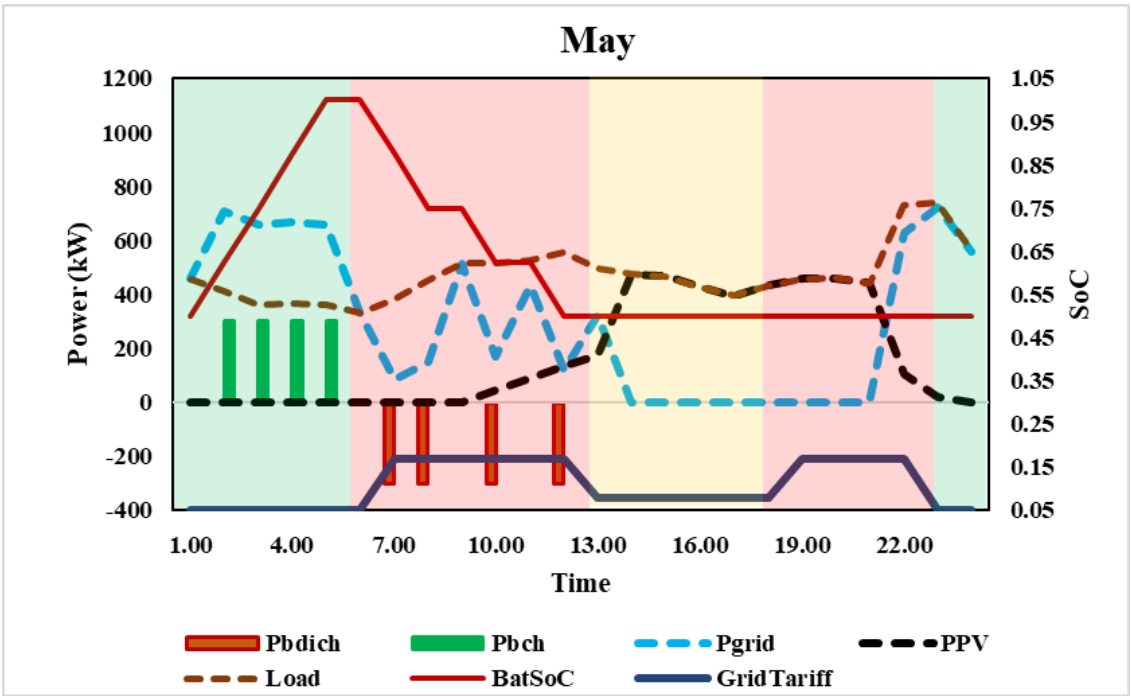

Figure 3-11: The microgrid dispatch for May for real-time operation of the Microgrid using RH control with the charge/discharge cycle limited to one cycle.

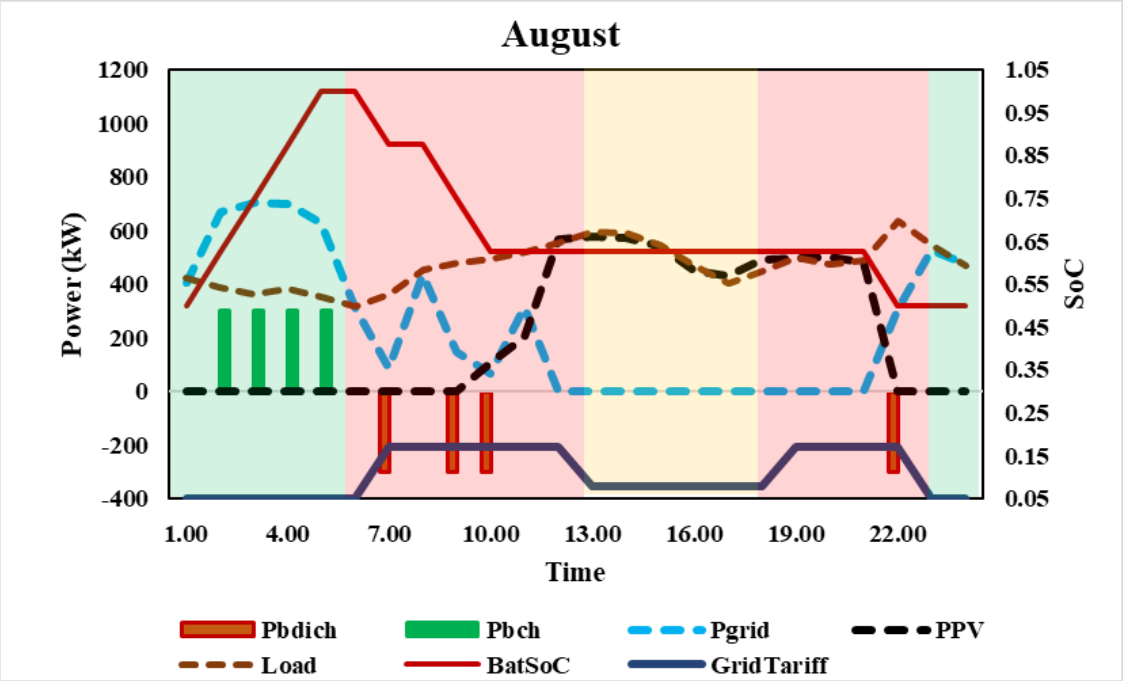

Figure 3-12: The microgrid dispatch for August for real-time operation of the Microgrid using RH control with the charge/discharge cycle limited to one cycle.

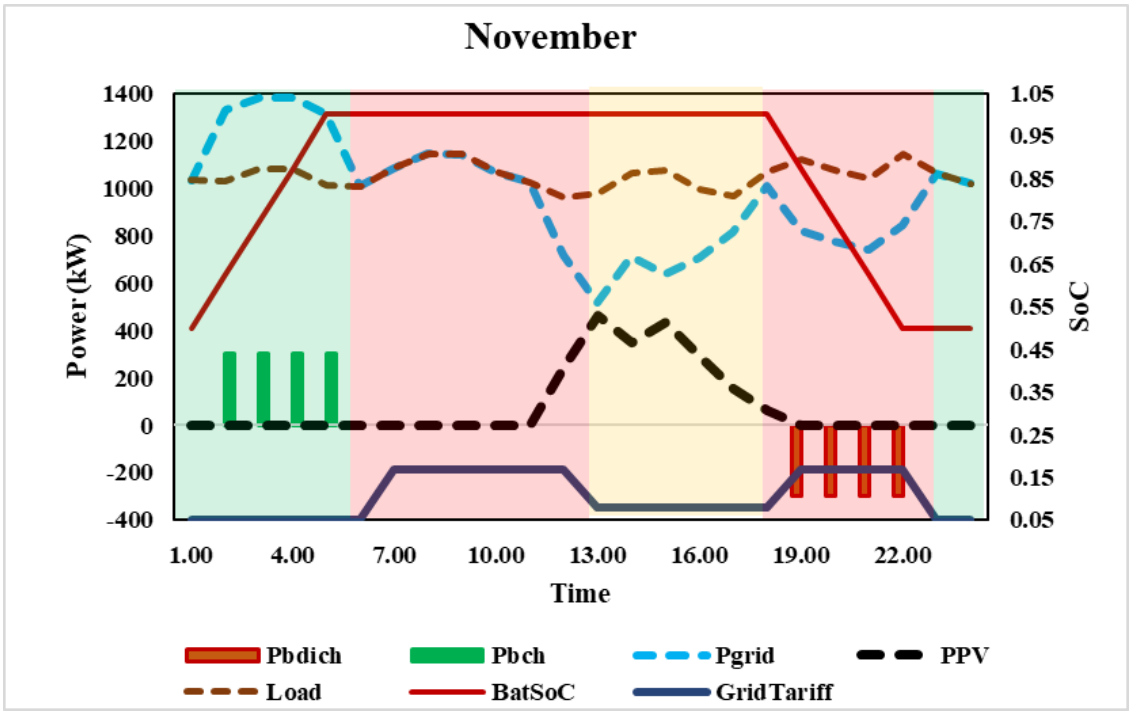

Figure 3-13: The microgrid dispatch for November for real-time operation of the Microgrid using RH control with the charge/discharge cycle limited to one cycle.

Figure 3-14 shows the daily optimal operating cost of the microgrid for the last day of every month of the year, for the benchmark, the real-time with RH control and the offline optimization using predicted data.

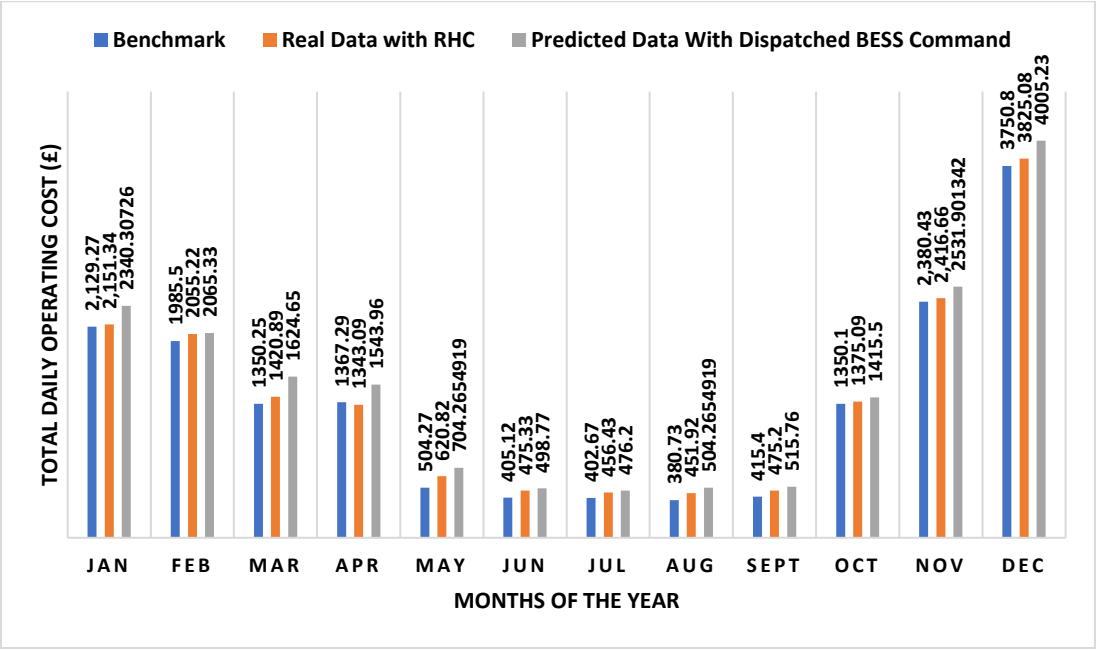

Figure 3-14: Optimal cost comparison between the benchmark, online and offline optimization

Table 3-4: Optimal cost comparison with average % difference between the two scenarios for K=3

Months	Optimal cost (£) (Benchmark)	Optimal cost (£) (Online Optimization)	Optimal cost (£) (Offline Optimization)	% Difference B/W the Two Scenarios
Jan	2,129.27	2,151.34	2,340.31	8.07
Feb	1,985.5	2,055.22	2,065.33	0.49
Mar	1,350.25	1,420.89	1,624.65	12.54
Apr	1,367.29	1,343.09	1,543.96	13.01
May	504.27	620.82	704.27	11.85
Jun	405.12	475.33	498.77	4.70
Jul	402.67	456.43	476.2	4.15
Aug	380.73	451.92	504.27	10.38
Sep	415.4	475.2	515.76	7.86
Oct	1,350.1	1,375.09	1,415.5	2.85
Nov	2,380.43	2,416.66	2,531.90	4.55
Dec	3,750.8	3,825.08	4,005.23	4.50
Total Cost	16,421.83	17,067.07	18,226.14	
% Closeness to the benchmark		**3.78**	**9.90**	
Total Cost % Difference B/W the Two Scenarios				**6.12**

To validate the outcome of the BESS charge/discharge limiting algorithm, further simulation is carried out, limiting the BESS charge/discharge cycle to two by increasing the value of K from 3 to 7 for January, May, August, and November. The result shows that BESS starts charging at the beginning of the day when the ToU tariff is at its lowest rate (the green region) and discharges when the TOU tariff is at its highest rate (the red region), and starts charging again when PV power becomes available or during the mid-peak ToU tariff (pink region), and finally discharges during the second peak of the TOU tariff as seen in Figure 3-15 to 3-19. This charge/discharge pattern of the battery is consistent throughout the year and makes it easy to calculate the life of the battery BESS based on the standard cycle life vs depth of discharge (DOD) curve of BESS. The optimal cost comparison with reference to the benchmark for the two scenarios is presented in Figure 3-19 and Table 3-5, with the online approach outperforming the offline approach by 3.3% for the system under study.

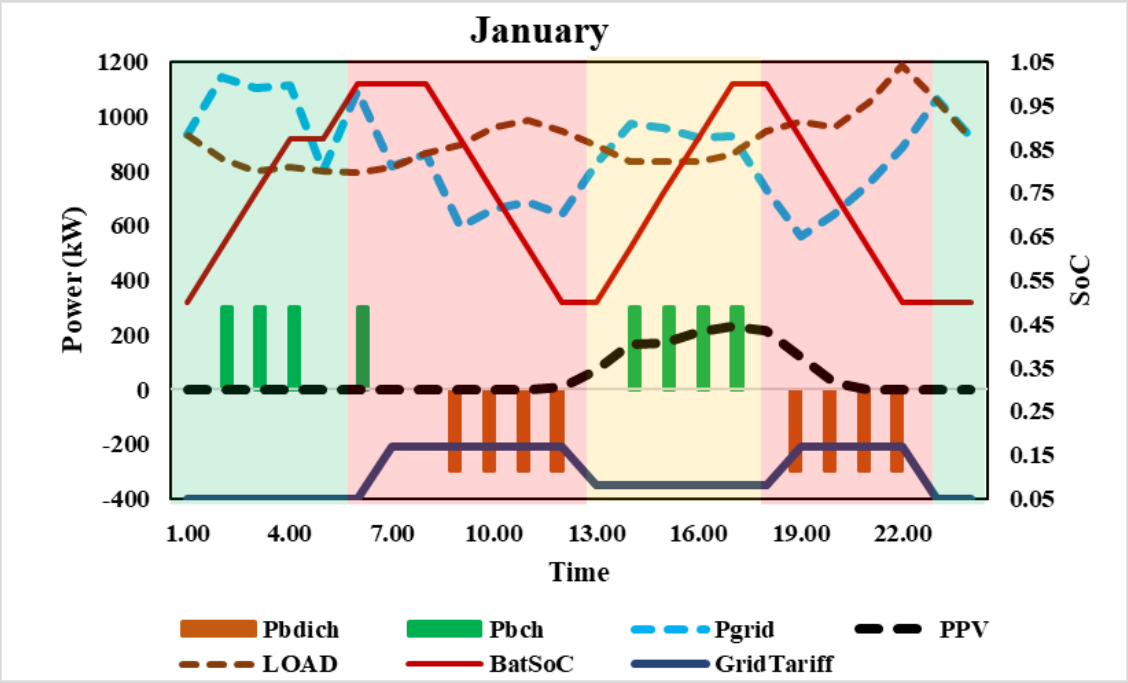

Figure 3-15: The microgrid dispatch for January for real-time operation of the Microgrid using RH control with the charge/discharge cycle limited to two cycles.

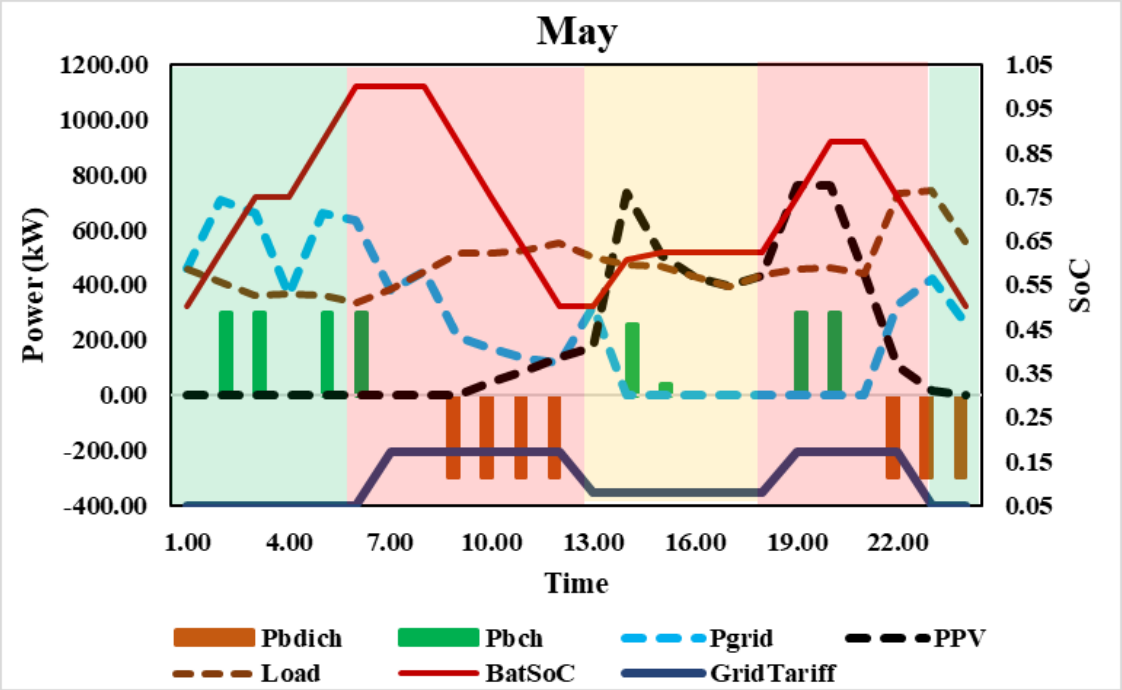

Figure 3-16: The microgrid dispatch for May for real-time operation of the Microgrid using RH control with the charge/discharge cycle limited to two cycles.

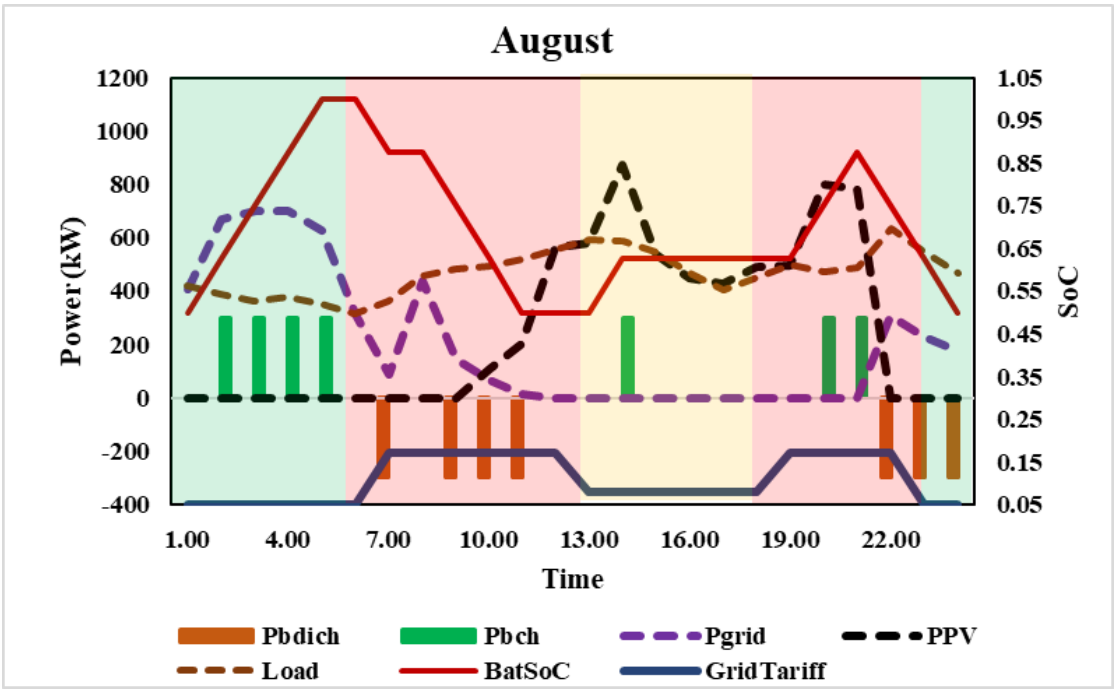

Figure 3-17: The microgrid dispatch for August for real-time operation of the Microgrid using RH control with the charge/discharge cycle limited to two cycles.

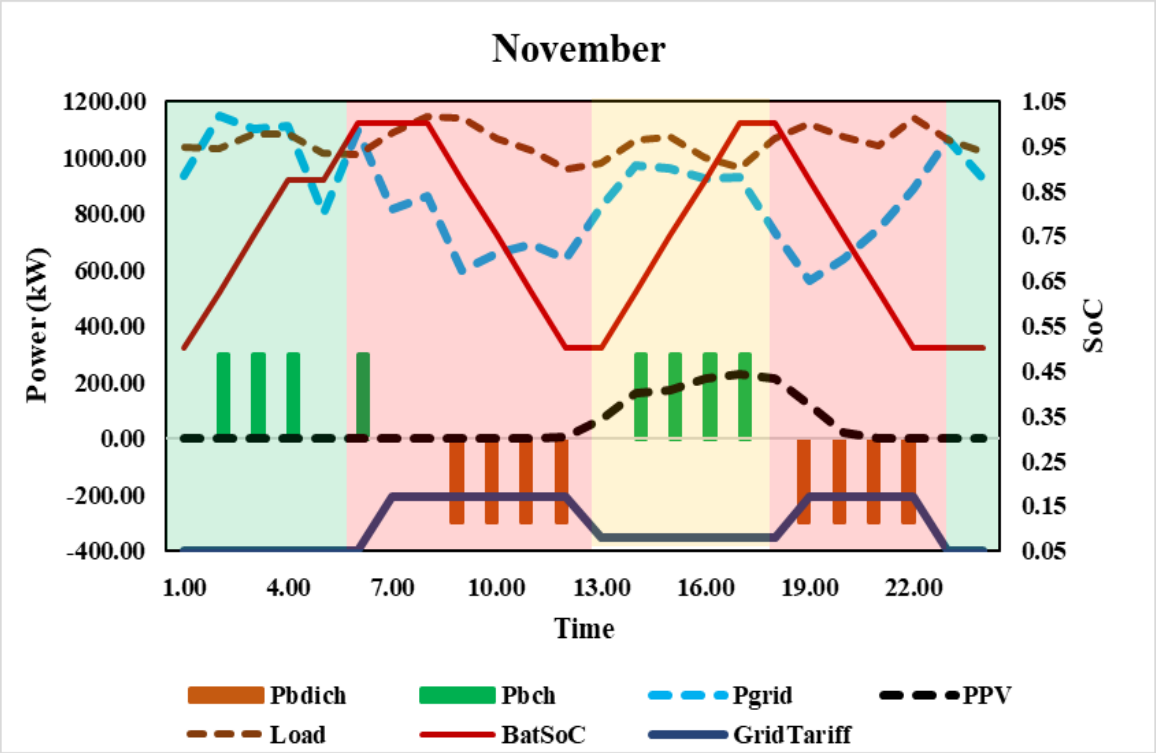

Figure 3-18: The microgrid dispatch for November for real-time operation of the Microgrid using RH control with the charge/discharge cycle limited to two cycles.

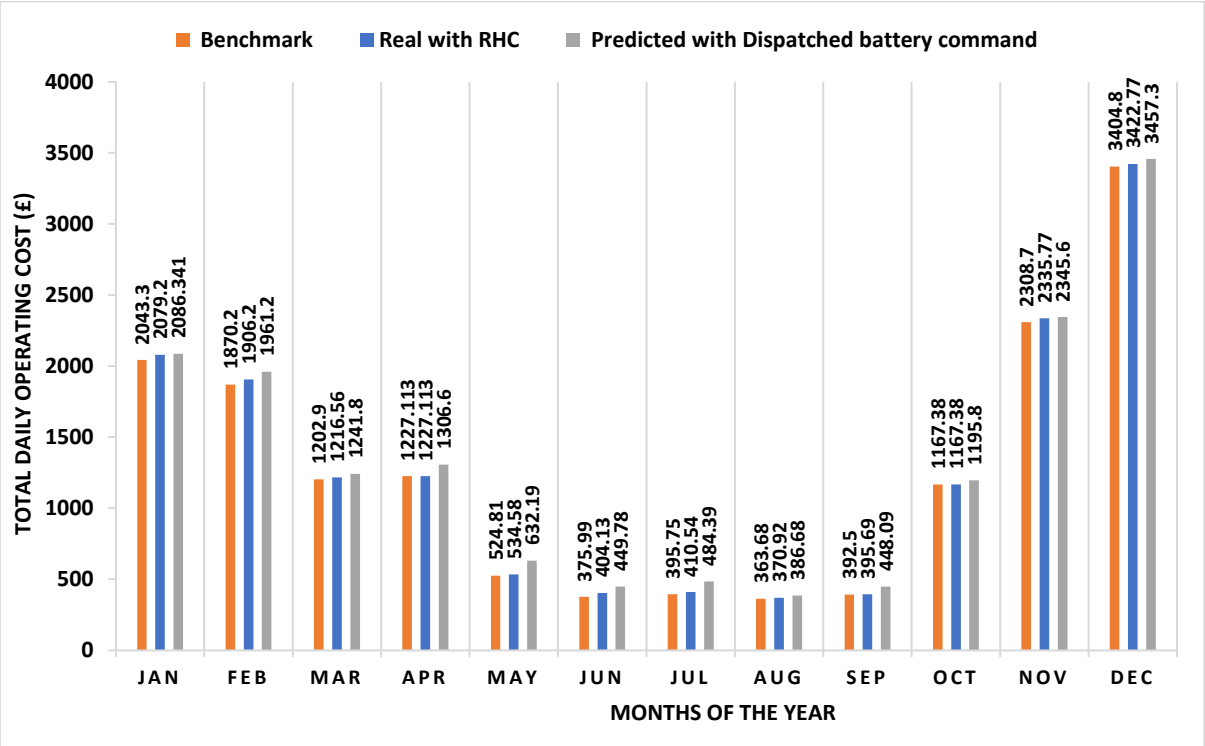

Figure 3-19: Optimal cost comparison between the benchmark, online and offline optimization.

Table 3-5: Optimal cost comparison with average % difference between the two scenarios for K=7

Months	Optimal cost (£) (Benchmark)	Optimal cost (£) (Online Optimization)	Optimal cost (£) (Offline Optimization)	% Difference B/W the Two Scenarios
Jan	2043.30	2079.20	2086.30	0.342
Feb	1870.20	1906.20	1961.20	2.804
Mar	1202.90	1216.56	1241.80	2.033
Apr	1227.11	1227.11	1306.60	6.083
May	524.81	534.58	632.19	15.440
Jun	375.99	404.13	449.78	10.149
Jul	395.75	410.54	484.39	15.246
Aug	363.68	370.92	386.68	4.076
Sep	392.50	395.69	448.09	11.694
Oct	1167.38	1167.38	1195.80	2.376
Nov	2308.70	2335.77	2345.60	0.419
Dec	3404.80	3422.77	3457.30	0.998
Total Cost	**15, 277.123**	**15,470.853**	**15,995.771**	
% Closeness to the benchmark		**1.252**	**4.493**	
Total Cost % Difference B/W the Two Scenarios				**3.3**

3.5 Summary/Discussion

This chapter presents an EMS to minimise the daily operating cost and control the charge/discharge cycle of BESS in a grid-tied microgrid. At the same time, it guarantees the security of supply and respects-imposed constraints. The optimality of this approach is evaluated based on the daily operating cost of energy and the limits placed on the battery charge/discharge cycle. Furthermore, the result from simulation studies carried out on the two scenarios considering different sets of data throughout the year shows that the online optimization adopting the LSTM-MILP-RH (online) control strategy is more effective in terms of reducing the daily operating cost when compared to the LSTM-MILP (offline) optimization approach, with the benchmark daily operating cost set as a

reference. The approach is general enough to be used with different TOU tariff models and could be applied to commercial, residential, standalone, and community-based microgrids.

Finally, since BESS degradation depends largely on the charge/discharge cycles, this approach guarantees a longer life for the BESS as the utilization of the BESS charge/discharge cycle limiting constraint is implemented in both scenarios. In this case, the charge/discharge cycle was first limited to one with the value of K= 3 and then limited to two with the value of K=7 using equations (3-15)–(3-19)**.** The findings indicate that the running costs of the microgrid will be proportionally higher if the number of charge/discharge cycles is decreased. On the other hand, the BESS is likely to have a longer lifespan, resulting in cost savings in the long term. For the model under study, comparing the like to like in *Table 3-6*, limiting the charge/discharge cycle to one gives a higher operating cost for the three scenarios with a percentage cost saving of 7.3, 9.4 and 12.3%, respectively. From an operating cost point, it seems to have a higher number of charges/discharges is better. However, this affects the BESS's health, which will mean a higher capital expenditure as the BESS will be replaced more frequently.

Table 3-6: Comparison between the two limits under study for K=3 and K=7

Description	Limiting Charge/discharge cycle to one (K=3)	Limiting Charge/discharge cycle to two (K=7)	Percentage cost savings
Optimal cost (£) (Benchmark)	16,421.83	15, 277.123	7.3%
Optimal cost (£) (Online Optimization)	17,067.07	15,470.853	9.4%
Optimal cost (£) (Offline Optimization)	18,226.14	15,995.771	12.3%

Further research should be carried on the economic benefit of limiting the charge/discharge cycle of the BESS with more empasis on the replacement frequency and replacement cost.

In the next chapter of the thesis, an analysis is carried out considering different TOU tariffs (i.e., UK economy 7, UK economy10 and UK standard tariff) to observe the effect of the TOU tariff on the battery charge/discharge cycle limits and how a change in the TOU tariff will affect the impact of the charge/discharge cycle limit constraint and the daily operating cost of the microgrid.

Chapter 4

Analysis of the Impact of Time-Of-Use (TOU) and Standard Tariffs Schemes in Energy Management for Grid-Connected Microgrids with Energy Storage.

4.1 Introduction

This chapter analyses the impact of various tariff schemes on the EMS of the grid-connected microgrid system consisting of the solar PV system and BESS. The selection of appropriate rates for buying electricity also influences the solar PV and BESS performance. Electricity tariffs such as standard and TOU would influence energy import from the grid, thereby affecting the economic performance of the entire system [170]. For example, consumers would benefit from the relatively low electricity prices during the TOU scheme's off-peak period. Conventionally, optimal sizing of solar PV has always been studied using a single electricity pricing tariff; this needs to be extended to several electricity pricing tariffs. Several studies have investigated the system performance under different electricity tariffs, such as flat rates, TOU rates, and real-time pricing (RTP) rates [171], [172]. However, in all those studies, the developed EMS is based on the net metering scheme. The net metering scheme is the simplest EMS which sells the extra power of PV to the grid without considering the electricity rate after supplying the load and charging the BESS [173][174].

In addition, research on renewable energy systems conducted under various energy tariffs was rarely reported. The majority of the findings from the simulation may be attributed to a single power pricing (Standard or TOU electricity rates) [175]. Due to the number of variables involved in energy management decisions in grid-connected microgrids, it is essential to recalculate outcomes under

different sets of assumptions to determine the impact of a variable under sensitivity analysis. This is helpful to test the robustness of a system or model in the presence of uncertainty and identify the model input that causes significant uncertainty in the output.

Sensitivity analysis is essential for model building and quality assurance for models involving many input variables. National and international agencies involved in impact assessment studies have included sections devoted to sensitivity analysis in their guidelines. Examples are the European Commission (see, e.g. the guidelines for impact assessment), the White House Office of Management and Budget, the Intergovernmental Panel on Climate Change and the US Environmental Protection Agency's modelling guidelines [176]. Sensitivity analysis aims to observe the system response following modifications in the design parameters of a system. Understanding the parameters' relationships and relative importance helps achieve optimum energy management performance[177]. However, there are no formal rules and well-defined procedures for performing sensitivity analysis for energy management systems in microgrids; this is because the objective of each study and the energy management model may be different [178].

In most cases, perturbation techniques and sensitivity methods are used to study input parameters' impacts on different simulation outputs compared to a base case situation[179]. The concept is straightforward, but it is crucial to understand what sensitivity analysis can do for energy management systems studies and interpret the results [180]. A background theory study can provide a better picture of the sensitivity figures and their implications. In this Chapter, the sensitivity of the performance of the energy management model in Chapter 3 is evaluated

considering the different TOU and standard flat tariffs as the changing input parameter. The aim is to determine the effect of the ToU tariff on the BESS charge/discharge cycle limits and how a change in the BESS charge/discharge cycle limit will affect the daily operating cost of the microgrid using a simple input-output simulation analysis.

4.2 System Model and Configuration

The proposed EMS, as developed in chapter 3, is general and suitable for all typical grid-connected PV-BESS systems to optimise their usable capacity and control the power flow. In this study, the case study presents a typical grid-connected system of an island community. The layout for a typical community installation of EMS controlled microgrid is shown in Figure 2-1. The data received by the EMS, such as the PV generation, the load demand profile, and energy tariffs, will be explained in this section. The annual data of the solar PV generation and load demand of 8760 hours for Ushant Island are shown in Figure 4-1 and Figure 4-2. The load demand is higher throughout the winter and Autumn months due to increased power usage. During the remaining seasons, however, power use is modest. The average load and peak demand for one year are 773kWh, and 1707kWh, respectively and the total annual energy consumption of the Island is 6773.4 MWh. The average daily PV generation and Load demand for January, April, July, and October, representing the four seasons of the year, are presented in Figure 4-3 and Figure 4-4, respectively.

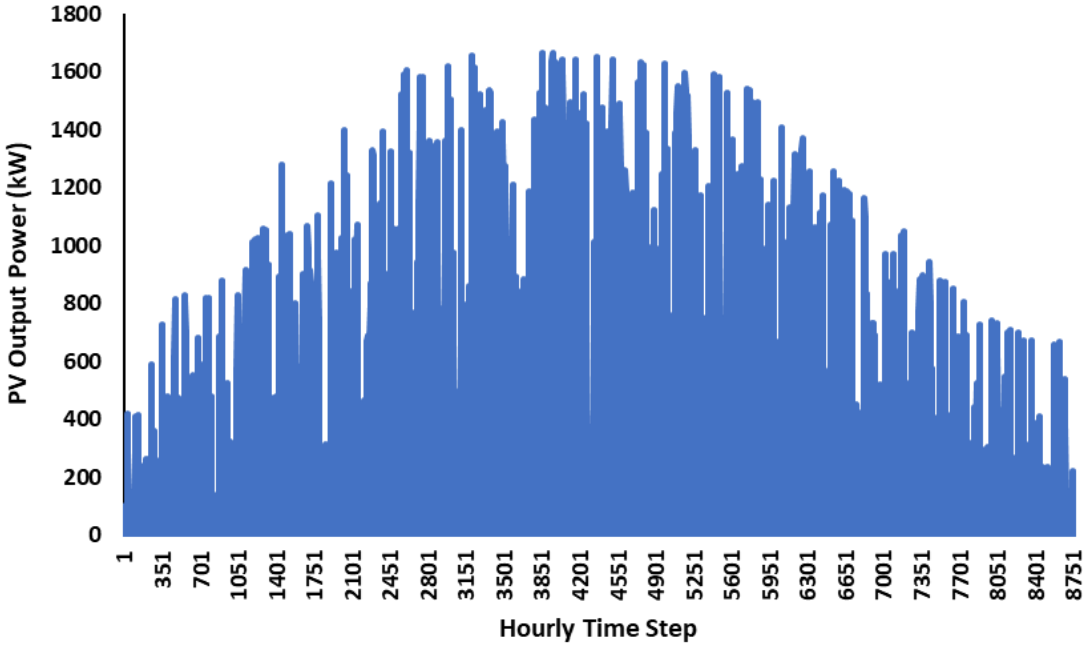

Figure 4-1: Ushant Island Annual Solar PV Generation

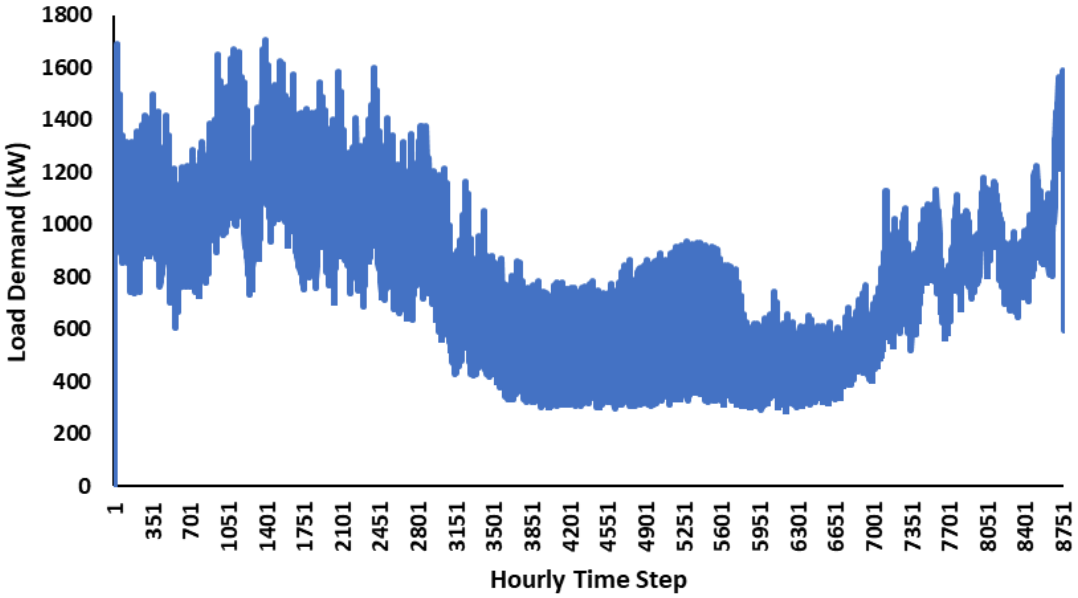

Figure 4-2: Ushant Island annual Load Demand Distribution

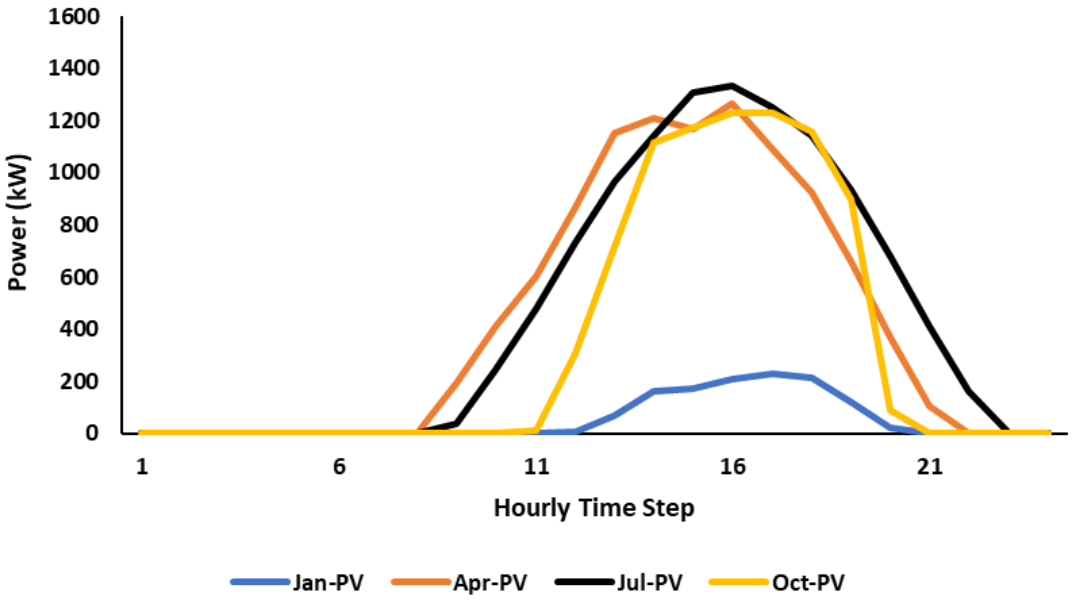

Figure 4-3: Ushant Island Average Daily PV Generation for January, April, July and October

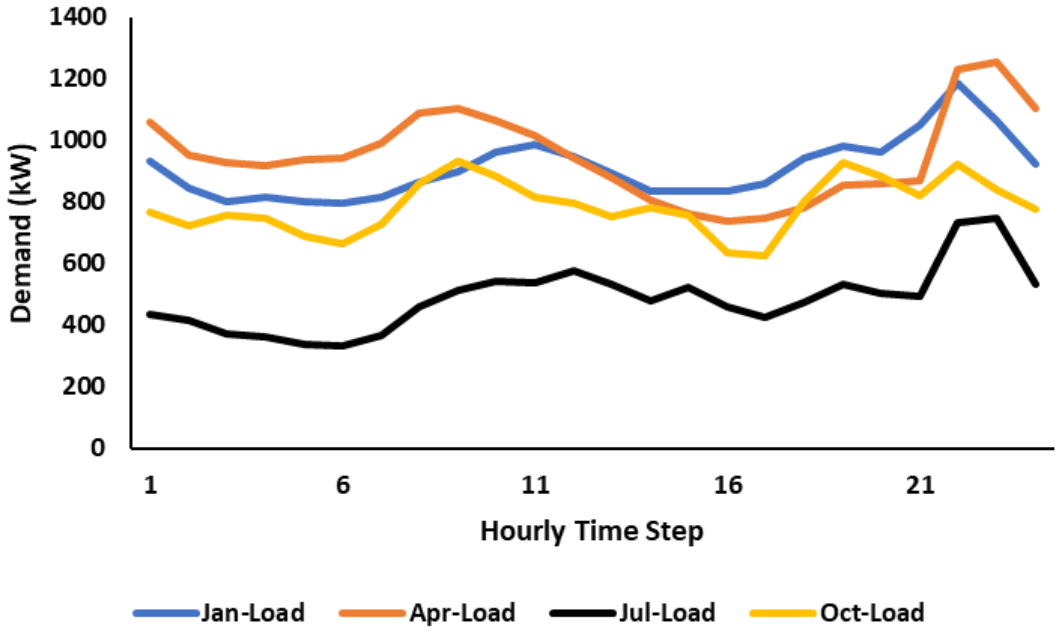

Figure 4-4: Ushant Island Average Daily Load Demand for January, April, July and October

Electricity buying prices for the standard and TOU tariffs are presented in Figure 4-5. The electricity buying price for standard rates is 0.13 £/kWh, which is more than two times the cost of exporting power to the grid at the rate of 0.055 £/kWh, assuming the excess generated solar PV power was to be sold to the grid. The

electricity price for ToU rates is not fixed and varies with different periods [181]. In this study, we have considered three types of time of use (TOU) tariffs, which are the UK economy seven tariff (E7T), the economy ten Tariff (E10T), the residential time of use tariff (RTOU) and the standard tariff (STD). For E7T, the peak period means that the demand is usually high, and it starts from 7 AM to 11:59 PM. The off-peak period indicates lower usage of electricity, and it is between 12 AM and 7 AM. The retail electricity price during the peak and off-peak periods are 0.15 and 0.07 £/kWh, respectively. For E10T, the off-peak period is between 9 PM to 4 AM and 1 PM to 4 PM at the rate of 0.07 and 0.15 £/kWh, respectively. While that of the RTOU has an off-peak period from 10 PM to 3 AM, peak period from 4 AM to 9 AM and 6 PM to 9 PM, and mid-peak from 12 PM to 5 PM. The STD tariff is the same throughout the day at the rate of 0.13£/kWh.

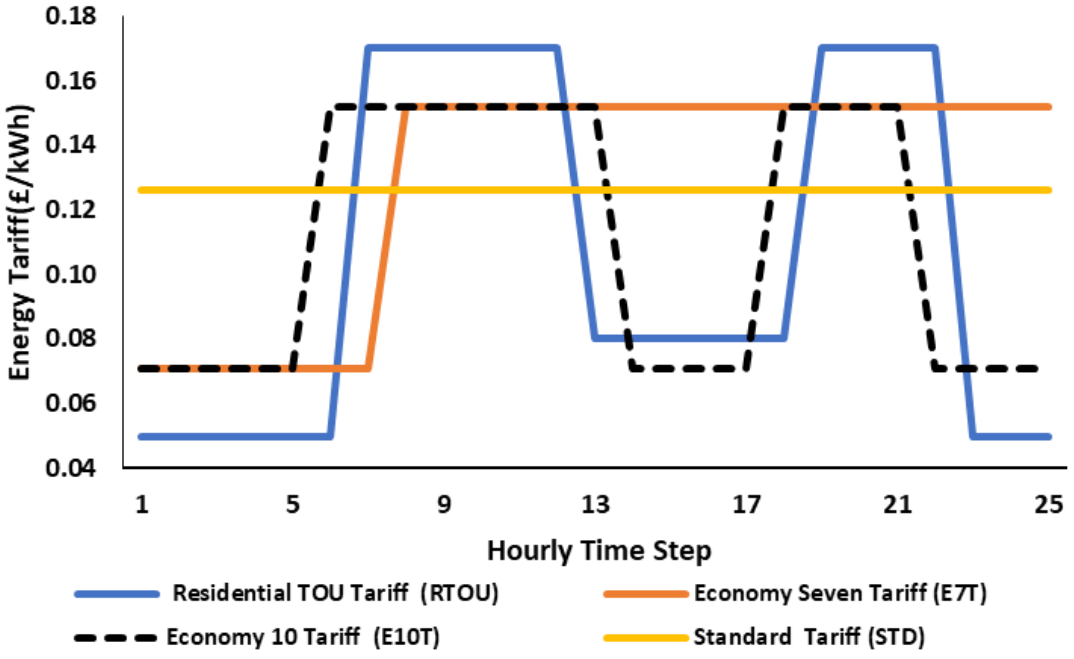

Figure 4-5: Cost of energy under the standard (STD) and TOU tariff rates

Table 4-1 demonstrates the parameters of the solar PV and BESS. The minimum and maximum limitations of the BESS SOC are selected as 20% and 100%, respectively.

Table 4-1: Parameters of the Solar PV and BESS

Parameter Description	Value
Solar PV Capacity	2700 kW_p
BESS Capacity	5.6 MWh
BESS Minimum SOC	20%
BESS Maximum SOC	100%
BESS Efficiency	95%
Maximum Charge and Discharge Power	5300 kW (1C)

4.3 Operational Strategy

The proposed system is intended to be used in a community microgrid setting linked to the main grid and comprised of the solar PV system and BESS designed for a power purchase agreement program. In this study, This research operates on the presumption that the behind-the-meter BESS systems installed are unable to engage in power trading with the primary grid. To determine the optimal power flow between these resources, the EMS gathers information from sources such as the renewable power supplied by the solar PV, the available charge and discharge power of the BESS, the load demand of the community, the grid constraint, and the prices of electricity supplied by the grid. The community energy demand at all times is met by a combination of power from the PV, denoted as $P_{pv}(t)$ power from the BESS $P_{bat}(t)$ and power from the grid, as described in equation (4-1).

$$P_{demand}(t) = P_{pv}(t) + P_{grid}(t) + P_{bat}^{d}(t) - P_{bat}^{ch}(t). \quad (4\text{-}1)$$

To solve the economic dispatch problem here, we employ the same approach used in chapter 3 to determine the minimum operating cost while respecting imposed constraints and guaranteeing the security of the supply.

Within the scope of this research, an EMS is developed for the various system configurations. A sensitivity analysis is performed on the different TOU and Standard tariffs to identify which tariff is the most appropriate for the system's functioning from an economic point of view. The EMS is selected for simplicity, practicality, user-friendliness, ease of implementation in practice, and low calculation requirement [182]. This facilitates achieving a feasible system operation and hence optimal planning. Different electricity tariffs like STD and TOU directly affect electricity trading between the components of the microgrid and, in turn, affect the overall operating cost of the system. Therefore, the EMS can be developed under four different schemes in terms of electricity buying tariffs.

4.4 Results and Discussions

This section presents the economic and technical findings of the optimised system for the case study. The power flow analysis and sensitivity analysis are presented. First, the optimal result shows the annual contribution of the PV and the BESS for four different tariff structures, as seen in Figure 4-6. It is observed that the ability of the BESS to reduce the peak demand on the grid effectively depends mainly on the tariff structure. However, in this study, we have set a charge and discharge limit on the BESS, which makes it impossible for the BESS to perform more than two charge/discharge cycles within 24 hours. This limit cannot be implemented in the algorithm when solving the problem annually (i.e. t=8760). Therefore, to achieve the result in Figure 4-6, the limit on the charge/discharge cycle is not considered, and the optimal operating cost for the four different tariff structures is compared. The STD tariff structure produces the highest optimal operating cost, and the RTOU tariff structure gives the lowest

(best) operating cost. Since the RTOU pricing structure is intended for residential users, it may not be utilised for a community grid-microgrid system, except the community comprises residential settlements only [18]. After evaluating the BESS participation and the optimal operating cost while considering the E7T, E10T, and the STD tariff Schemes, it can be seen that the E10T scheme is the one that provides the best guarantee for the lowest possible optimal operating cost as well as the most efficient usage of the BESS without considering any limit on the BESS charge/discharge cycle.

With the charge/discharge cycle limit in place, the optimisation is performed every 24 hours considering the RTOU tariff, E7T, E10T and the STD tariff. The results using the average daily load demand profile and PV daily profile for January, April, July and October, representing the four seasons of the year, are presented based on the four tariff schemes mentioned above in the technical and operating cost analysis subsections below.

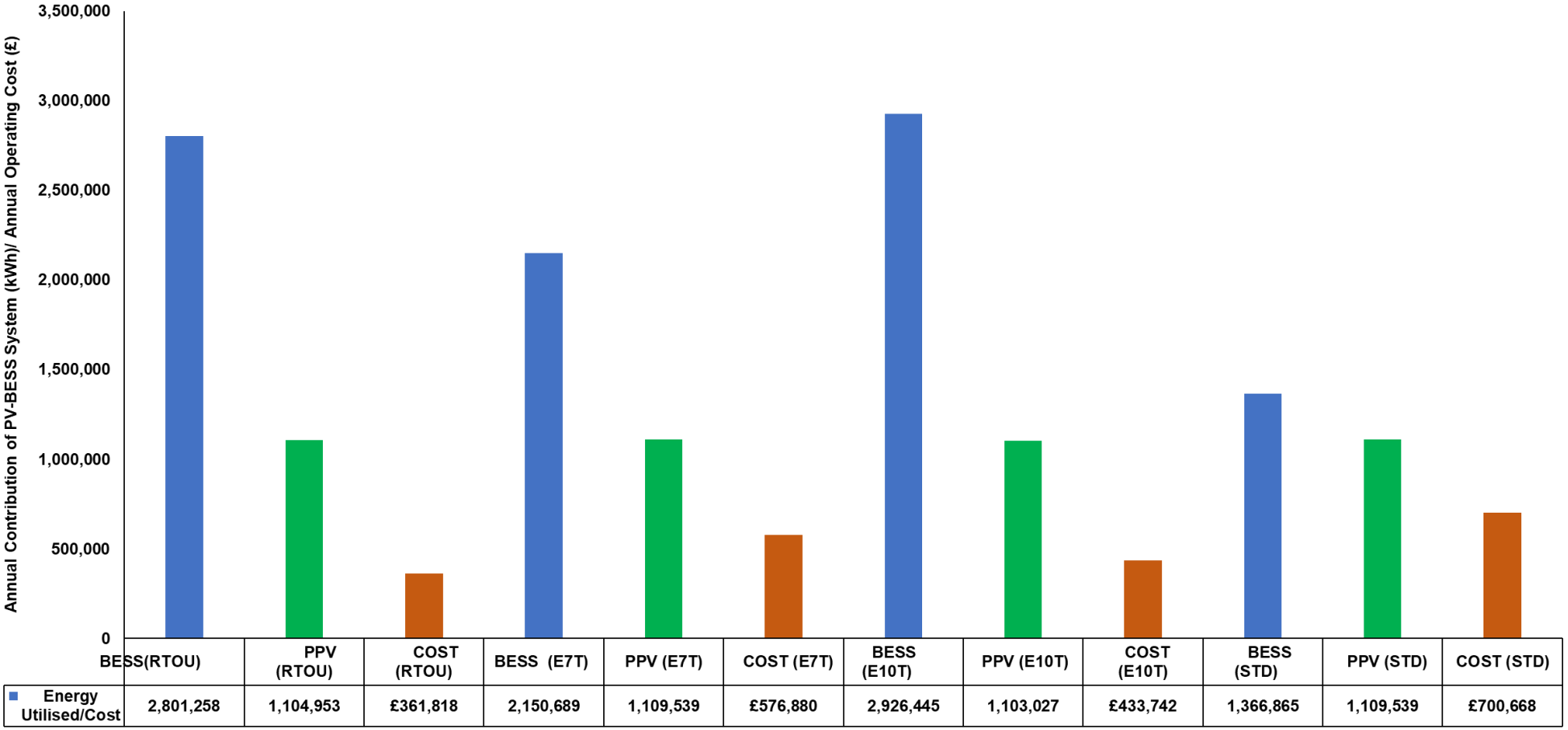

	BESS(RTOU)	PPV (RTOU)	COST (RTOU)	BESS (E7T)	PPV (E7T)	COST (E7T)	BESS (E10T)	PPV (E10T)	COST (E10T)	BESS (STD)	PPV (STD)	COST (STD)
Energy Utilised/Cost	2,801,258	1,104,953	£361,818	2,150,689	1,109,539	£576,880	2,926,445	1,103,027	£433,742	1,366,865	1,109,539	£700,668

Figure 4-6: Comparison of the optimal result for four tariff schemes based on an annual optimal approach (t=8760)

4.4.1 Technical Analysis Based on the Four Tariff Schemes

For the purpose of the technical analysis, rather than considering an annual operation of the PV-BESS grid-connected microgrid system, a 24-hour sample was obtained from the daily average of the monthly data for four months of the year.

4.4.1.1 Scheme 1: Residential Time of use (RTOU) Tariff

For this scheme, the electricity buying price is based on the residential TOU tariff, where the retail price of electricity is relatively high during the peak period. However, for this tariff structure, the BESS is made to charge during the off-peak and mid-peak periods and discharge during the peak period, thereby reducing the peak demand on the grid. For January, the BESS is charged with the grid only during the off-peak period since the PV generation is less than the load demand throughout the month, as seen in Figure 4-7. During the spring, summer and autumn seasons (April, July and October), when the load demand drops and the PV generation is greater than the load demand in the middle of the day, the BESS is charged during the off-peak period in the early hours of the morning and discharge during the first peak period of the day to create space for PV charging and discharges again during the second peak period of the day as seen in Figure 4-8 to Figure 4-10.

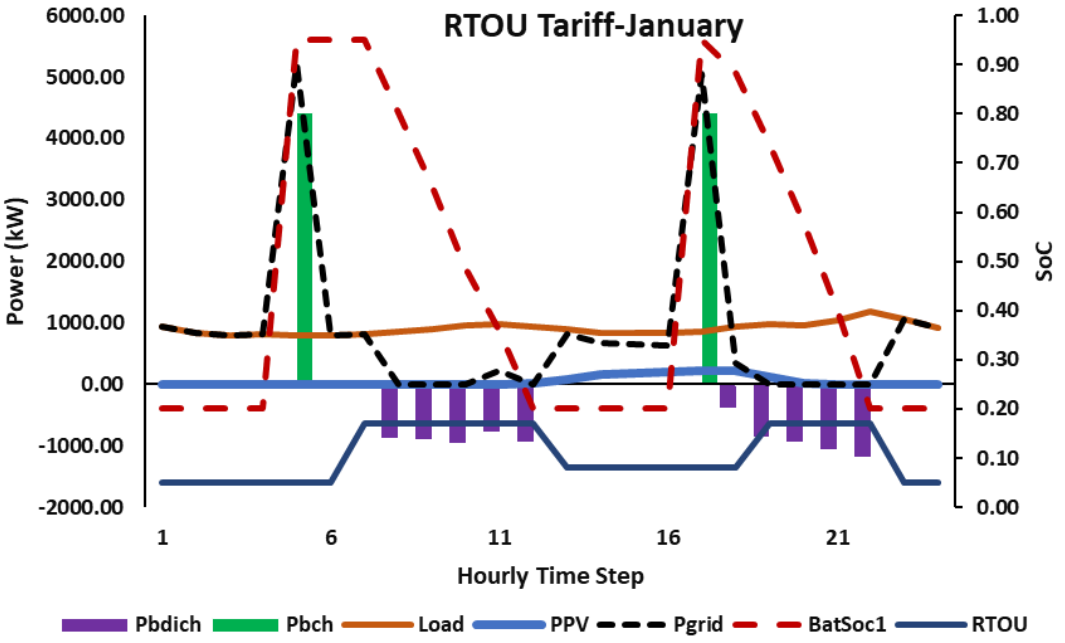

Figure 4-7: Microgrid Dispatch commands for January using the RTOU Tariff

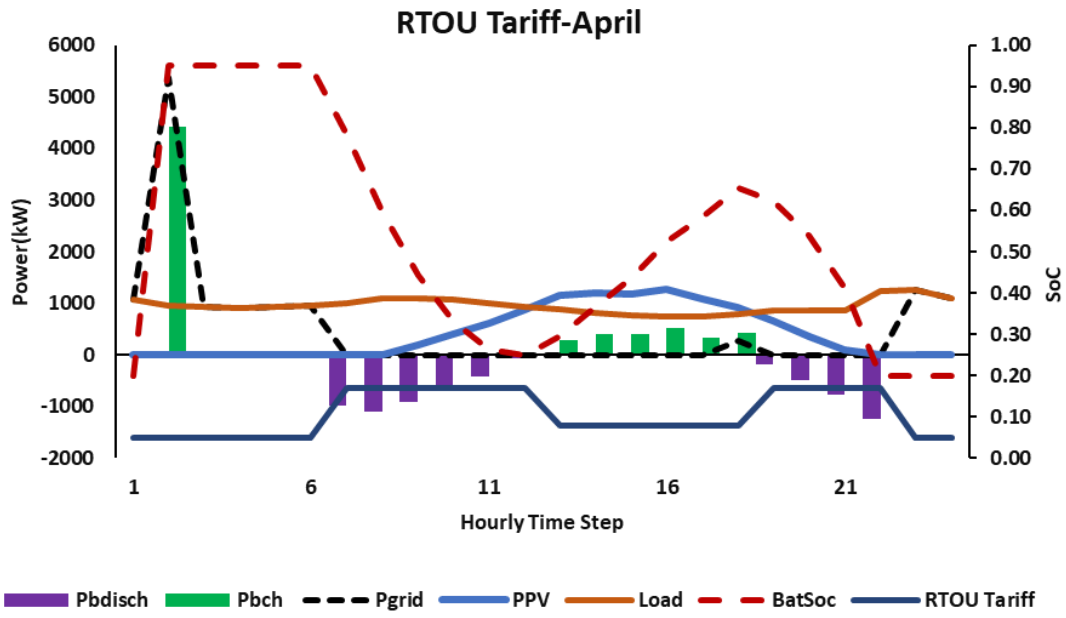

Figure 4-8: Microgrid Dispatch commands for April using the RTOU Tariff

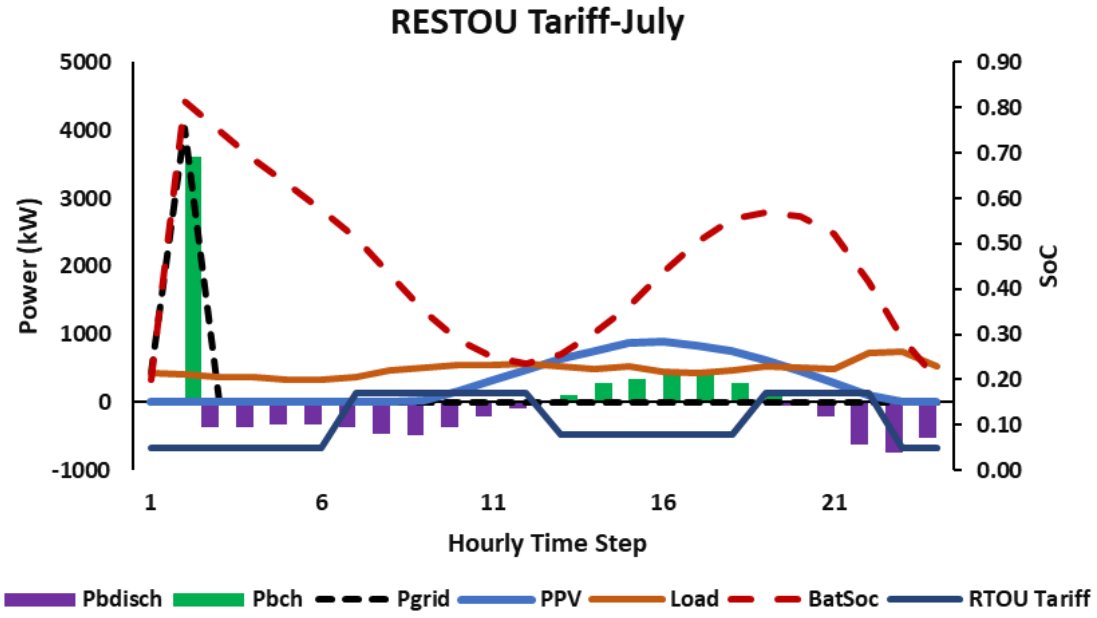

Figure 4-9: Microgrid Dispatch commands for July using the RTOU Tariff

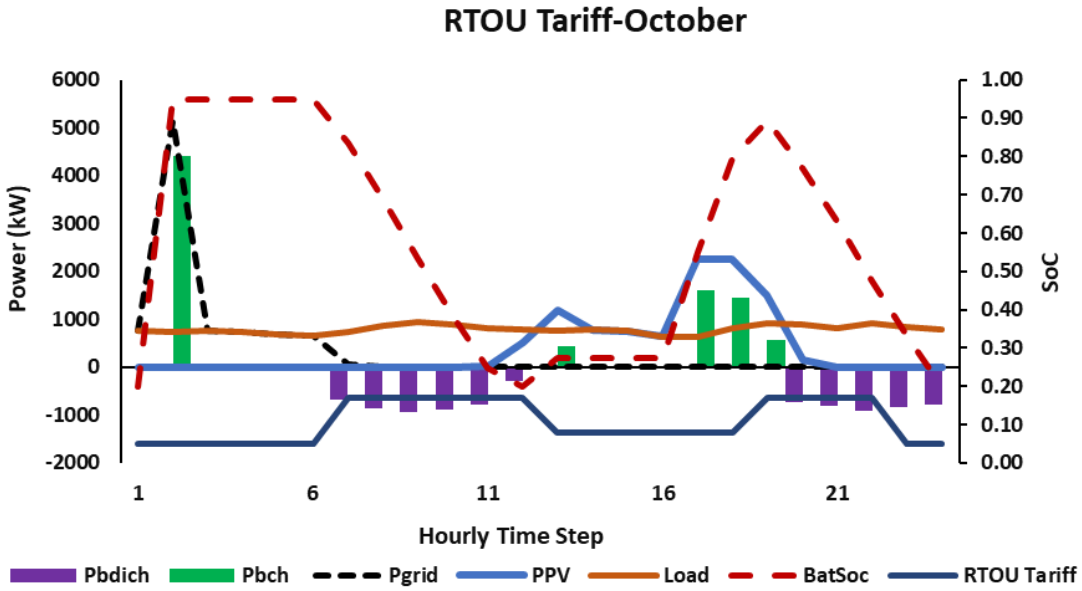

Figure 4-10: Microgrid Dispatch commands for October using the RTOU Tariff

4.4.1.2 Scheme 2: Economy Seven (E7) Tariff

In this scheme, during the off-peak period between 12 AM and 7 AM for the four seasons of the year, the BESS is charged when PV generation is unavailable with the grid, as seen in Figure 4-11 -Figure 4-14. However, because the EMS has an understanding of the amount of PV power available in the future from predicted data, it schedules the discharge of the BESS to create space for PV

charging. In January, during the winter season, when the PV generation is less than the load demand, the BESS discharges once during the peak period with just one charge/discharge cycle. However, for the rest of the seasons of the year, when PV generation is greater than the load demand, the BESS discharges during the peak period. It creates space for PV charging, then charges with the excess PV generated, and discharges again when the PV generation becomes less than load demand. The control strategy for this scheme remains the same as that of the RSTOU tariff. Therefore, the demand on the grid is reduced or even eliminated when the BESS is charged during the off-peak period or with PV generation and discharged during the peak period.

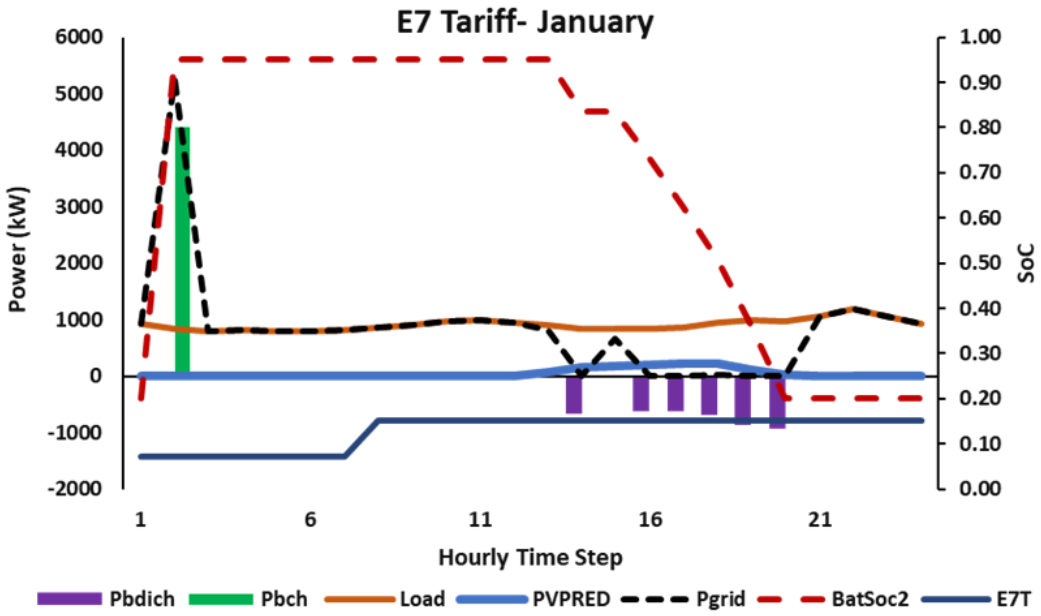

Figure 4-11: Microgrid Dispatch commands for January using the E7 Tariff

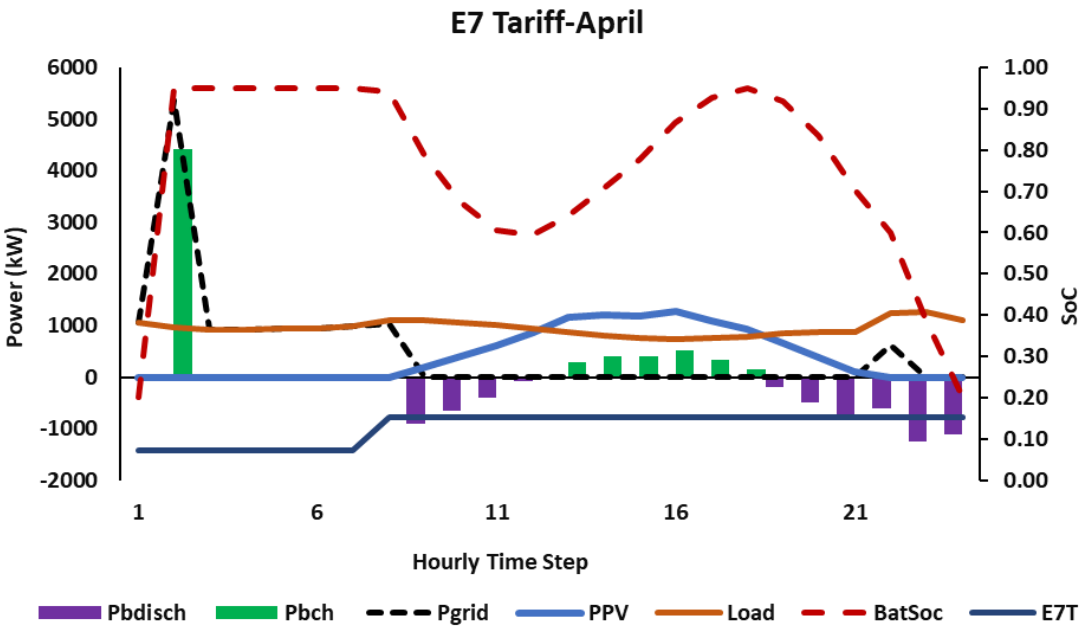

Figure 4-12: Microgrid Dispatch commands for April using the E7 tariff

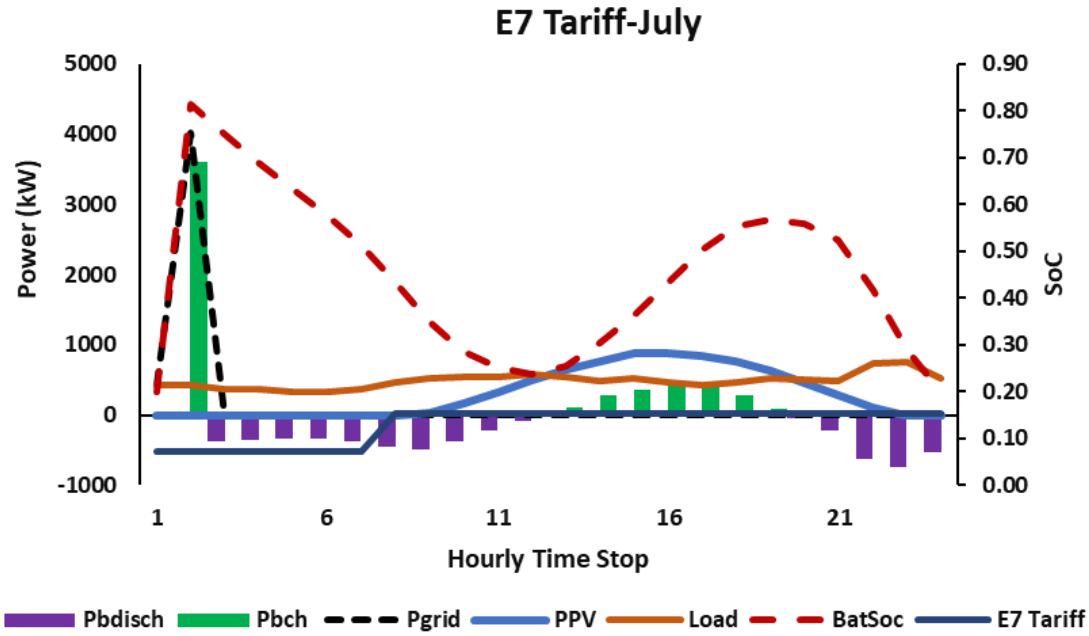

Figure 4-13: Microgrid Dispatch commands for July using the E7 Tariff

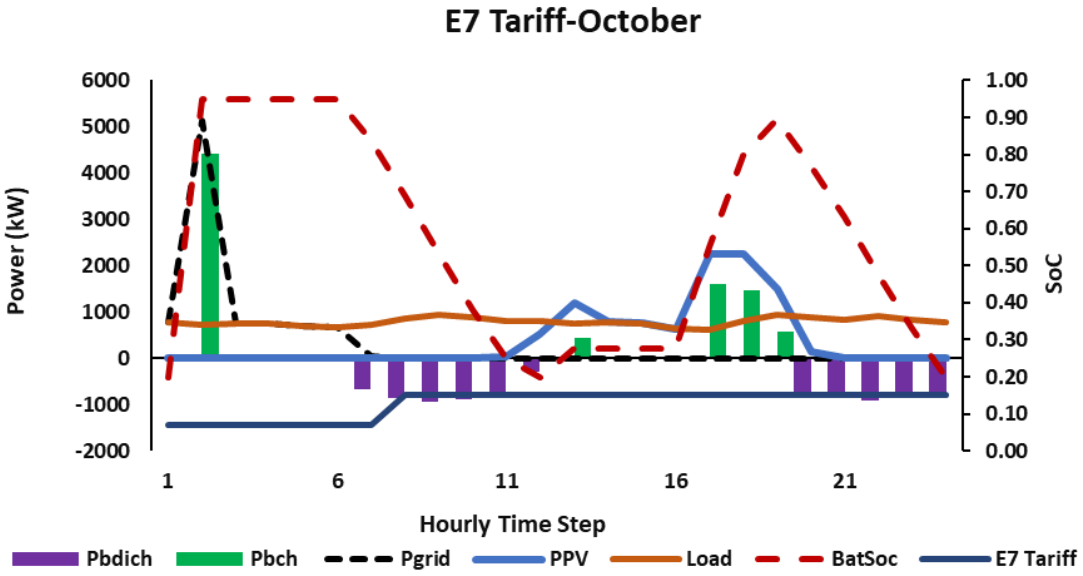

Figure 4-14: Microgrid Dispatch commands for October using the E7 tariff

4.4.1.3 Scheme 3: Economy Ten (E10) Tariff

The E10 Tariff Scheme is very similar to the RTOU tariff scheme; the only difference is that for the E10T, there is no mid-peak which means in terms of the peak and off-peak, it relates closely with the E7T scheme. For this scheme, the electricity buying price is at its peak twice during the day, when the retail price of electricity is relatively high. During the off-peak period, which occurs in the early morning hours and around mid-day, the BESS is charged for the winter (January) season and discharged during the peak period, thereby reducing the peak demand on the grid, as shown in Figure 4-15. During the spring, summer and autumn seasons (April, July and October), when the demand drops and the PV generation is greater than the load demand during the greater part of the day, the BESS is charged during the off-peak period in the early hours of the morning and discharge during the first peak period of the day to create space for PV charging and discharges again during the second peak period of the day as seen in FiguresFigure 4-15 to Figure 4-18.

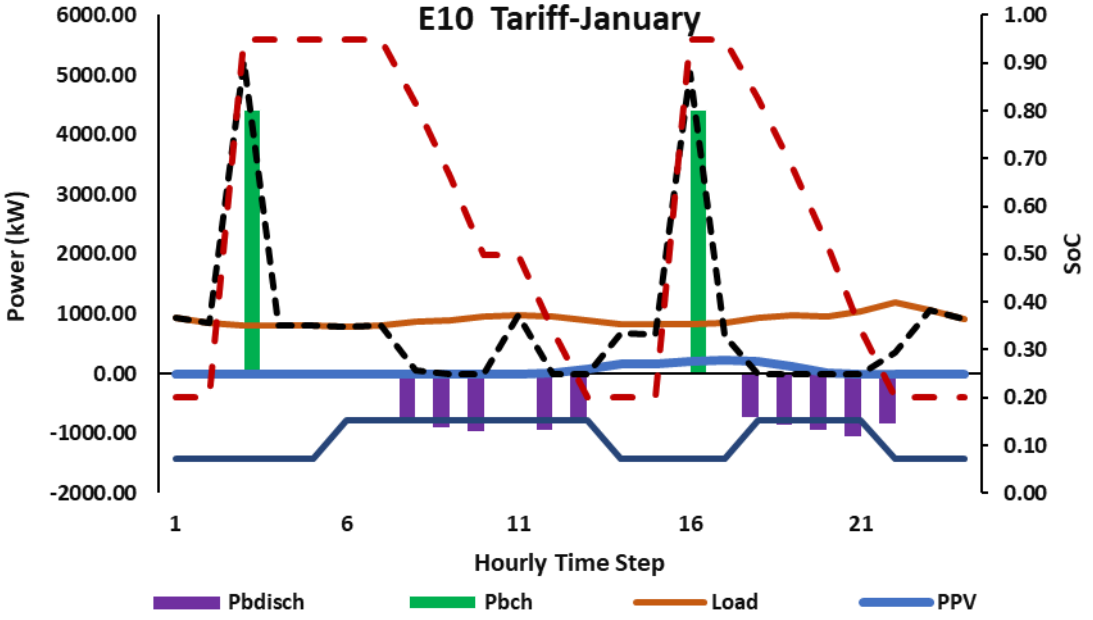

Figure 4-15: Microgrid Dispatch commands for January using the E10 Tariff

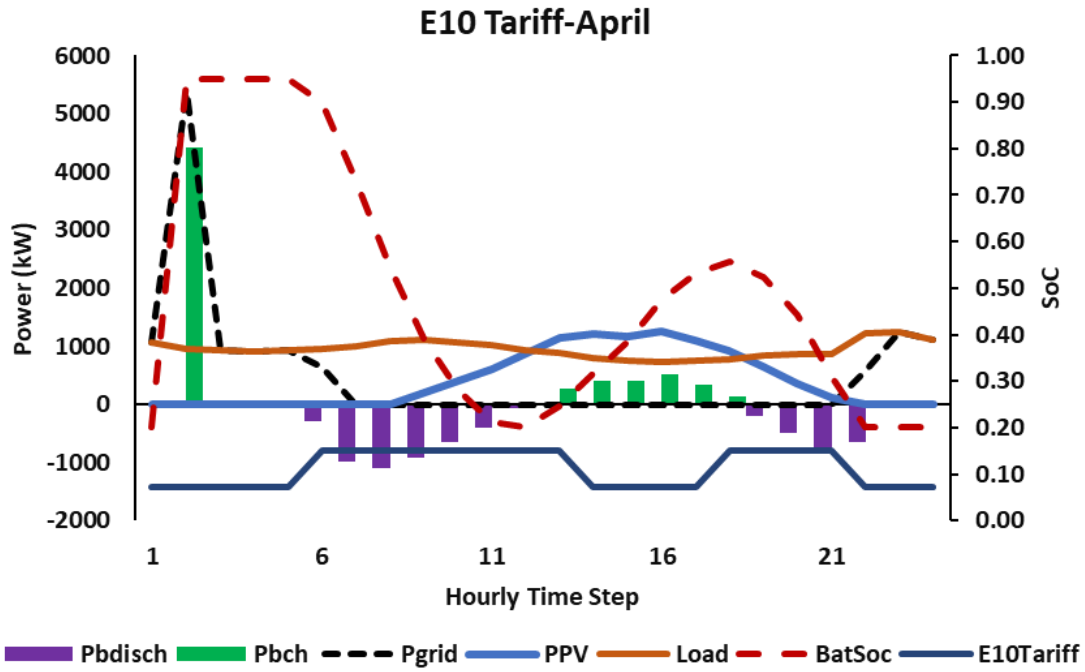

Figure 4-16: Microgrid Dispatch commands for April using the E10 Tariff

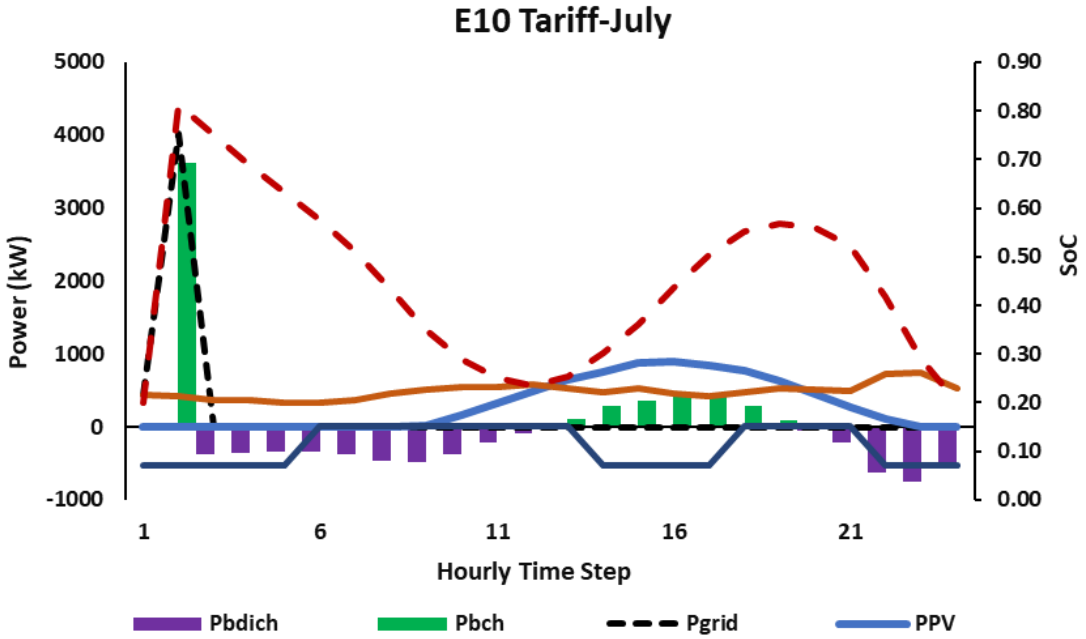

Figure 4-17: Microgrid Dispatch commands for July using the E10 Tariff

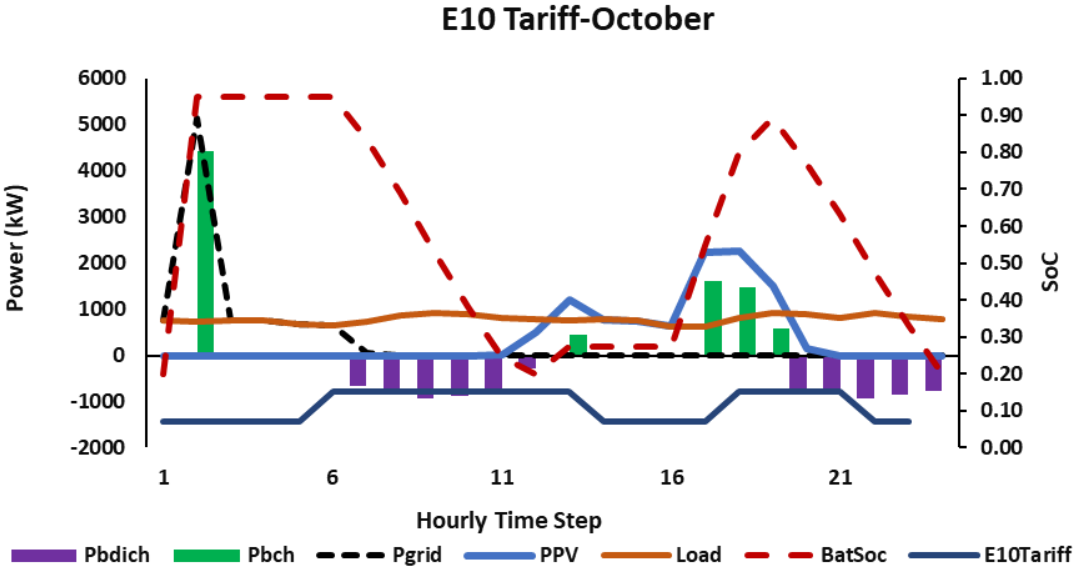

Figure 4-18: Microgrid Dispatch commands for October using the E10 tariff

4.4.1.4 Scheme 4: Standard (STD) Tariff

This scheme is relatively different from the other three schemes as the tariff is the same throughout the day. This scheme will only function very well if the system is designed to sell excess generated power from the PV to the grid. This is so because the PV system can be oversized so that during the days of poor solar

irradiation, its generation will be greater than the demand, giving room for the BESS charging from the PV. During the summer, the excess PV generation after charging the BESS is then sold to the grid. However, since this is not the case in this study, this Tariff structure tends to pose a challenge as the BESS will be idle during the winter seasons, as seen in Figure 4-19. Since the tariff is flat, there will be no cost-benefit if the BESS is charged from the grid. In Figures 4-21 to 4-23, it is seen that as the PV generation rises above the demand during the day for the spring, summer and autumn months, the BESS is charged with excess PV generations and discharges when PV generation begins to drop in the evening. As a result, if the PV system is not oversized (which is not advisable for economic reasons except the excess generation is to be sold to the grid at a reasonable rate), it is not advisable to have a BESS inclusive microgrid using the STD tariff structure.

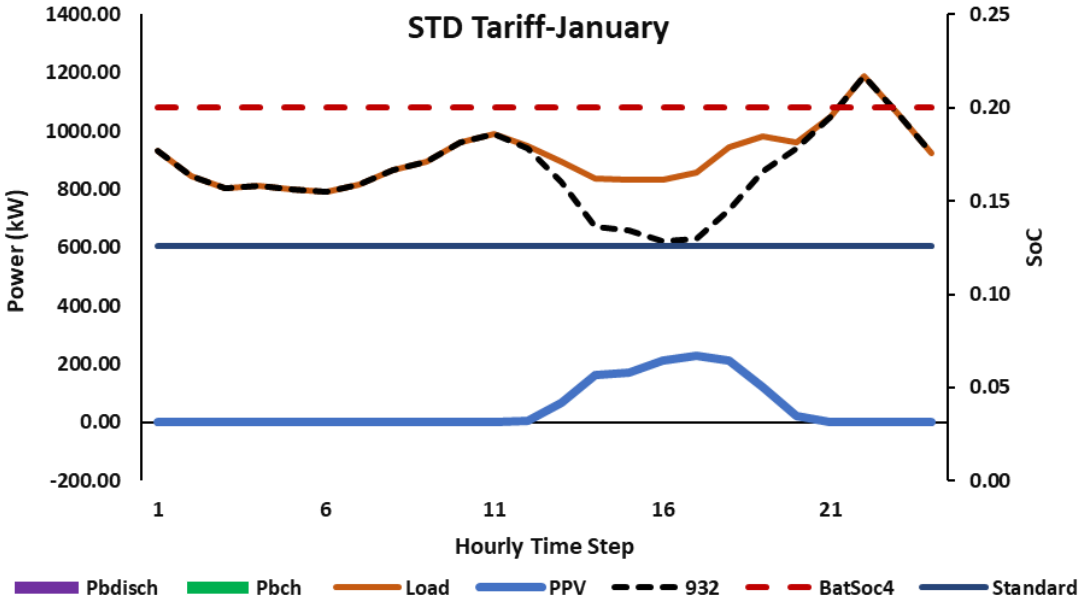

Figure 4-19: Microgrid Dispatch commands for January using the STD Tariff

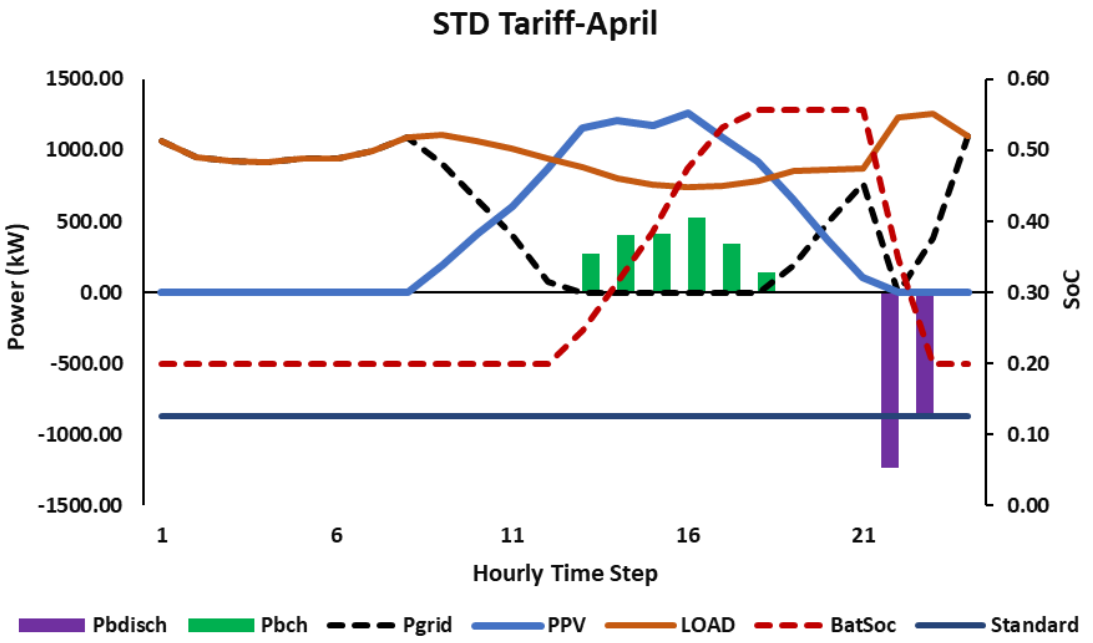

Figure 4-20: Microgrid Dispatch commands for April using the STD Tariff

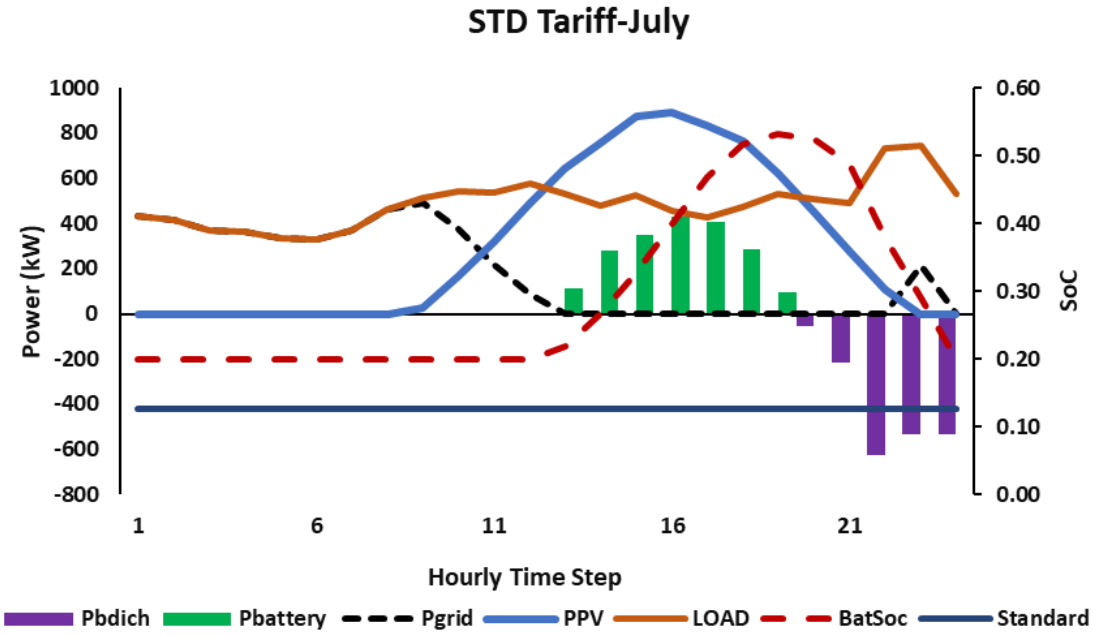

Figure 4-21: Microgrid Dispatch commands for July using the STD Tariff

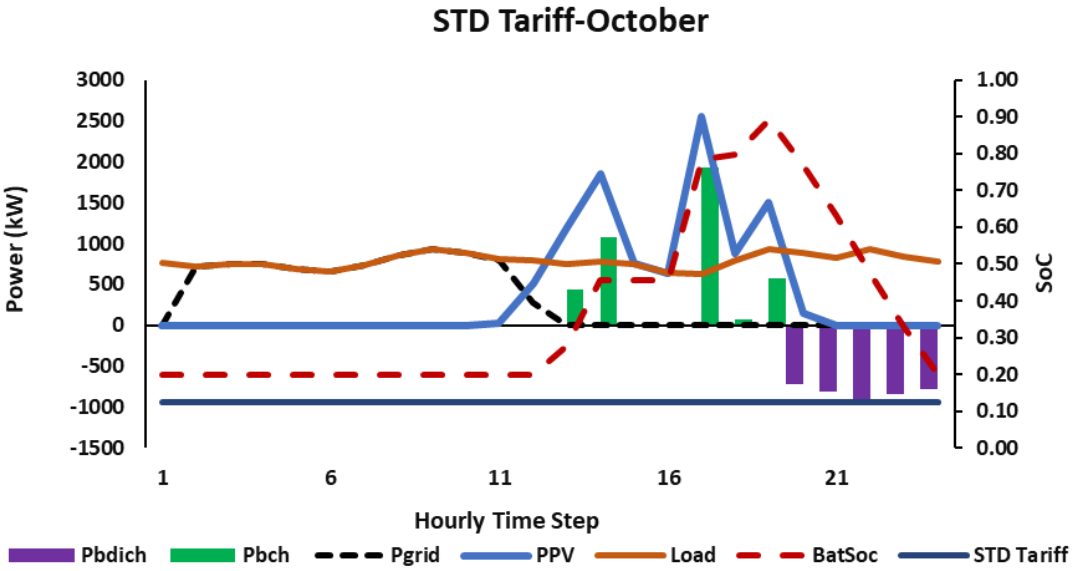

Figure 4-22: Microgrid Dispatch commands for October using the STD Tariff

4.4.2 Optimal Operating Cost Analysis Based on the Four Tariff Schemes

This section presents the operational cost analysis of this study, considering the four tariff schemes. Although the study initially considered the entire year in the operational analysis, it is important to note that the BESS charge/discharge limit operation cannot be implemented on an annual basis; as a result, the operational analysis has been illustrated for a 24 hours sample time for the four seasons of the year using the data for January, April, July and October to represent the seasons. Notably, these four sample days for different seasons were selected due to high, medium and low solar irradiation and temperature in summer, autumn, spring and winter, respectively. Figure 4-23 shows the optimal operating cost for the four tariff schemes for each month, with the STD and RSTOU tariffs having the highest and the lowest operating cost for all four sample months, respectively. As the solar irradiation increases and the load demand decreases, the operating cost difference between the tariff schemes also reduces, with July having the lowest operating cost difference between the tariff schemes.

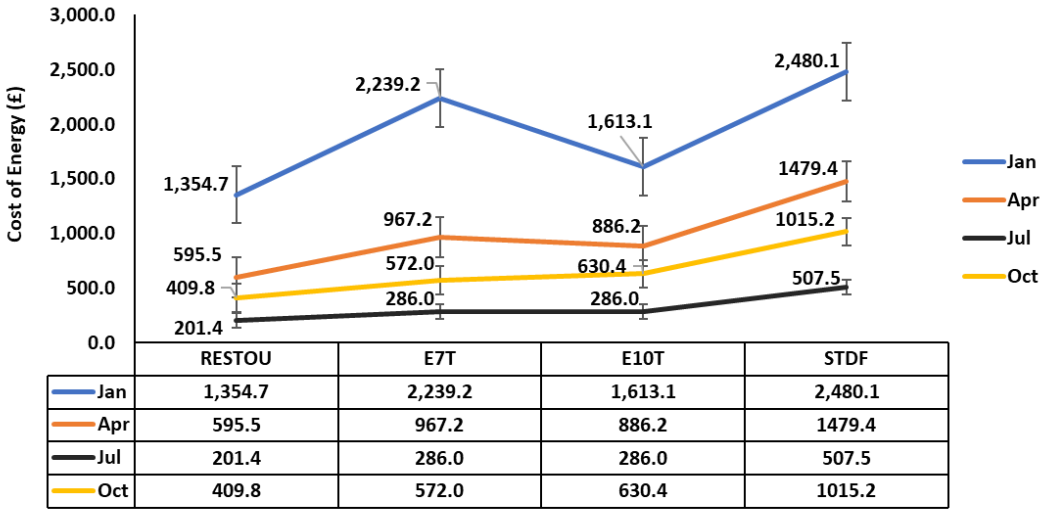

	RESTOU	E7T	E10T	STDF
Jan	1,354.7	2,239.2	1,613.1	2,480.1
Apr	595.5	967.2	886.2	1479.4
Jul	201.4	286.0	286.0	507.5
Oct	409.8	572.0	630.4	1015.2

Figure 4-23: Optimal Operating Cost comparison for the four Tariff schemes for Jan, Apr, Jul and May.

Figure 4-24 and Figure 4-25 show the daily average optimal operating cost for each tariff scheme every month for PV-BESS grid-connected and grid-only operations, respectively. For the SPV-BESS grid-connected operations, the STD tariff scheme has the highest daily operating cost across the year; this is slightly different for the grid-only operations, where the E7T scheme has the highest daily operating cost across the year. This shows the benefit of the grid-connected microgrid in terms of operating cost reduction. In general, this study shows that all four tariff schemes can greatly benefit grid-connected microgrid operations; however, tariff structures such as STD may not guarantee the economic and technical benefits of grid-connected microgrid systems with energy storage.

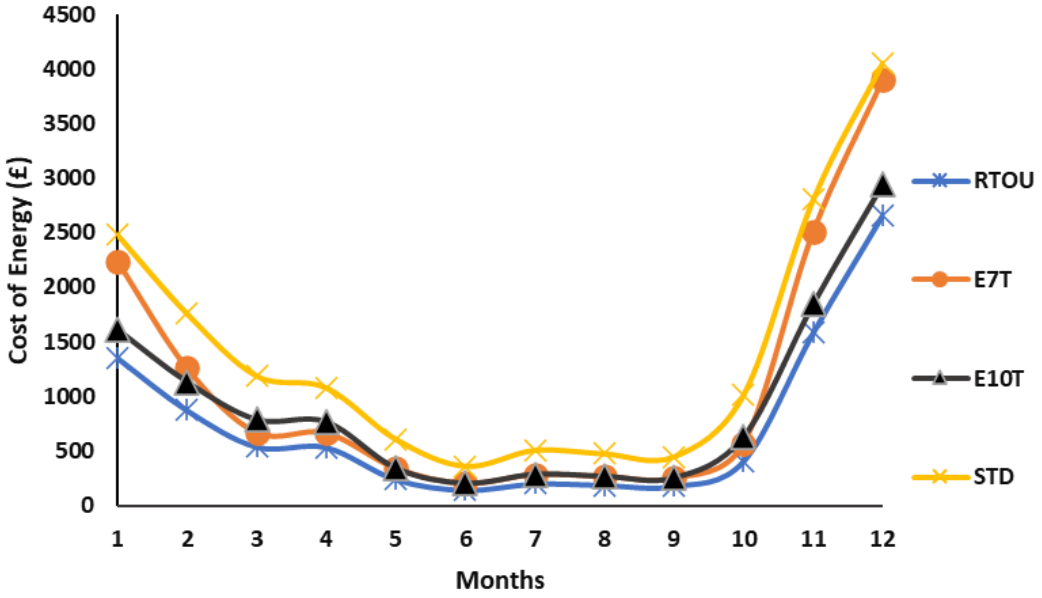

Figure 4-24:Daily Average Optimal Operating cost for each Tariff Scheme on a Monthly Basis for the PV-BESS Grid-Connected Operations.

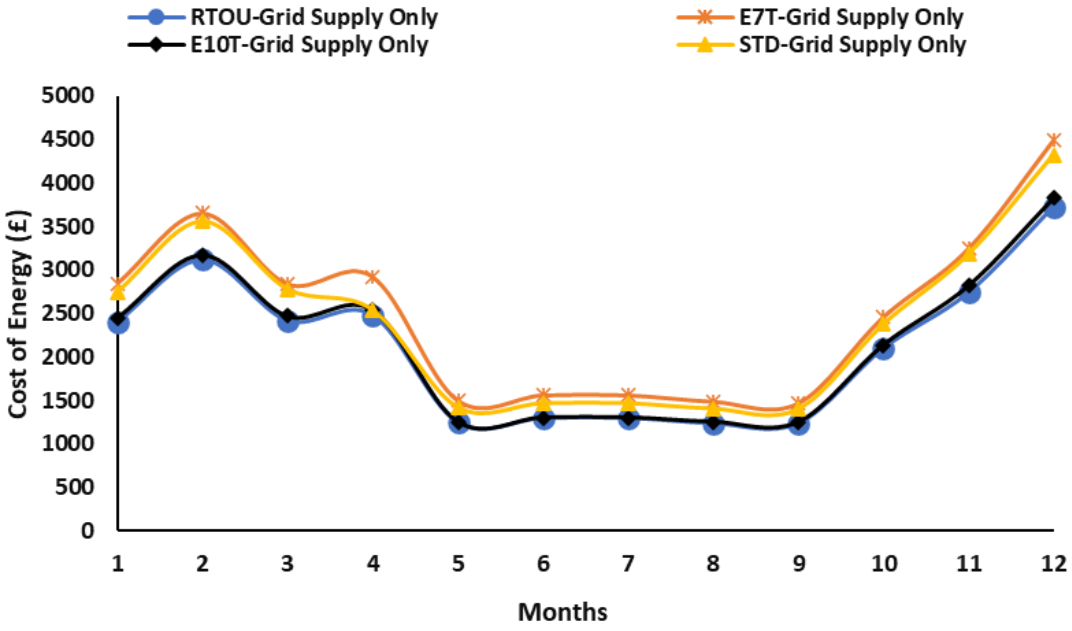

Figure 4-25: Daily Average Operating cost for Grid Operations only on a Monthly Basis.

Figure 4-26 compares the annual operating cost for the grid-only supply operations and grid-connected PV-BESS system, which is used to calculate the yearly operational cost percentage savings between the grid-only supply and the grid-connected PV-BESS microgrid supply, as shown in Table 4-2.

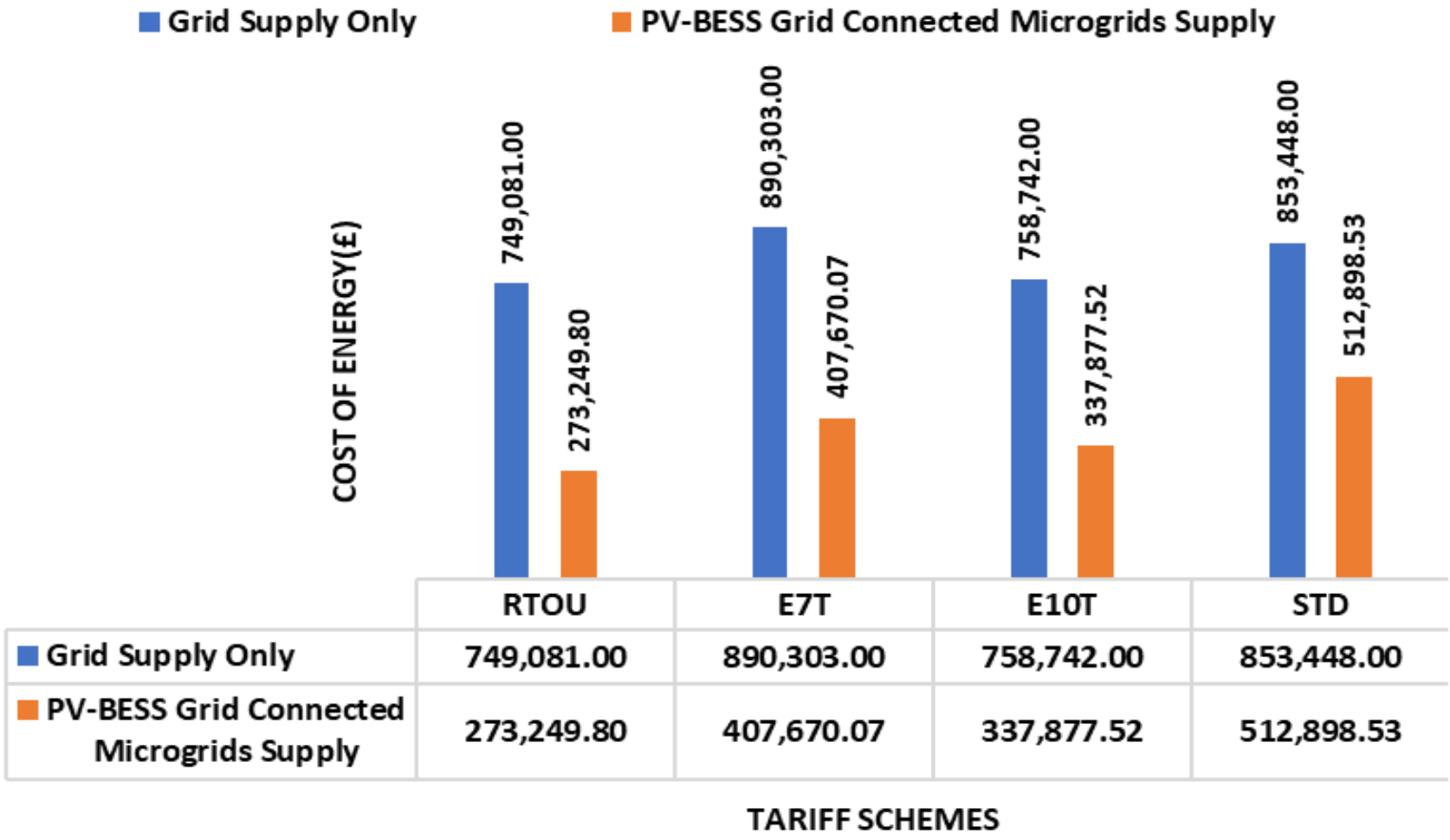

Figure 4-26: Annual Operating Cost Comparison between Grid supply only and Grid-Connected PV-BESS Supply.

Table 4-2: Yearly Operational cost savings for PV-BESS grid-connected microgrid considering the Tariff schemes.

Description	Residential TOU Tariff	Economy 7 Tariff	Economy 10 Tariff	Standard Flat Tariff
Annual Operating Cost (Grid-Only)	£749,081	£890,303.0	£758,742.0	£853,448.0
Annual Operating Cost (Grid-Connected SPV-BESS)	£273,249.	£407,670.07	£337,877.5	£512,898.53
Percentage savings	63.5%	54.2%	55.5%	39.9%

4.5 Conclusion

The main contribution of this Chapter of the thesis was to perform the optimal operation of the PV-BESS grid-connected microgrid according to different TOU and standard flat tariff schemes for community microgrid application. For the four tariff schemes: (1) Residential TOU tariff (RTOU), (2) Economy seven tariff (E7T), (3) Economy ten tariff (E10T), and (4) Standard tariff (STD), it was found that the RTOU tariff scheme gives the lowest operating cost, followed by the E10T tariff scheme with savings of 63.5% and 55.5%, respectively, compared to the grid-only operation. However, the RTOU and E10 tariff scheme is mainly used for residential applications with the duck curve load demand structure. For community grid-connected microgrid applications, the E7T and STD are the most likely options offered by energy suppliers. It was found that even though the E7T is the most expensive for grid-only applications, as seen in Table 4-2, it has a cost savings of 54.2% for the PV-BESS configuration as against 39.9% of the STD tariff scheme. Notably, a case study using data from Ushant Island was

considered to evaluate the methodology; however, the proposed method can be applied to other case studies.

This work can further be extended to include grid-connected systems with the ability to export excess PV-generated power to the grid, considering a combination of tariff schemes for buying and exporting power to the grid. The possible tariff combinations are (1) the TOU-STD scheme (i.e., energy is imported based on the TOU tariff and exported based on the STD tariff), (2) the TOU -TOU scheme, and (3) the STD-TOU scheme. Furthermore, works can be extended to the grid-connected system in developing countries where grid supply is inconsistent and requires the microgrid owner/operator to determine the tariff for which energy is sold to the consumers.

Chapter 5

Real-Time Economic Dispatch of CHP Systems with Energy Storage for Behind-the-Meter Industrial Distributed Energy Application

5.1 Introduction

The use of CHP systems has recently increased due to their high combined efficiency and low emissions. Using CHP systems in behind-the-meter applications, however, can introduce some challenges: Firstly, the CHP system must operate in a load-following mode to prevent power export to the grid. Secondly, if the load drops below a predefined threshold, the engine will operate at a lower temperature. Hence, lower efficiency as the fuel is only half-burnt, creating significant emissions. The aforementioned issues may be solved by combining CHP with a BESS; however, the dispatch of CHP and BESS must be optimised. Offline optimisation methods based on load prediction will not prevent power export to the grid due to prediction errors. Therefore, this chapter builds on the previously developed EMS and extends its application to control CHPs and BESS in behind-the-meter applications. The EMS uses a combination of LSTM neural networks, MILP, and RH control strategy. The RH control strategy is suggested to reduce the impact of prediction errors and enable real-time implementation of the EMS exploiting actual generation and demand data on the day. Simulation results show that the proposed method can prevent power export to the grid and reduce the operational cost by 8.75% compared to the offline method.

5.2 System Description

The grid-connected CHP system with EMS under study is presented in Figure 5-1 with red dotted lines showing the communication link between the components of the microgrid and the EMS. It comprises two CHP units rated at 250 kW_e connected to the grid, a 1000 kWh BESS, and a heat storage buffer tank. The present study considers the case of an animal feed processing factory which has both electrical and thermal energy requirements.

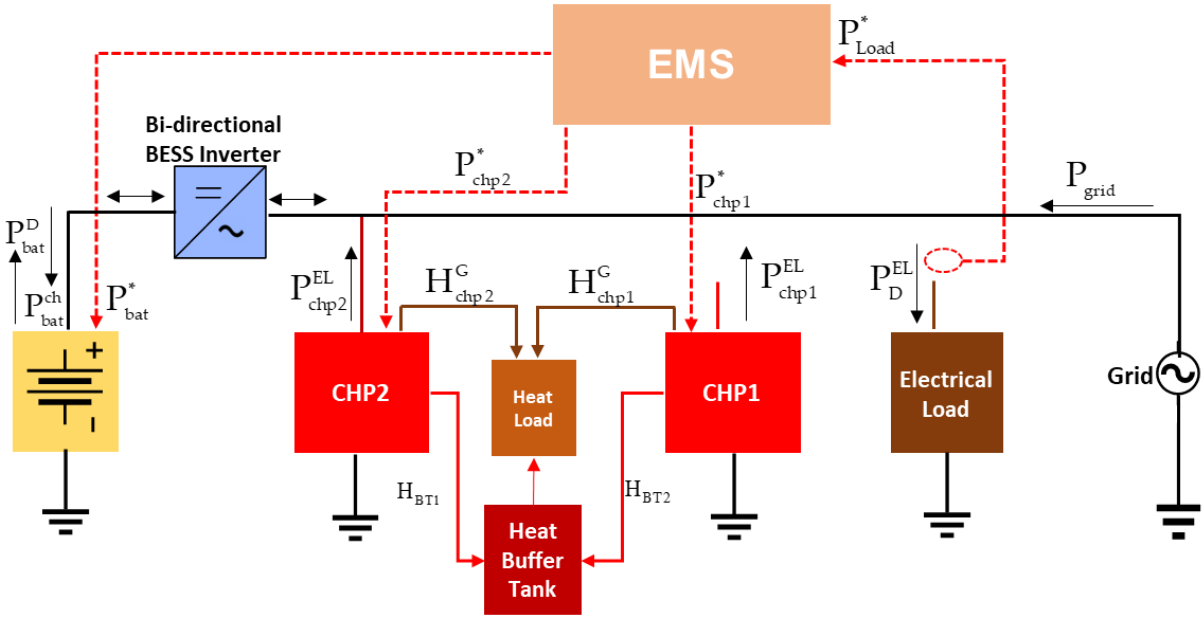

Figure 5-1: Grid-connected CHP system with energy storage (CHP+BAT+GRID).

The system is designed so that the electrical load is met by the combination of the electrical power generated from the two CHP units, power discharged from the BESS, and energy from the grid, while the recoverable heat from the CHP units should be greater than, or equal to the heat demand at all times and any excess heat will be taken by the buffer tank and utilised when the system is out of operation. This is represented in equations (5-1) and (5-2) below:

$$P^{EL}_{chp1}(t)+P^{EL}_{chp2}(t)+P^{D}_{bat}(t)+P_{grid}(t)=P^{EL}_{d}(t), \quad (5\text{-}1)$$

$$H^{G}_{chp1}(t)+H^{G}_{chp2}(t)=H_{D}(t)+H_{BT}, \quad (5\text{-}2)$$

where, $P_{chp1}^{EL}(t)$ and $P_{chp2}^{EL}(t)$ are the electrical power generated by the CHP systems, $P_{bat}^{D}(t)$ is power discharged from the BESS, $P_{grid}(t)$ is the power utilised from the grid and $H_{chp1}^{G}(t), H_{chp2}^{G}(t)$, $H_{D}(t)$, and $H_{BT}\left(H_{BT}=H_{BT1}+H_{BT2}\right)$ are the recoverable heat from the CHP units, the heat demand, and heat stored in the buffer tanks respectively.

Up to two-thirds of the energy produced by conventional electricity generation is wasted in heat. The heat recovered from the system can be calculated using equation (5-2)representing the relationship between the electrical power generated by the CHP system and the recoverable heat as:

$$H_{chp}^{G}(t)=P_{chp}^{EL}(t)\times Q_{hrr}, \qquad (5\text{-}3)$$

where, $H_{chp}^{G}(t)$ is the total heat recovered from the CHP system, and Q_{hrr} is the useful heat recovery rate.

The useful heat recovery rate Q_{hrr} shown in equation (5-3) depends mainly on the fuel consumed by the prime mover and the fuel offset. On the other hand, the fuel offset depends on the amount of useful heat recovery achieved by the CHP system, which measures the effectiveness with which the thermal energy is recovered from the prime mover and used to meet on-site thermal needs [183].

5.3 Problem Formulation

The problem formulation is based on the model shown in Figure 5-1. Since running the CHP generators under 50% capacity is harmful, the scheduling problem will consider real-time demand uncertainties and ensure that the CHP generators operate within safety limits, as stated in the manufacturer's datasheet [184].

5.3.1 Economic Operation of the Hybrid CHP System using MILP

Economic dispatch, as part of unit commitment, represents the scheduling of generators to minimise the total operating cost, which can be cast as a constrained optimisation problem. The operation of the CHP system is very similar to that of the diesel generators, which have a nonlinear quadratic cost function, as seen in equation (5-4):

$$f(x) = ax^2 + bx + c, \quad \underline{x} \le x \le \overline{x} \tag{5-4}$$

where, $\{a, b, c\}$ are the fuel cost coefficients and x is the electrical power output (power generation) of the CHP unit.

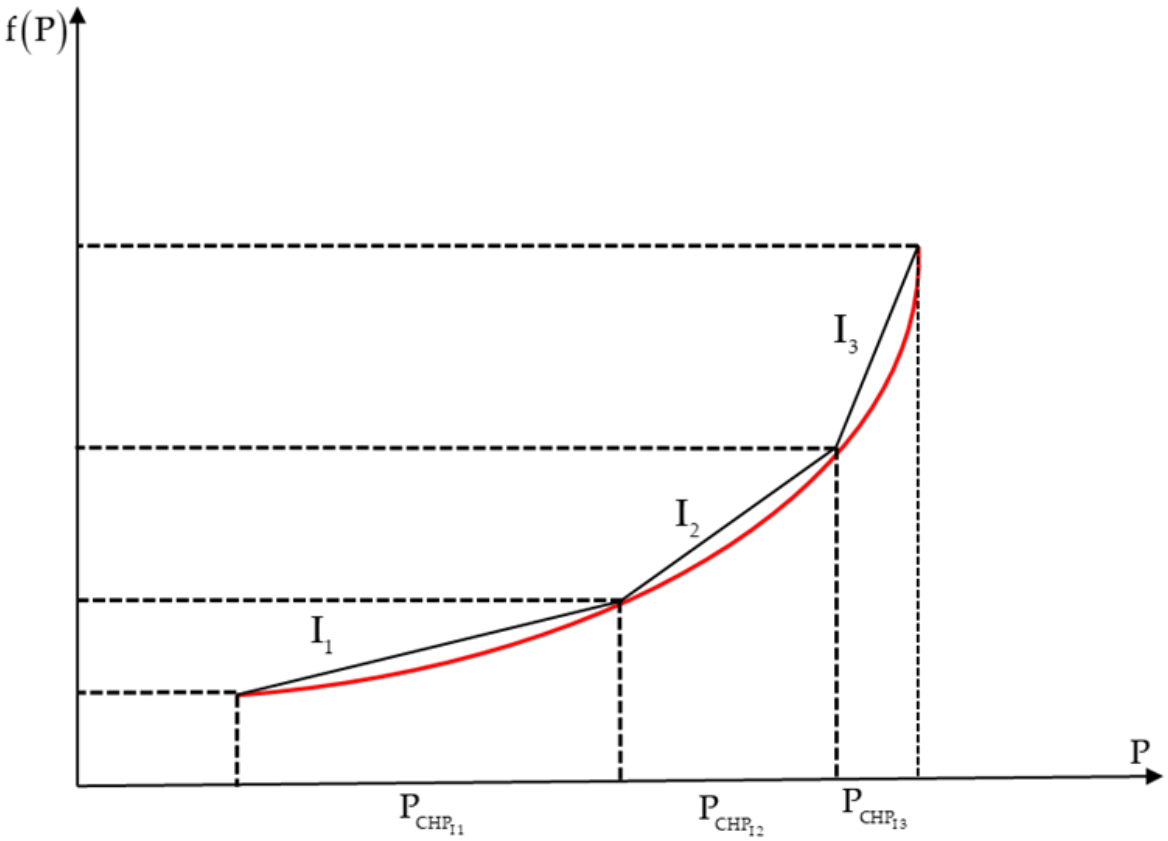

Figure 5-2: Nonlinear cost function approximated by piecewise linear approximation.

This makes it difficult to solve its economic dispatch problem using linear programming. Thus, a piecewise linear approximation of the quadratic function is suggested to make the nonlinear quadratic cost function a mixed integer linear

program (MILP) problem by approximating the nonlinear function as a series of straight-line segments [49]-[185], as shown in Figure 5-2.

The next formulation shows how the economic dispatch problem can be structured as a MILP program. At first, the nonlinear cost function is expressed as a set of linear functions from a series of straight-line segments by approximating the operation using a piecewise-linear approach divided into three operating segments, as seen in. The three segments of the CHP system are represented as I_1, I_2 and I_3 with variables $P_{CHP_{I1}}, P_{CHP_{I2}}$ and $P_{CHP_{I3}}$ that represents the marginal production in each segment. Each segment will have a slope designated as S_{I1}, S_{I2} and S_{I3} $\left(S_{I1} < S_{I2} < S_{I3}\right)$. The fuel cost is a function of the power dispatch of the CHP system and is the sum of the cost at P_I^{min} plus the sum of the linearised cost for each segment which is the slope(i.e. the slope multiplied by the $P_{CHP_{Ij}}$ variable such as:

$$F_I\left(P_{CHP_I}\right) = F_I\left(P_{CHP_I}^{min}\right) + S_{I1}P_{CHP_{I1}} + S_{I2}P_{CHP_{I2}} + S_{I3}P_{CHP_{I3}}. \quad (5\text{-}5)$$

where $S_{I1}P_{CHP_{I1}} + S_{I2}P_{CHP_{I2}} + S_{I3}P_{CHP_{I3}}$ is the sum of the linear cost function for each segment.

where,

$$0 \le P_{CHP_{Ik}} \le P_{CHP_{Ik}}^{max}. \quad (5\text{-}6)$$

for $k \in \{1,2,3\}$ and

$$P_{CHP_I} = P_{CHP_I}^{min} + P_{CHP_I} + P_{CHP_{I1}} + P_{CHP_{I2}} + P_{CHP_{I3}}. \quad (5\text{-}7)$$

$$S_{Ik} = \frac{F_I\left(P_{CHP_{Ik+1}}\right) - F_I\left(P_{CHP_{Ik}}\right)}{\left(P_{CHP_{Ik+1}}\right) - \left(P_{CHP_{Ik}}\right)}. \quad (5\text{-}8)$$

The cost function is now made up of a linear expression in the three new optimisation variables $P_{CHP_{I1}}$, $P_{CHP_{I2}}$ and $P_{CHP_{I3}}$ as an update of equation (5-8).

$$\left(\sum_{I=1}^{N_{CHP}} P_{CHP_I}\right) + P_{bat}^{D} + P_{grid} = P_{Load} \quad . \tag{5-9}$$

*w*here, N_{CHP} is the number of CHP systems in the power system.

The MILP is then formulated to solve the economic dispatch problem based on finding the minimum operating cost while respecting the imposed constraints considering decision variables in Table 5-1.

Table 5-1: MILP economic dispatch continuous and binary decision variables

Decision Variable	Variable Type	Description
$P_{grid}^{EL}(t)$	Continuous	Power from the Grid to the Electrical Load
$P_{grid}^{bat}(t)$	Continuous	Power from the Grid to the BESS
$P_{chp}^{EL}(t)$	Continuous	Power from the CHP to the Electrical Load
$P_{chp}^{bat}(t)$	Continuous	Power from the CHP to the BESS
$\gamma_{bat}^{CH}(t)$	Binary	On/off state of the BEESS charge
$\gamma_{bat}^{D}(t)$	Binary	On/off state of the BESS discharge

Figure 5-3 shows the flow chart used for the modelling framework implementation of the MILP algorithm in MATLAB environment. The set of constraints for the optimisation is explained below.

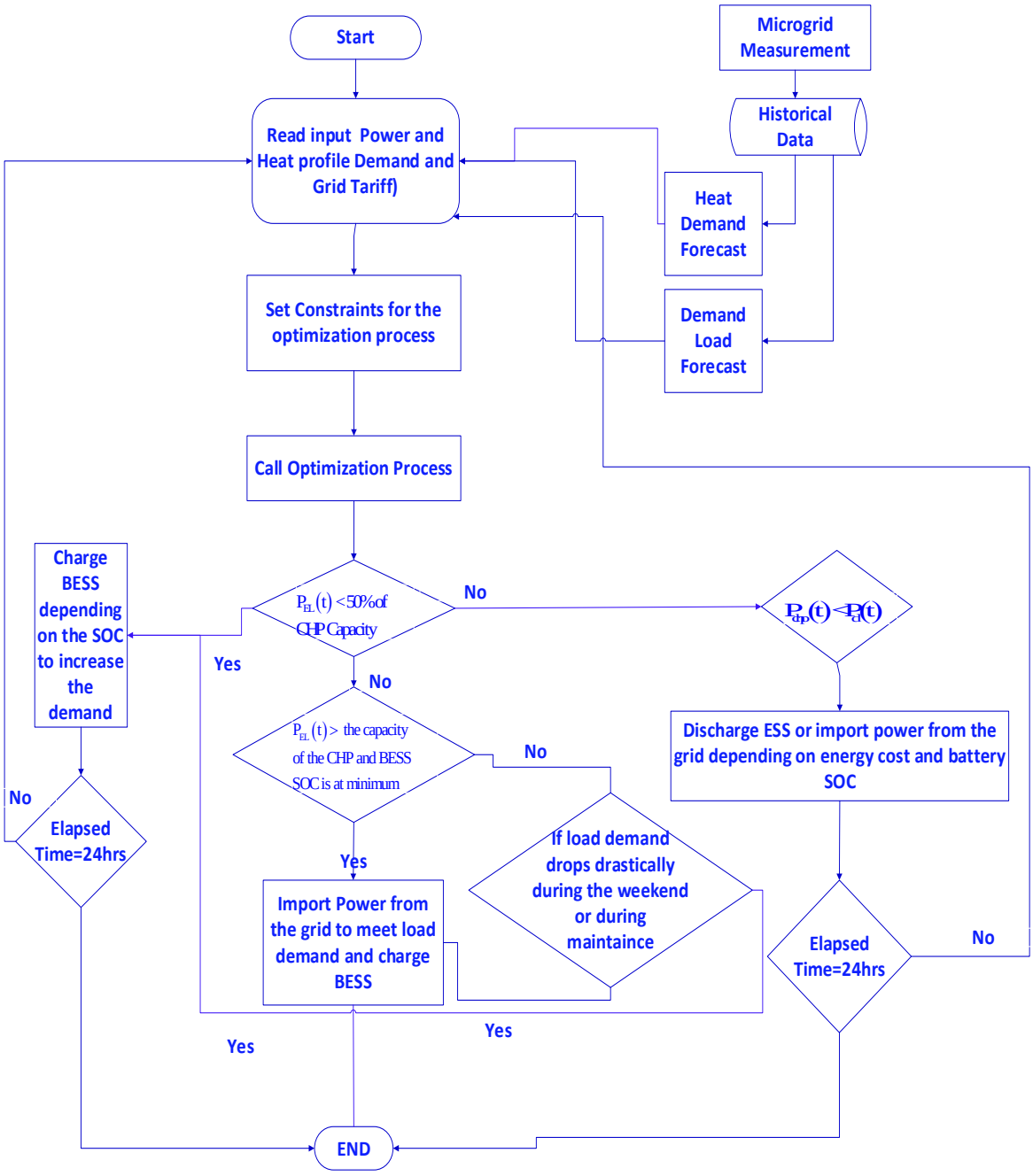

Figure 5-3: Flow chart for implementing the MILP algorithm for the economic dispatch of the CHP Units.

The equality and inequality constraints imply that the produced electricity and heat should equal the electricity demand and be greater than or equal to the heat demand, as shown in equations (5-10) and (5-11). The power imported from the grid is given by:

$$P_{grid}(t) = P_{grid}^{EL}(t) + P_{grid}^{bat}(t). \qquad (5\text{-}10)$$

where, P_{grid}^{EL} is the power from the grid utilised by the electrical load, and P_{grid}^{bat} is the power from the grid used for charging the BESS. The BESS is charged with the power from the CHP units P_{CHP}^{bat} and the power from the grid P_{grid}^{bat}.

$$P_{bat}^{CH}(t) = P_{chp}^{bat} + P_{grid}^{bat}(t). \quad (5\text{-}11)$$

The power from the BESS utilised by the electrical load is given in equation (5-12) as:

$$P_{bat}^{EL}(t) = P_{EL}(t) - P_{grid}^{EL}(t) - P_{CHP}^{EL}. \quad (5\text{-}12)$$

The grid power and CHP power utilised by the BESS at any time should be greater than or equal to zero as:

$$\left.\begin{aligned} &P_{grid}(t) \geq 0, \\ &P_{CHP}^{bat}(t) \geq 0,\ P_{grid}^{bat}(t) \geq 0 \end{aligned}\right\}. \quad (5\text{-}13)$$

The SOC is constrained by the minimum and maximum operating limits of the BESS as follows:

$$\beta_{soc}^{min} \leq \beta_{soc}(t) \leq \beta_{soc}^{max} \quad (5\text{-}14)$$

where, β_{soc} represents the BESS SOC state of charge. The inequality constraints for the BESS state of charge are given in equations (5-15) and (5-16):

$$\varphi_{BESS}\beta_{soc}(t) + P_{bat}^{CH}(t)\eta_c\Delta t - P_{bat}^{D}(t)\eta_d\Delta t \leq \varphi_{BESS}. \quad (5\text{-}15)$$

$$\beta_{soc}(t+1) = \beta_{soc}(t) - \phi_{BESS}P_{bat}^{D}(t)\times\eta_d(t) + \phi_{BESS}P_{bat}^{CH}(t)\times\eta_c(t). \quad (5\text{-}16)$$

where, φ_{EESS} represents the BESS capacity and ϕ_{EESS} is the a coefficient associated with the physical features of the BESS and converts the BESS charge/discharge from its kW units to a percentage; η_d and η_c are the charge/discharge efficiencies of the BESS, respectively.

During the optimisation process, it is important that the charging and discharging of BESS is not scheduled simultaneously. Therefore, an inequality constraint for the ‘‘on’’ and ‘‘off’’ state of the BESS charge and discharge is formulated as an integer in equation (5-17) as:

$$\gamma_{bat}^{CH}(t)+\gamma_{bat}^{D}(t)\le 1, \tag{5-17}$$

where, γ_{bat}^{CH} and γ_{bat}^{D} are binary variables representing the ‘‘on/off’’ and ‘‘off’’ states of the BESS charge and discharge, respectively. The inequality constraints for charging and discharging the BESS are shown in equation as follows:

$$\left.\begin{aligned} P_{bat}^{CH}(t) &\le P_{bat}^{CH_{max}}\times\gamma_{bat}^{CH}(t)\\ P_{bat}^{D}(t) &\le P_{bat}^{D_{max}}\times\gamma_{bat}^{D}(t)\end{aligned}\right\}. \tag{5-18}$$

The general objective function for the entire system is formulated as an economic dispatch problem in equation (5-19) as:

$$\min: Z=\sum_{t=1}^{T} P_{CHP_1}(t)\times T_{CHP_1}(t)+T_{SU_{CHP_1}}(t)+P_{CHP_2}(t)\times T_{CHP_2}(t)+T_{SU_{CHP_2}}(t)+P_{grid}(t)\times T_{grid}(t) \tag{5-19}$$

Subject to equations (5-1), (5-9)–(5-18), where, T_{SU} is the start-up cost of the CHP units, T_{chp_2} and T_{grid} are the cost of operating the CHP, and the grid tariff, respectively.

5.4 EMS Implementation

Two implementation methods for the MILP optimisation-based EMS are proposed: offline and online. The two methods are explained in detail.

5.4.1 Offline Implementation

The offline implementation is based on historical and predicted day-ahead load demand. To implement the MILP optimisation presented above, a 24-hours load profile is needed as an input. This profile is predicted using an LSTM network, a

recurrent neural network (RNN), as shown in Figure 3. The predicted data profile is then fed into the MILP optimiser, which determines the dispatch commands for the battery and CHPs for the next 24 hours. The pre-determined dispatched commands are then applied in real-time. Due to the expected anticipated error between the LSTM predicted load profile and the real-time load profile, violations of the optimisation constraints are likely to occur, particularly in the reverse flow of the grid power, i.e. power injected into the grid.

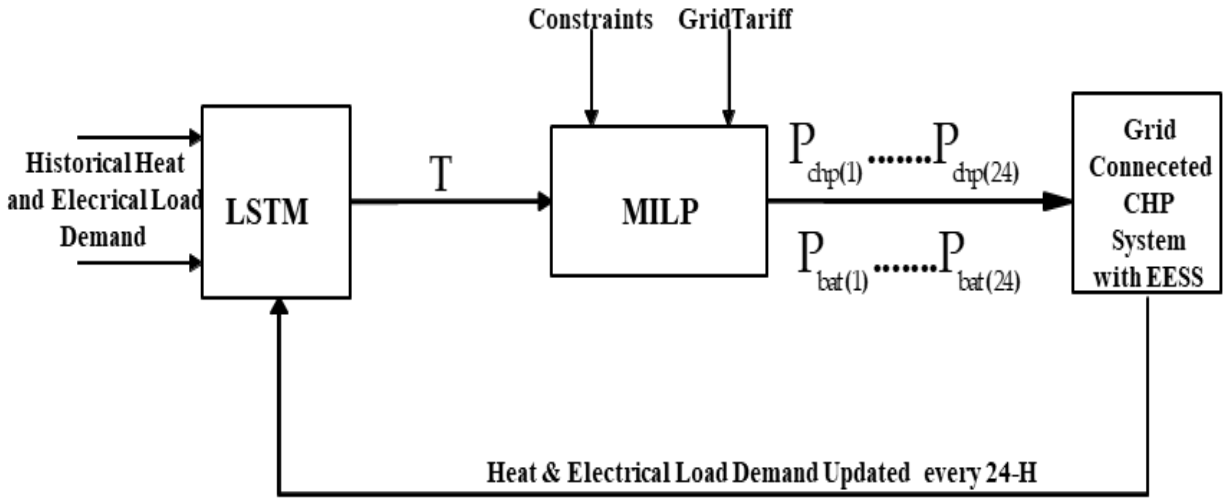

Figure 5-4: LSTM-MILP flow model for real-time operation of the grid-connected CHP system (offline optimisation scheme).

One way of solving this problem is by dispatching only the CHP commands from the offline, 'day ahead' optimisation. The BESS then operates in real-time, balancing the difference between generation and load demand. While the reverse grid power can be prevented with this scenario, the system is likely to operate sub-optimally, as the battery commands are not optimised.

5.4.2 Online Implementation using RH

The RH strategy is a concept adopted from the model predictive control (MPC), which solves control problems by using online model-based optimisation to determine the current control action [168]. It is a general-purpose control scheme that repeatedly solves a constrained optimisation problem, using future

generation and demand prediction over a moving time horizon to choose the control action. The RH control handles constraints, such as limits on control variables, directly and naturally, and generates precisely calculated control actions, respecting the constraints. The basic RH policy is straightforward. At time *t*, we consider an interval extending *T* steps into the future: $t, t+1, \ldots\ldots\ldots, t+T$ as shown in Figure 4. This method can effectively correct errors in predicting the load in future iterations for energy systems scheduling problems with high dependency on the forecasted values of load demand [169]. The RH is suggested to reduce the impact of the prediction error and enable real-time implementation of the economic dispatch problem that benefits from using real-time load data. The implantation of the online EMS is illustrated in Figure 5-5.

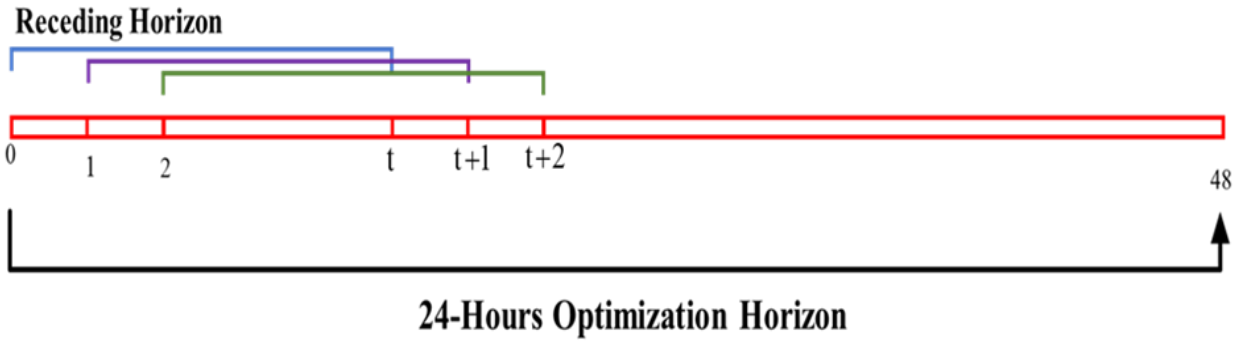

Figure 5-5: Illustration of the RH control strategy.

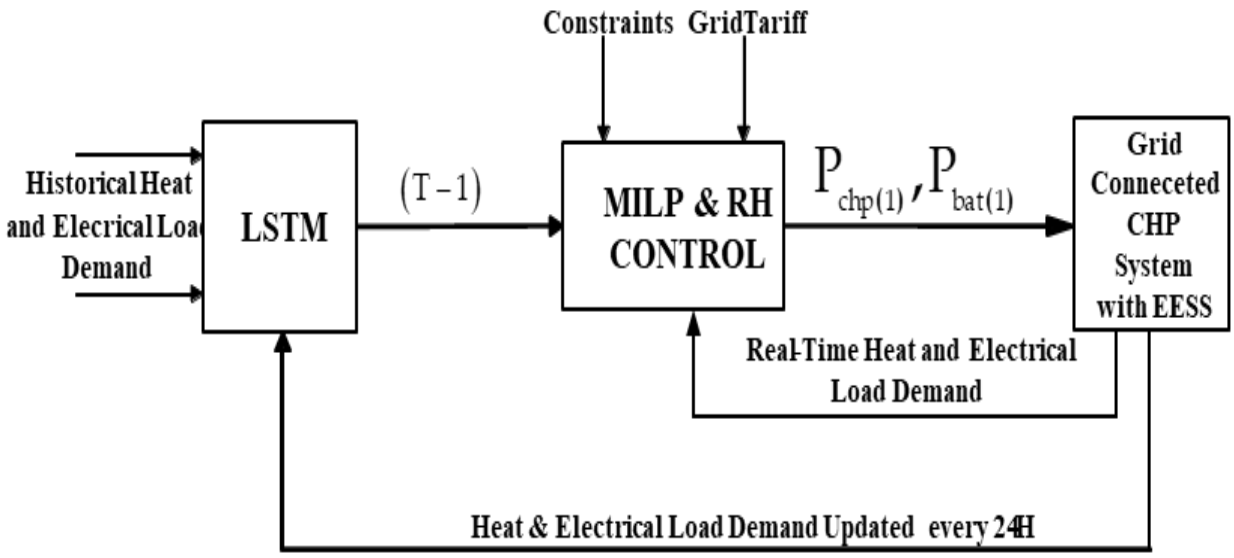

Figure 5-6: LSTM-MILP-RH flow model for real-time operation of the grid-connected CHP system (online optimisation).

The system considered here is modelled as an economic load dispatch optimisation problem for 24 hours consisting of 48-time steps using MILP. The LSTM predicts the PV generation and the load data for the next time horizon. The dispatch problem is then solved using MILP and RH control strategy [162]. Only the dispatch command for the real-time (first-time step) is applied to the CHP Units and BESS, and the process is repeated.

5.5 Simulation Results

In this section, the details of the case study and the results of the EMS implementation are presented to show the technical specification of the six-in-line cylinder gas engine CHP units (GXC250-NG) [182]. The values in Table 5 3 are calculated from Table 5 2. Tables 5 4, and 5 5 present the characteristics of the lithium-ion battery package and the daily time of use tariff cost of gas, respectively.

Table 5-2: CHP Power and Efficiency @ 50Hz

Description	Full Load Operation	75% Load Operation	50% Load Operation
Load	100%	75%	50%
Electrical Power (kW_e)	250	187.5	125
Heat Power (kW_{th})	333	249.75	166.5
Fuel/Energy Input (kW)	710	522	361
Electrical Efficiency	35.5%	35.9%	34.3%
Heat Efficiency	47.3%	47.8%	45.9%
Total Efficiency	82.8%	83.7%	80.2%

Table 5-3: The CHP Input-Output Curve

Description	Values (CHP)
a	7.045×10^{-5}
b	0.0297
c	2.0654

Table 5-4: Characteristics of the Lithium-Ion BESS Package

Description	Value
Rated Depth of Discharge (DOD) %	70
Maximum charging power (kW)	250
Battery charge efficiency (%)	95
Battery discharge efficiency (%)	95
Maximum State of Charge (%)	100
Minimum State of Charge (%)	30
Nominal EESS Capacity @ 100% SoC (kWh)	1000

Table 5-5: Daily TOU Electricity Tariff / Cost of Gas

Description	Time	Tariff
Off-peak time	00:00 AM -7:30 AM	0.106 £/kWh
Peak time	08:00 AM-23:30 PM	0.14 £/kWh
Cost of Gass		0.0198£/kWh

The economic dispatch and energy management system simulation was performed in MATLAB with a 32 GB 64-bit operating system computer, dual-core i7, 2.70–2.90 GHz. The average computational time of the simulation was about 11.93 ± 2.012 seconds. The offline and online economic dispatch results with

optimal cost comparison are presented below. The proposed economic dispatch simulation was performed in MATLAB language.

5.5.1 Load Prediction using LSTM

The LSTM model is trained with the RMSE loss function, Adam optimiser (adaptive movement optimisation), which is an alternative optimisation algorithm for stochastic gradient descent for training deep learning models. 500 max epoch with a single gradient threshold and initial learn rate of 0.005 have been chosen. The RMSE indicates the deviation between the predicted value and the measured value, and it is a measure of the forecasting error [162] [166]. Before training or testing a neural network, the training and testing data must go through a series of pre-processing steps. Normalisation was used as a pre-processing approach in this case since it lowers the impact of various scales on the acquired data, as well as interpolating any missing data points and arranging the data (historical load demand) in chronological order. The normalised data is utilised as an input to the LSTM network in the next step [162]. The initial predicted electrical load and heat demand are shown in Figure 5-7 and Figure 5-8.

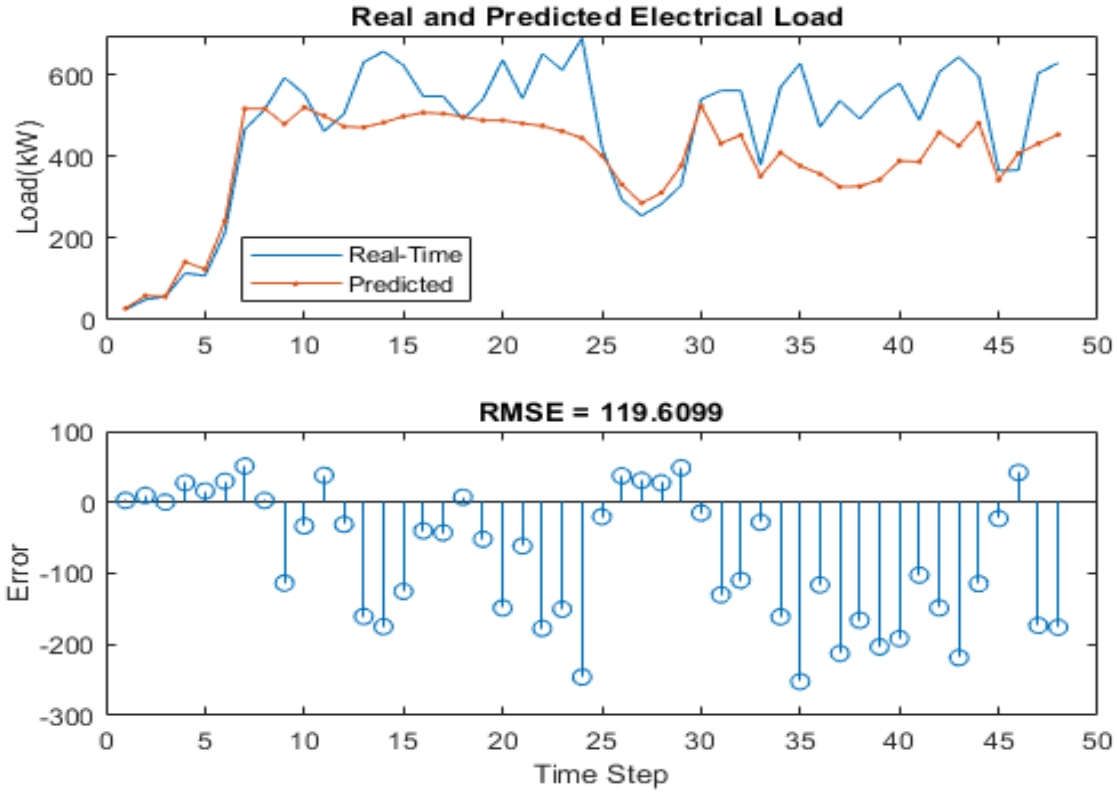

Figure 5-7: Real and predicted electrical load with RMSE

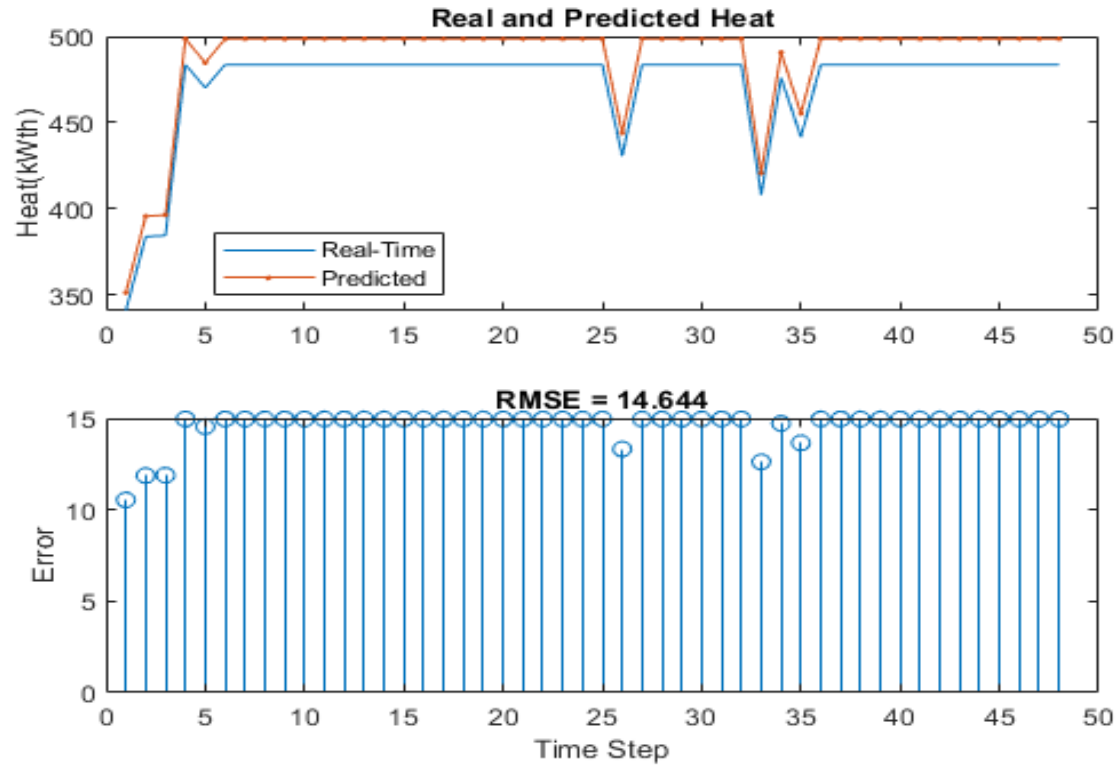

Figure 5-8: Real and Predicted Heat Demand with RMSE.

5.5.2 EMS Implementation Results

Four Scenarios are considered in our simulations:

- Scenario 1, predicted data is the same as that of the real data; offline EMS provides dispatch commands to CHPs and the battery. This represents the ideal scenario, which is not achievable and does not exist in reality but provides a best case. The results provide a benchmark for comparing the other scenarios.
- Scenario 2, predicted data is different from real data; offline EMS provides dispatch commands to CHPs and batteries.
- Scenario 3, predicted data is different from real data; offline EMS provides dispatch commands to CHPs only. The battery operates to balance generation and load in real-time.
- Scenario 4, predicted data is different from real data; online EMS provides dispatch commands to CHPs and batteries.

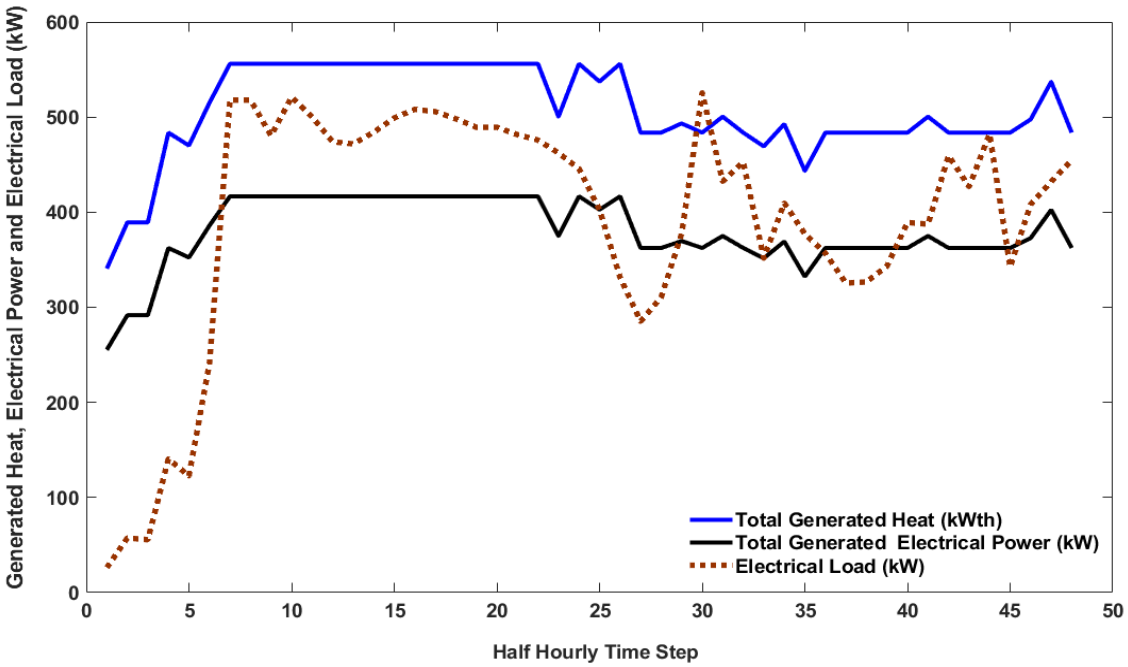

Figure 5-9: Total output electrical power and heat generated from 2×250kWe CHP units using predicted load demand data.

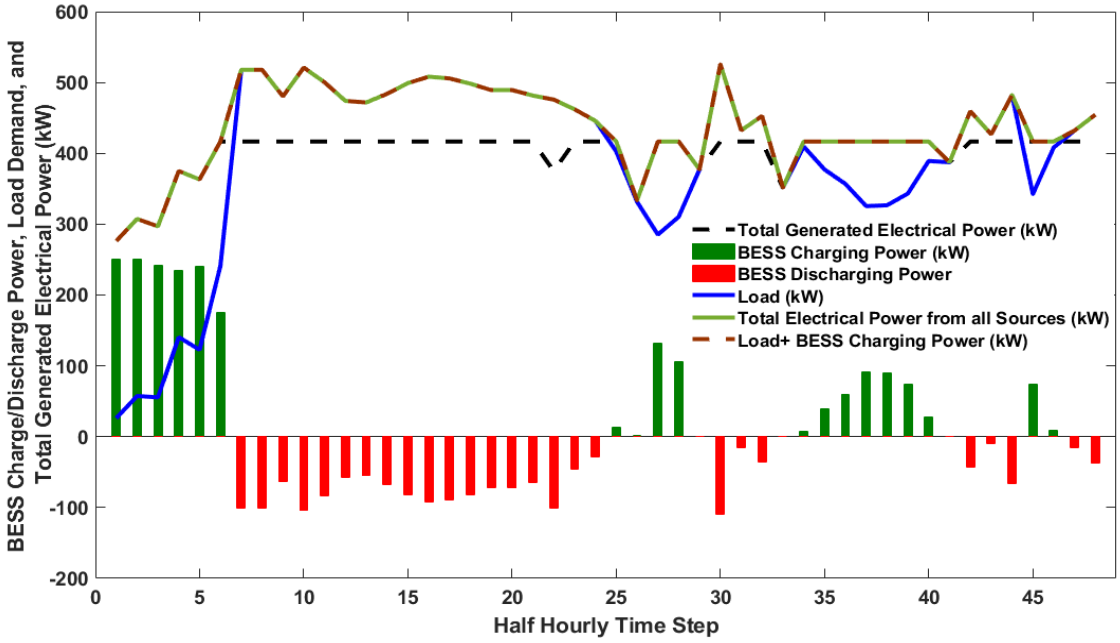

Figure 5-10: Total electrical power generated, the ideal real-time load demand and BESS charge/discharge command (scenario 1).

Figure 5-9 shows the electrical power, the heat generated from the CHP units and the predicted load demand resulting from the offline optimisation in scenario one using predicted data. The result of the first scenario, which is the ideal case, is shown in Figure 5-10. There is no power exported to or imported from the grid, and total generation equals load plus battery discharge power.

For the second scenario, the commands of the CHP units and the BESS from the offline optimisation are dispatched on the real-time data. The results are presented in Figure 5-11, and Figure 5-12 show that power is exported to the grid whenever there is an excess generation, which violates the constraints that cannot be enforced in the offline architecture. In the third scenario, only the CHP command is dispatched from the offline optimisation. At the same time, the BESS offsets the difference between the load demand and the dispatched CHP command in real-time. Total power generated equals the load demand plus battery charge power, and power is not exported into the grid, as seen in Figure 5-13 and Figure 5-14. Since the CHP command for the three scenarios is based

on offline optimisation, the total generated heat for all scenarios remains the same as in Figure 5-15, where the total generated heat is greater than or equal to the heat demand with excess generated heat stored in the heat buffer tank, respecting the constraint in equation (5-2).

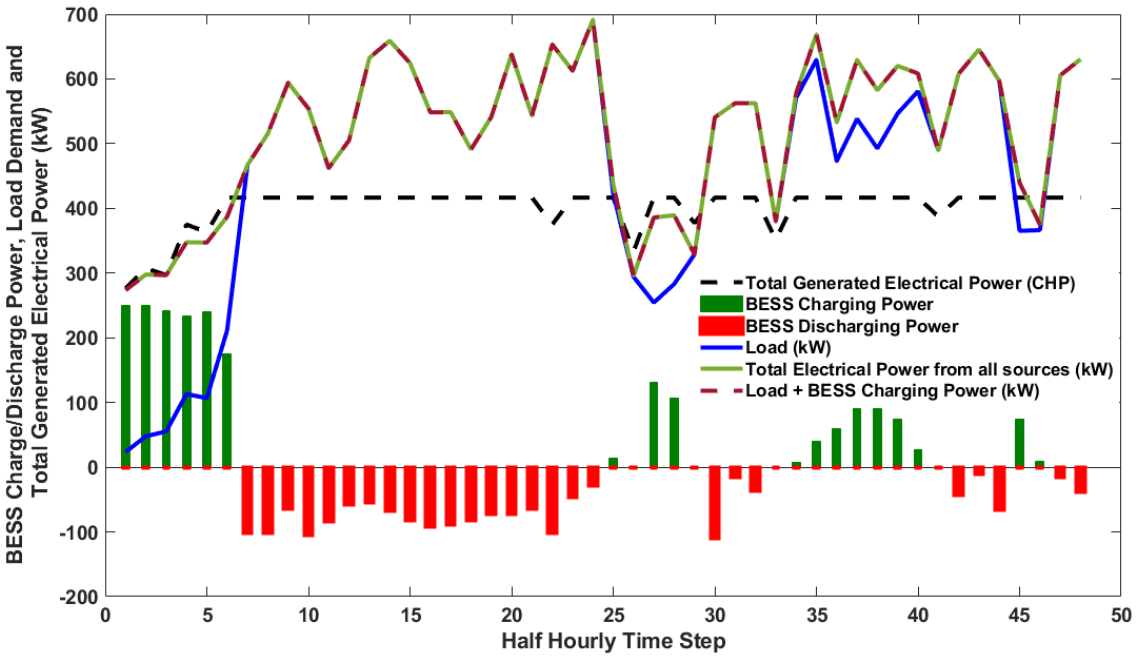

Figure 5-11: Total electrical power generated, real-time load demand and BESS charge/discharge command (Scenario 2).

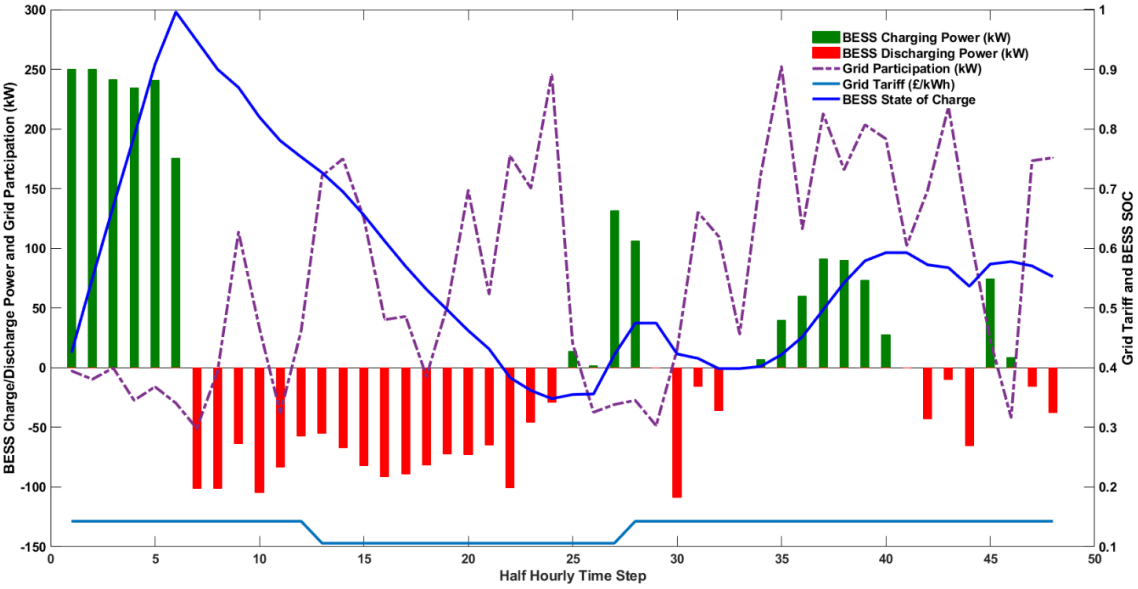

Figure 5-12: Grid participation, BESS SOC, grid tariff and BESS charge/discharge command (Scenario 2).

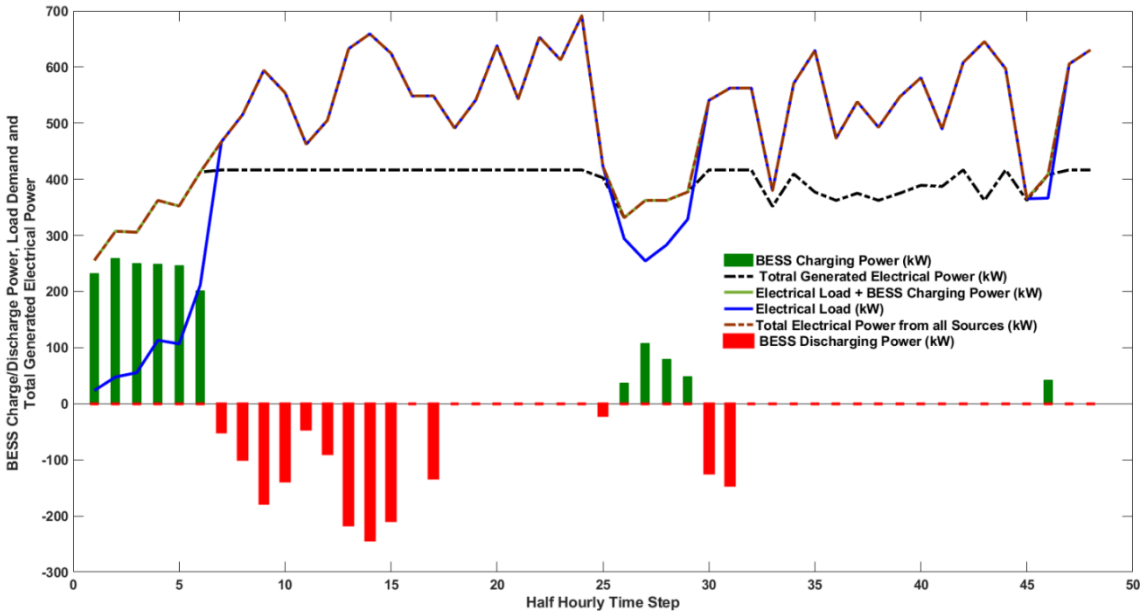

Figure 5-13: Total electrical power generated, real-time load demand and BESS charge/discharge command (Scenario 3).

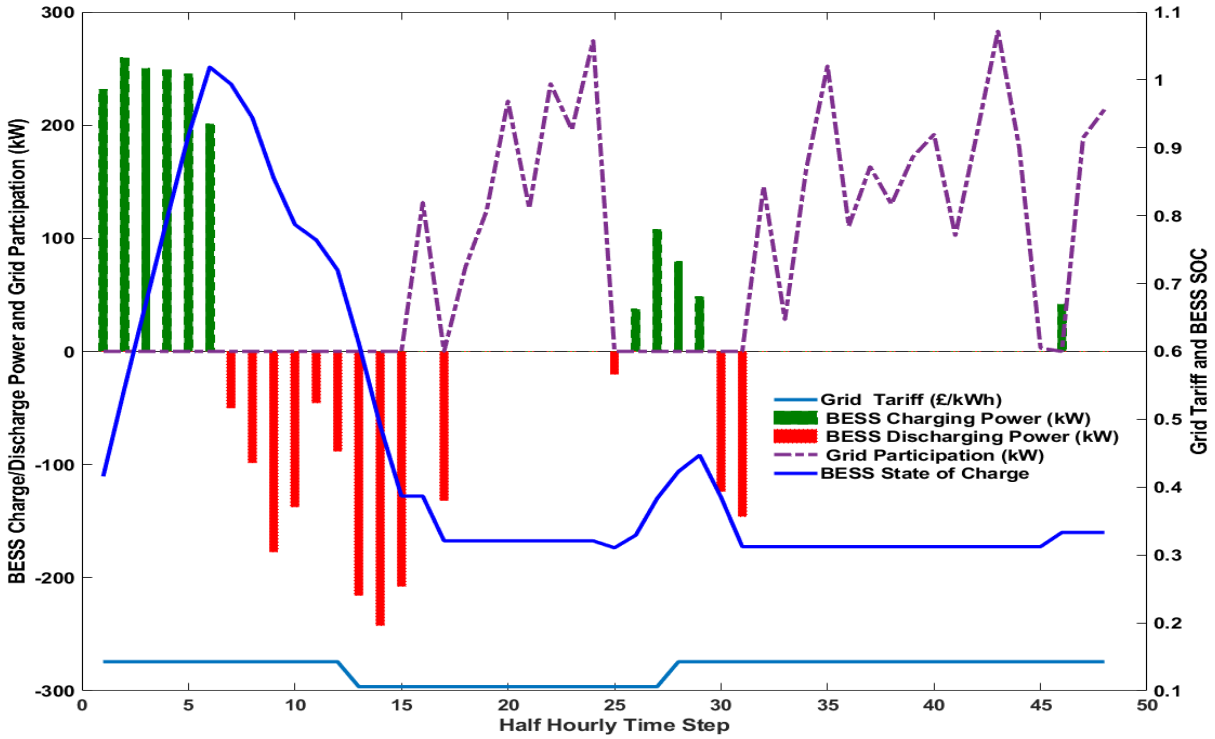

Figure 5-14: Grid participation, BESS SOC, grid tariff and BESS charge/discharge command (Scenario 3).

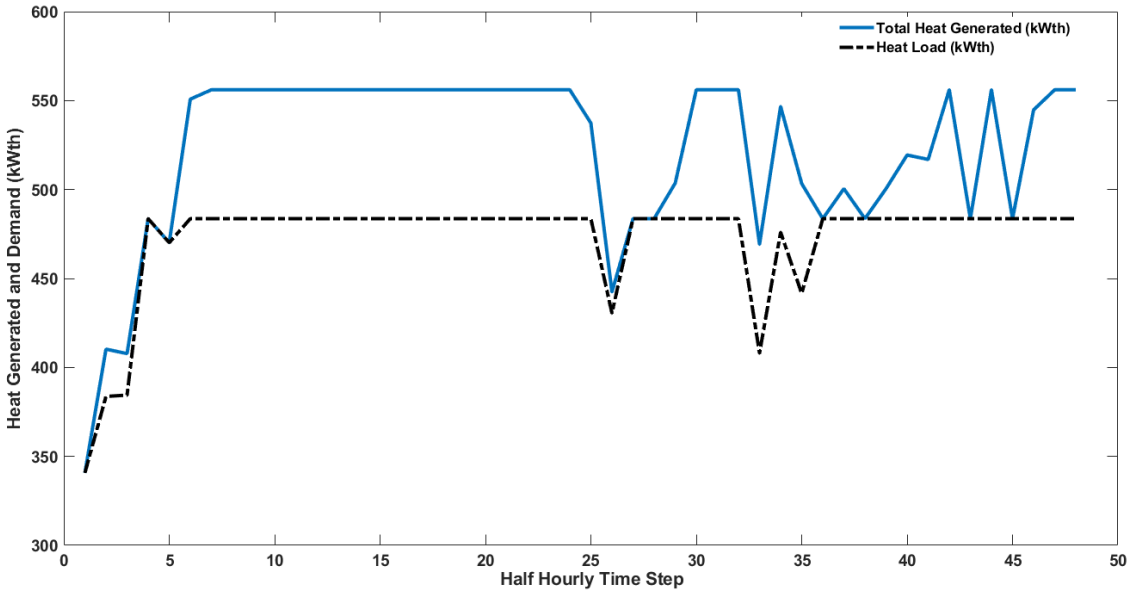

Figure 5-15: Total heat generated by the CHP units and heat demand (offline optimization).

For online optimisation (Scenario 4), the LSTM-MILP-RH approach has been used. The results are presented in Figure 5-16-Figure 5-19. Figure 5-16 shows the total power generated by the two CHP units, the recoverable heat, and the difference between the power generated by the CHP units and the real-time load demand. Figure 5-17 shows that with the online optimisation, the total generated power from all sources can meet the load demand in real-time using the RH control strategy. The charge/discharge power of the BESS, the state of charge and the power imported from the grid is shown in Figure 5-18. This confirms that the concept of real-time load following can easily be achieved using the proposed online optimisation method. Figure 5-19 shows the total generated heat and heat demand, where the total generated heat is greater than or equal to the heat demand, also respecting the constraint in equation (5-2).

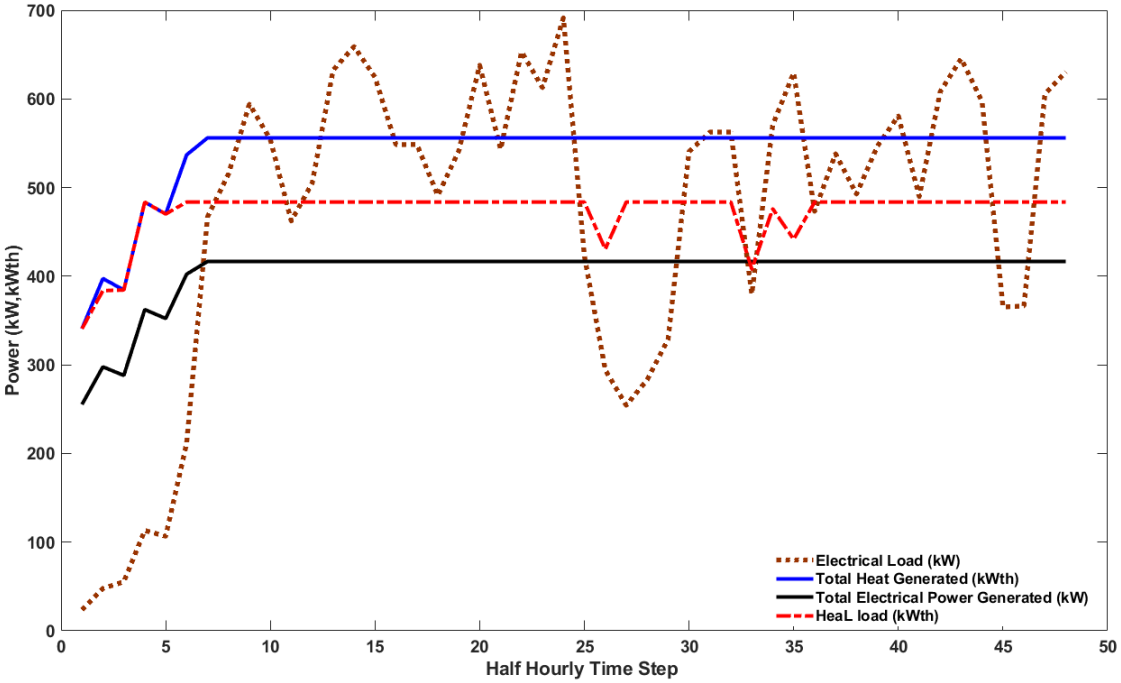

Figure 5-16: Total power and heat generated from 2×250kWe CHP units vs real-time electrical load (online optimization).

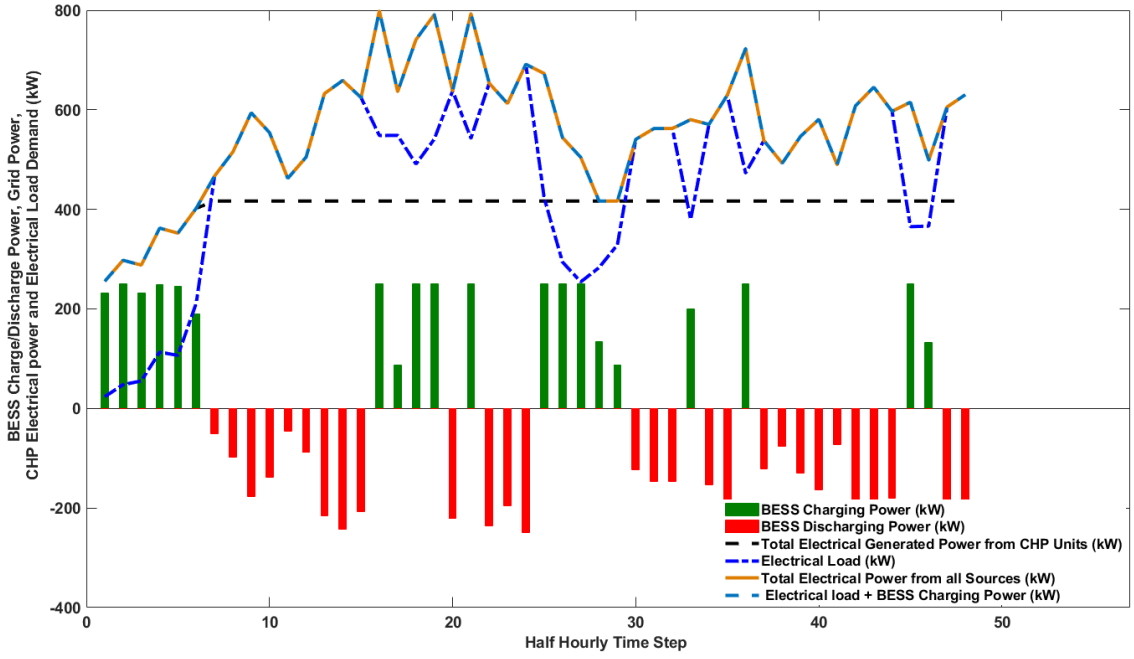

Figure 5-17: Total electrical power generated, real-time load demand and BESS charge/discharge command (scenario 4).

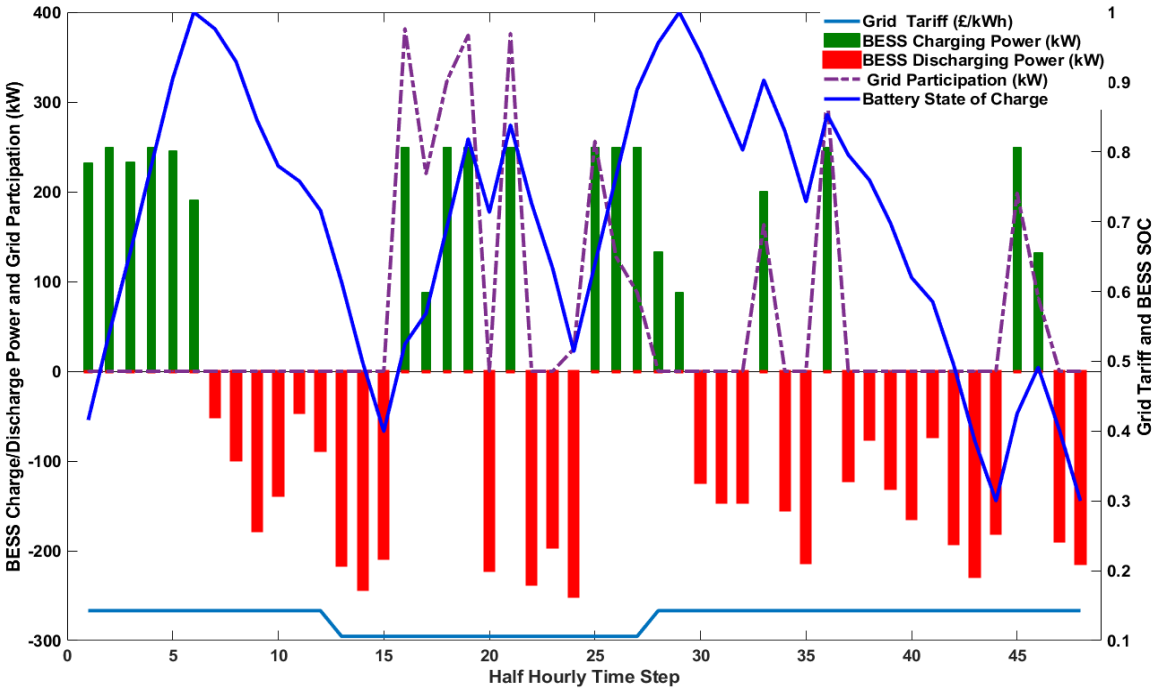

Figure 5-18: Grid participation, BESS SOC, grid tariff and BESS charge/discharge command (scenario 4).

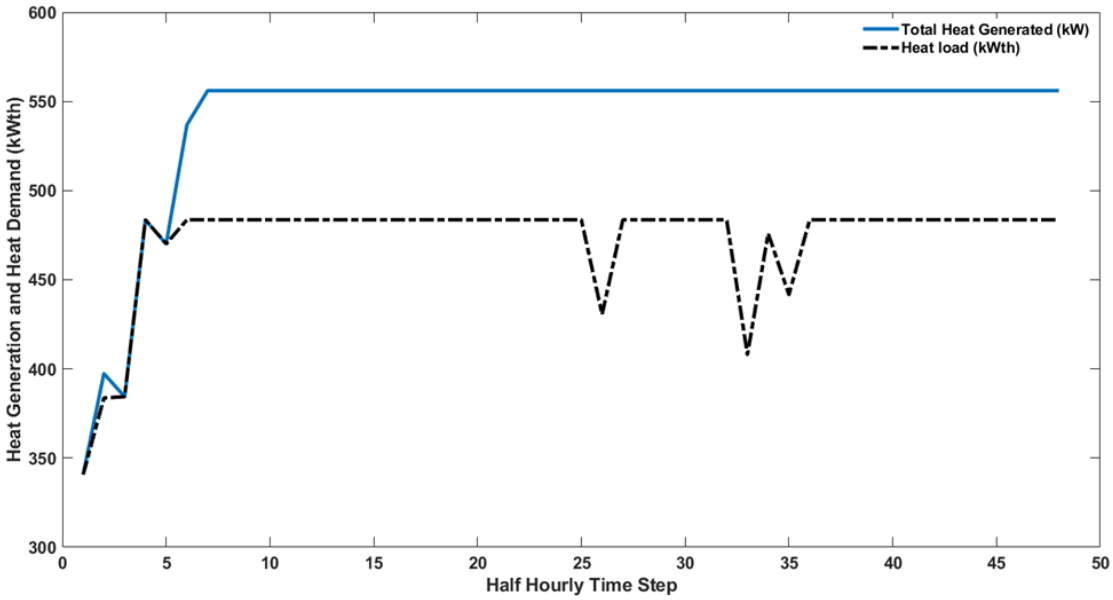

Figure 5-19: Total heat generated by the CHP units and heat demand (online optimization).

Table 5-6: Total Daily Operating cost and % Saving for all Scenarios

Description	Scenario 1 (Ideal)	Scenario 2 (0ffline)	Scenario 3 (Offline)	Scenario 4 (Online)	Grid Supply Only
Total Daily Operating (£)	333.65	602.15	453	413.4	731.98
% Daily Cost Savings WRT Grid Supply Only	54.4	17.7	38.1	43.5	-

Table *5-6* shows the operating cost of the grid-connected CHP system from the offline and online optimisation implemented in real-time compared with the operating cost of the factory when supplied with the grid only. As seen from the percentage cost savings, the results of the offline optimisation (when only the CHP command is dispatched in real-time) are compared with the result of the online optimisation. It is seen that the online optimisation approach is way better in terms of grid utilisation, total operating cost, and percentage cost savings for the model under study. The online approach in scenario four outperforms the offline approach in scenario three by 8.75% in terms of cost savings between the two scenarios and 5.4% when both scenarios are compared to grid supply only, as seen in Table 5-6 and about 7.1% when both scenarios are compared to scenario one (Ideal Scenario).

5.6 Summary/ Discussion

This chapter evaluates the economic operation of a hybrid grid-connected CHP system designed to meet a production factory's electrical and heat demand. The focus is to ensure that the CHP remains in operating mode throughout the period of production, having set a minimum operating condition with fluctuating load demand that sometimes falls below the minimum safe and economical operating condition for the CHP Units. The chapter has proposed an RH-based real-time EMS which forecasts the load demand using LSTM and optimises the operation using MILP. Simulation results have shown that the proposed online EMS can reduce the operational cost compared to the offline EMS thanks to its ability to correct forecast errors using real-time data. Furthermore, the online EMS has been able to meet all the constraints, particularly limiting power from

being injected into the grid and preventing CHP units from operating below their safe limits.

Chapter 6

Conclusion and Future Works

6.1 Conclusion

This study focuses on the techno-economic analysis of BESS application in energy management for microgrids. It proposes an energy management system to control BESS systems in grid-connected microgrids and CHP applications. After a careful review of several pieces of research done in the area of energy management systems for grid-connected microgrids, it is clear that the application of energy storage in the control and operation of microgrids cannot be overemphasized. However, the optimization models utilised in the energy management of microgrids that incorporate BESS have not taken into consideration the real-time control of the charge/discharge cycle of the BESS. Because of its long-term memory, the LSTM network was used in the first part of this study work to operate the EMS in real-time. This was done in order to make predictions regarding variables in systems like load demand and PV generation. After that, the RH control technique was used for the optimisation every hour, considering the predicted load demand and PV generation. The LSTM predicts the PV generation and load data for the entire day, and the MILP algorithm solves the optimal dispatch problem. The dispatchable BESS directives for the first hour are implemented in real-time. The real data was utilised to update the LSTM input, which was then repeated for the subsequent time step. The EMS can reduce the unpleasant challenges related to the stochasticity of the PV generation and the real-time power imbalances by utilising this strategy. The proposed approach was evaluated by comparing the daily operating cost against a reference benchmark. The MILP optimization strategy was chosen because it

offers a flexible and reliable solution for resolving complicated issues by discovering the optimal energy management link between the plants and utilities and making quick energy management choices using integer decision variables. In order to operate the microgrid with the greatest resource efficiency and lowest operating cost while adhering to the operational limits of the system, it systematically determines the optimum trade-off. The most recent projections and information about the strategy were used by the RH control strategy to adjust to new events and operational situations.

The proposed MILP-LSTM optimization framework was executed considering two scenarios: Online Optimization - Execution in every hour in real-time using a receding horizon of 24 hours and Offline Optimization – Execution once a day using a single set of LSTM predicted data.

Simulations were carried out for different operating conditions for 12 months. The BESS's charge and discharge timings depend on the grid's TOU tariff, and the microgrid's ideal performance is assessed in terms of the daily operating cost of energy. Through the process of optimising the microgrid, one may determine the most effective schedule for the grid-connected microgrid. This solution ensures a longer life for the BESS since it uses the BESS charge/discharge cycle, limiting restriction in all circumstances as BESS deterioration heavily relies on the charge/discharge cycle.

Furthermore, the results of the simulation studies that were performed on the two different scenarios throughout the year show that the LSTM-MILP-RH (online) control strategy used in the online optimization is more effective in terms of reducing the daily operating cost when compared to the LSTM-MILP (offline) optimization approach, with the benchmark daily operating cost being used as a

reference. The conclusion was reached after the simulation studies were carried out on the two different scenarios. This method is flexible enough to be utilised with a variety of TOU tariff types and has the potential to be implemented in commercial, residential, and stand-alone microgrids.

The defined optimization models simultaneously optimize the use of all the controllable resources at the operation level and show that the proposed online strategy outperforms the offline optimisation strategy reducing the operating cost by 6.12% in the first case and 3.3% in the second while guaranteeing the limits placed on the BESS charge/discharge cycle. However, the optimal operating cost for the first scenario is always higher than that of the second.

An analysis of the EMS model is evaluated in the next chapter of the thesis. This evaluation takes into account various TOU and standard tariffs with the intention of determining the effect of the TOU on the BESS charge/discharge cycle limits and how a change in the BESS charge/discharge cycle limit will affect the daily operating cost of the microgrid through the use of a simple input-output simulation analysis. The contribution of this chapter of the thesis was to perform the optimal operation of the PV-BESS grid-connected microgrid according to different TOU and standard flat tariff schemes for community microgrid application. For the four tariff schemes: (1) Residential TOU tariff (RTOU), (2) Economy seven tariff (E7T), (3) Economy ten tariff (E10T), and (4) Standard flat tariff (STDF). It was found that the RTOU tariff scheme gives the lowest operating cost, followed by the E10T tariff scheme with savings of 63.5% and 55.5%, respectively, with a consistent BESS charge/discharge cycle of two per day when compared to the grid-only operation. However, the RTOU and E10 tariff scheme is mainly used for residential applications with the duck curve load demand structure. For

community grid-connected microgrid applications, the E7T and STD are the most likely options offered by energy suppliers, except it is a residential-only community. It was found that even though the E7T is the most expensive for grid-only applications, as seen in Table 4-2, it has a cost savings of 54.2% for the PV-BESS configuration as against 39.9% of the STD tariff scheme.

Finally, the last chapter of the thesis takes a look at the economic operation of a hybrid grid-connected CHP system designed to meet a production factory's electrical and heat demand. The focus is to ensure that the CHP remains in operating mode throughout the period of production, having set a minimum operating condition with fluctuating load demand that sometimes falls below the minimum safe and economical operating condition for the CHP Units. This Chapter has proposed an RH-based real-time EMS which forecasts the load demand using LSTM and optimises the operation using MILP. Simulation results have shown that the proposed online EMS can reduce the operational cost compared to the offline EMS thanks to its ability to correct forecast errors using real-time data. Furthermore, the online EMS has been able to meet all the constraints, particularly limiting power from being injected into the grid and preventing CHP units from operating below their safe limits.

6.2 Future Works

In addition to the contribution of this research work which has provided a considerable effort to solve the problem of the transition from a traditional power grid system to a modern smart grid system by integrating renewable energy resources, there is the possibility of promising future research works considering the methods developed in this thesis since the microgrid and smart grid are now very active research areas that will attract substantive investments in the next decade.

The first will be to conduct an experimental determination considering the control of BESS charge/discharge limits in grid-connected microgrids to reduce the gap between optimization theory and experimental operation of microgrids under different scenarios. Secondly will be to evaluate the effects of the proposed EMS solution, considering the problem from the DNO's point of view and the proposed feasible solution.

This work can also be extended to grid-connected and island-based interconnected microgrid systems, with each microgrid having its EMS and a centralized EMS between the interconnected system that actively participates in the energy market. Considering the use of the BESS, two scenarios can be considered as follows:

1. The system is designed in such a way that each microgrid within the interconnected system should have their own BESS
2. Implementation of a centralised BESS system.

A robust demand side management which would include a more complex system with EV charging and the possibility of excess generated energy exported to the grid, is another area of research that should be looked at considering the EMS and the implementation strategy proposed in this thesis.

References

[1] H. Zhang, F. Mollet, C. Saudemont, and B. Robyns, “Experimental validation of energy storage system management strategies for a local DC distribution system of more electric aircraft,” *IEEE Transactions on Industrial Electronics*, vol. 57, no. 12, pp. 3905–3916, 2010, DOI: 10.1109/TIE.2010.2046575.

[2] Z. Zhang, J. Wang, and X. Cao, “Economic dispatch of microgrid considering optimal management of lithium batteries,” in *POWERCON 2014 - 2014 International Conference on Power System Technology: Towards Green, Efficient and Smart Power System, Proceedings*, 2014, no. Powercon, pp. 3194–3199. DOI: 10.1109/POWERCON.2014.6993716.

[3] J. P. Fossati, A. Galarza, A. Martín-Villate, and L. Fontán, “A method for optimal sizing energy storage systems for microgrids,” *Renew Energy*, vol. 77, pp. 539–549, 2015, DOI: 10.1016/j.renene.2014.12.039.

[4] C. Chen ; S. Duan ; T. Cai ; B. Liu ; G. Hu, “Smart energy management system for optimal microgrid economic operation title,” *IET Renewable Power Generation*, vol. 5, no. 3, pp. 258–267, 2011, doi: 10.1049/iet-rpg.2010.0052.

[5] D. E. Olivares, C. A. Canizares, and M. Kazerani, “A centralized energy management system for isolated microgrids,” *IEEE Trans Smart Grid*, vol. 5, no. 4, pp. 1864–1875, 2014, DOI: 10.1109/TSG.2013.2294187.

[6] A. Chaouachi, R. M. Kamel, R. Andoulsi, and K. Nagasaka, “Multiobjective intelligent energy management for a microgrid,” *IEEE Transactions on Industrial Electronics*, vol. 60, no. 4, pp. 1688–1699, 2013, DOI: 10.1109/TIE.2012.2188873.

[7] M. Soroush and D. J. Chmielewski, “Process systems opportunities in power generation, storage and distribution,” *Comput Chem Eng*, vol. 51, pp. 86–95, 2013, DOI: 10.1016/j.compchemeng.2012.06.027.

[8] V. Sharma, M. H. Haque, and S. M. Aziz, “Energy cost minimization for net zero energy homes through optimal sizing of battery storage system,” *Renew Energy*, vol. 141, no. 2019, pp. 278–286, 2019, DOI: 10.1016/j.renene.2019.03.144.

[9] W. El-Khattam, K. Bhattacharya, Y. Hegazy, and M. M. A. Salama, “Optimal investment planning for distributed generation in a competitive electricity market,” *IEEE Transactions on Power Systems*, vol. 19, no. 3, pp. 1674–1684, 2004, DOI: 10.1109/TPWRS.2004.831699.

[10] A. Das and Z. Ni, “A computationally efficient optimization approach for battery systems in islanded microgrid,” *IEEE Trans Smart Grid*, vol. 9, no. 6, pp. 6489–6499, 2018, DOI: 10.1109/TSG.2017.2713947.

[11] T. A. Nguyen and M. L. Crow, “Stochastic Optimization of Renewable-Based Microgrid Operation Incorporating Battery Operating Cost,” *IEEE Transactions on Power Systems*, vol. 31, no. 3, pp. 2289–2296, 2016, DOI: 10.1109/TPWRS.2015.2455491.

[12] Y. Wang and D. Gladwin, “Power Management Analysis of a Photovoltaic and Battery,” 2021.

[13] Y. Wang, Y. Huang, Y. Wang, H. Yu, R. Li, and S. Song, “Energy management for smart multi-energy complementary micro-grid in the presence of demand response,” *Energies (Basel)*, vol. 11, no. 4, 2018, DOI: 10.3390/en11040974.

[14] R. Khezri, S. Member, A. Mahmoudi, S. Member, M. H. Haque, and S. Member, “A Demand Side Management Approach For Optimal Sizing of Standalone Renewable-Battery Systems,” vol. 12, no. 4, pp. 2184–2194, 2021.

[15] T. Wakui, T. Kinoshita, and R. Yokoyama, “A mixed-integer linear programming approach for cogeneration- based residential energy supply networks with power and heat interchanges,” vol. 68, pp. 29–46, 2014.

[16] M. Nemati, M. Braun, and S. Tenbohlen, “Optimization of unit commitment and economic dispatch in microgrids based on genetic algorithm and mixed integer linear programming,” *Appl Energy*, vol. 210, pp. 944–963, 2018, DOI: 10.1016/j.apenergy.2017.07.007.

[17] A. Parisio and L. Glielmo, “A mixed integer linear formulation for microgrid economic scheduling,” in *2011 IEEE International Conference on Smart Grid Communications, SmartGridComm 2011*, 2011, pp. 505–510. doi: 10.1109/SmartGridComm.2011.6102375.

[18] I. E. Agency, “Photovoltaic Module Energy Yield Measurements: Existing Approaches and Best Practice,” *Iea-Pvps Reports*, vol. 1, no., pp. 1–476, 2018.

[19] M. Konstantinou, S. Peratikou, and A. G. Charalambides, “Solar Photovoltaic Forecasting of Power Output Using LSTM Networks,” 2021.

[20] P. Xie, Y. Jia, C. Lyu, H. Wang, M. Shi, and H. Chen, “Optimal sizing of renewables and battery systems for hybrid AC / DC microgrids based on variability management,” vol. 321, no. October 2021, 2022.

[21] R. Luna-Rubio, M. Trejo-Perea, D. Vargas-Vázquez, and G. J. Ríos-Moreno, “Optimal sizing of renewable hybrids energy systems: A review of methodologies,”

Solar Energy, vol. 86, no. 4, pp. 1077–1088, 2012, DOI: 10.1016/j.solener.2011.10.016.

[22] A. M. Elshurafa, S. R. Albardi, S. Bigerna, and C. A. Bollino, “Estimating the learning curve of solar PV balance–of–system for over 20 countries: Implications and policy recommendations,” *J Clean Prod*, vol. 196, pp. 122–134, 2018, DOI: 10.1016/j.jclepro.2018.06.016.

[23] A. Jäger-Waldau, *Jrc Science for Policy Report*. 2019. doi: 10.2760/326629.

[24] L. Idoko, O. Anaya-Lara, and A. McDonald, “Enhancing PV modules efficiency and power output using multi-concept cooling technique,” *Energy Reports*, vol. 4, pp. 357–369, 2018, DOI: 10.1016/j.egyr.2018.05.004.

[25] C. M. Whitaker and J. D. Newmiller, “Photovoltaic Module Energy Rating Procedure, Final Subcontract Report, Endecon Engineering San Ramon, California,” *NREL/Sr-520-23942*, no. January, 1998.

[26] P. O. Oviroh and T. C. Jen, “The energy cost analysis of hybrid systems and diesel generators in powering selected base transceiver station locations in Nigeria,” *Energies (Basel)*, vol. 11, no. 3, pp. 7–9, 2018, DOI: 10.3390/en11030687.

[27] M. Zivic Djurovic, A. Milacic, and M. Krsulja, “A simplified model of quadratic cost function for thermal generators,” *23rd DAAAM International Symposium on Intelligent Manufacturing and Automation 2012*, vol. 1, no. 1, pp. 25–28, 2012.

[28] G. N. Bifulco, F. Galante, L. Pariota, and M. R. Spena, “A linear model for the estimation of fuel consumption and the impact evaluation of advanced driving assistance systems,” *Sustainability (Switzerland)*, vol. 7, no. 10, pp. 14326–14343, 2015, doi: 10.3390/su71014326.

[29] K. Kusakana, “Energy dispatching of an isolated diesel-battery hybrid power system,” *Proceedings of the IEEE International Conference on Industrial Technology*, vol. 2016-May, pp. 499–504, 2016, DOI: 10.1109/ICIT.2016.7474801.

[30] B. J. Donnellan, D. J. Vowles, and W. L. Soong, “A review of energy storage and its application in power systems,” *2015 Australasian Universities Power Engineering Conference: Challenges for Future Grids, AUPEC 2015*, 2015, DOI: 10.1109/AUPEC.2015.7324839.

[31] X. Luo, J. Wang, M. Dooner, and J. Clarke, “Overview of current development in electrical energy storage technologies and the application potential in power system operation,” *Appl Energy*, vol. 137, pp. 511–536, 2015, DOI: 10.1016/j.apenergy.2014.09.081.

[32] A. G. Ter-Gazarian, *Energy Storage for Power Systems*. Milton Keynes: IET Energy Series, 2008.

[33] M. Sufyan, N. A. Rahim, M. M. Aman, C. K. Tan, and S. R. S. Raihan, "Sizing and applications of battery energy storage technologies in smart grid system: A review," *Journal of Renewable and Sustainable Energy*, vol. 11, no. 1, 2019, DOI: 10.1063/1.5063866.

[34] K. Mongird *et al.*, "Energy Storage Technology and Cost Characterization Report | Department of Energy," no. July, 2019, [Online]. Available: https://www.energy.gov/eere/water/downloads/energy-storage-technology-and-cost-characterization-report

[35] EUROBAT, "Battery energy storage for smart grid applications," *Report of Smart Grids Task Force of EUROBAT's Industrial Battery Committee*, vol. 15, no. 2, p. 8, 2013.

[36] "Application of energy storage technology in the microgrid," in *Grid-scale Energy Storage Systems and Applications*, Elsevier, 2019, pp. 243–293. DOI: 10.1016/b978-0-12-815292-8.00007-1.

[37] F. Marra, G. Yang, C. Træholt, J. Østergaard, and E. Larsen, "A decentralized storage strategy for residential feeders with photovoltaics," *IEEE Trans Smart Grid*, vol. 5, no. 2, pp. 974–981, 2014, DOI: 10.1109/TSG.2013.2281175.

[38] H. C. Hesse, M. Schimpe, D. Kucevic, and A. Jossen, *Lithium-ion battery storage for the grid - A review of stationary battery storage system design tailored for applications in modern power grids*, vol. 10, no. 12. 2017. doi: 10.3390/en10122107.

[39] D. Hart, L. Bertuccioli, and X. Hansen, "Policies for Storing Renewable Energy: A SCOPING STUDY OF POLICY CONSIDERATIONS FOR ENERGY STORAGE (RE-STORAGE)," *Iea-Retd*, no. March, 2016.

[40] Deloitte Center for Energy Solutions, "Electricity Storage Technologies, Impacts, and Prospects," no. September 2015, p. 25, 2015.

[41] IRENA, "Utility-Scale Batteries," p. 7, 2019.

[42] IRENA, "Solutions to integrate high shares of renewable energy," no. June, p. 28, 2019.

[43] S. Khormali and I. Technology, "Optimal Integration of Battery Energy Storage Systems in Smart Grids Optimal Integration of Battery Energy Storage," 2015.

[44] H. C. Hesse, M. Schimpe, D. Kucevic, and A. Jossen, *Lithium-ion battery storage for the grid - A review of stationary battery storage system design tailored for*

applications in modern power grids, vol. 10, no. 12. 2017. doi: 10.3390/en10122107.

[45] T. Chen *et al.*, “Applications of Lithium-Ion Batteries in Grid-Scale Energy Storage Systems,” *Transactions of Tianjin University*, vol. 26, no. 3, pp. 208–217, 2020, DOI: 10.1007/s12209-020-00236-w.

[46] M. Jarnut, S. Wermiński, and B. Waśkowicz, “Comparative analysis of selected energy storage technologies for prosumer-owned microgrids,” *Renewable and Sustainable Energy Reviews*, vol. 74, no. April 2016, pp. 925–937, 2017, DOI: 10.1016/j.rser.2017.02.084.

[47] G. V. B. Kumar and K. Palanisamy, “A review of energy storage participation for ancillary services in a microgrid environment,” *Inventions*, vol. 5, no. 4, pp. 1–39, 2020, DOI: 10.3390/inventions5040063.

[48] D. K. Kim, S. Yoneoka, A. Z. Banatwala, Y.-T. Kim, and K.-Y. Nam, *Handbook on Battery Energy Storage System*, no. December. 2018. [Online]. Available: https://www.adb.org/publications/battery-energy-storage-system-handbook

[49] G. B. S. Allen J. Wood, Bruce F. Wollenberg, *Power Generation, Operation, and Control*, Third. New York.Chichester.Brisbane.Toronto.Singapore: John Wiley & Son, Inc., 2014.

[50] A. Hooshmand, B. Asghari, and R. K. Sharma, “Experimental demonstration of a tiered power management system for economic operation of grid-tied microgrids,” *IEEE Trans Sustain Energy*, vol. 5, no. 4, pp. 1319–1327, 2014, DOI: 10.1109/TSTE.2014.2339132.

[51] M. Nemati, M. Braun, and S. Tenbohlen, “Optimization of unit commitment and economic dispatch in microgrids based on genetic algorithm and mixed integer linear programming,” *Appl Energy*, vol. 210, pp. 944–963, 2018, DOI: 10.1016/j.apenergy.2017.07.007.

[52] S. M. Hashemi and V. Vahidinasab, *Energy management systems for microgrids*. 2021. DOI: 10.1007/978-3-030-59750-4_3.

[53] M. C. Antonio Carlos, Zambroni De Souza, “Microgrids Design and Implementation,” in *Microgrids Design and Implementation*, M. C. Antonio Carlos, Zambroni De Souza, Ed. Springer, 2018, pp. 97–137. DOI: 10.1007/978-3-319-98687-6_4.

[54] Y. Liu, “Demand response and energy efficiency in the capacity resource procurement: Case studies of forward capacity markets in ISO New England, PJM and Great Britain,” *Energy Policy*, vol. 100, no. September 2016, pp. 271–282, 2017, doi: 10.1016/j.enpol.2016.10.029.

[55] D. P. Jenkins, J. Fletcher, and D. Kane, “Model for evaluating impact of battery storage on microgeneration systems in dwellings,” *Energy Convers Manag*, vol. 49, no. 8, pp. 2413–2424, 2008, DOI: 10.1016/j.enconman.2008.01.011.

[56] M. J. B. Kabeyi and O. A. Olanrewaju, “Sustainable Energy Transition for Renewable and Low Carbon Grid Electricity Generation and Supply,” *Front Energy Res*, vol. 9, no. March, pp. 1–45, 2022, DOI: 10.3389/fenrg.2021.743114.

[57] A. Hirsch, Y. Parag, and J. Guerrero, “Microgrids: A review of technologies, key drivers, and outstanding issues,” *Renewable and Sustainable Energy Reviews*, vol. 90, no. September 2017, pp. 402–411, 2018, DOI: 10.1016/j.rser.2018.03.040.

[58] W. Shi, N. Li, C. C. Chu, and R. Gadh, “Real-Time Energy Management in Microgrids,” *IEEE Trans Smart Grid*, vol. 8, no. 1, pp. 228–238, 2017, DOI: 10.1109/TSG.2015.2462294.

[59] A. Rahman, V. Srikumar, and A. D. Smith, “Predicting electricity consumption for commercial and residential buildings using deep recurrent neural networks,” *Appl Energy*, vol. 212, no. October 2017, pp. 372–385, 2018, DOI: 10.1016/j.apenergy.2017.12.051.

[60] IEA, “World Energy Outlook 2020: Part of World Energy Outlook,” 2020.

[61] S. Monesha, S. G. Kumar, and M. Rivera, “Microgrid energy management and control: Technical review,” *2016 IEEE International Conference on Automatica, ICA-ACCA 2016*, pp. 1–7, 2016, DOI: 10.1109/ICA-ACCA.2016.7778452.

[62] D. Gielen, F. Boshell, D. Saygin, M. D. Bazilian, N. Wagner, and R. Gorini, “The role of renewable energy in the global energy transformation,” *Energy Strategy Reviews*, vol. 24, no. January, pp. 38–50, 2019, DOI: 10.1016/j.esr.2019.01.006.

[63] BBC, “The rising demand for energy - Reasons for increase in demand for energy - Higher Geography Revision.” 2020.

[64] O. Green and G. Studies, “OECD Green Growth Studies,” *Director*, p. 104, 2012.

[65] M. Faisal, M. A. Hannan, P. J. Ker, A. Hussain, M. Bin Mansor, and F. Blaabjerg, “Review of energy storage system technologies in microgrid applications: Issues and challenges,” *IEEE Access*, vol. 6, pp. 35143–35164, 2018, DOI: 10.1109/ACCESS.2018.2841407.

[66] Y. E. G. Vera, R. Dufo-López, and J. L. Bernal-Agustín, “Energy management in microgrids with renewable energy sources: A literature review,” *Applied Sciences (Switzerland)*, vol. 9, no. 18, 2019, DOI: 10.3390/app9183854.

[67] L. Olatomiwa, S. Mekhilef, M. S. Ismail, and M. Moghavvemi, “Energy management strategies in hybrid renewable energy systems: A review,”

Renewable and Sustainable Energy Reviews, vol. 62, pp. 821–835, 2016, DOI: 10.1016/j.rser.2016.05.040.

[68] T. Weitzel and C. H. Glock, “Energy management for stationary electric energy storage systems: A systematic literature review,” *Eur J Oper Res*, vol. 264, no. 2, pp. 582–606, 2018, DOI: 10.1016/j.ejor.2017.06.052.

[69] W. Yanzi, X. Changle, and W. Wang, “Energy management strategy based on fuzzy logic for a new hybrid battery-ultracapacitor energy storage system,” *IEEE Transportation Electrification Conference and Expo, ITEC Asia-Pacific 2014 - Conference Proceedings*, pp. 1–5, 2014, DOI: 10.1109/ITEC-AP.2014.6940850.

[70] N. Dorsch, S. Böcker, and C. Wietfeld, “ICT Requirements and Recent Developments,” in *Pathways to a Smarter Power System*, Elsevier, 2019, pp. 343–369. DOI: 10.1016/b978-0-08-102592-5.00012-0.

[71] H. S. Salama, M. Abdel-Akher, and M. M. Aly, “Development energy management strategy of SMES-based Microgrid for stable islanding transition,” *2016 18th International Middle-East Power Systems Conference, MEPCON 2016 - Proceedings*, pp. 413–418, 2017, DOI: 10.1109/MEPCON.2016.7836924.

[72] D. Michaelson, H. Mahmood, and J. Jiang, “A Predictive Energy Management System Using Pre-Emptive Load Shedding for Islanded Photovoltaic Microgrids,” *IEEE Transactions on Industrial Electronics*, vol. 64, no. 7, pp. 5440–5448, 2017, DOI: 10.1109/TIE.2017.2677317.

[73] A. Hirsch, Y. Parag, and J. Guerrero, “Microgrids: A review of technologies, key drivers, and outstanding issues,” *Renewable and Sustainable Energy Reviews*, vol. 90, no. September 2017, pp. 402–411, 2018, DOI: 10.1016/j.rser.2018.03.040.

[74] J. Cerquides, A. Farinelli, and P. Meseguer, “A tutorial on optimisation for multi-agent systems,” *Comput J*, pp. 1–27, 2014.

[75] O. P. Mahela, S. Member, M. Khosravy, and N. Gupta, “Comprehensive Overview of Multi-agent Systems for Controlling Smart Grids,” vol. 8, no. 1, pp. 115–131, 2022, DOI: 10.17775/CSEEJPES.2020.03390.

[76] M. Mao, P. Jin, N. D. Hatziargyriou, and L. Chang, “Multiagent-based hybrid energy management system for microgrids,” *IEEE Trans Sustain Energy*, vol. 5, no. 3, pp. 938–946, 2014, DOI: 10.1109/TSTE.2014.2313882.

[77] L. Raju, A. A. Morais, R. Rathnakumar, S. Ponnivalavan, and L. D. Thavam, “Micro-grid grid outage management using multi-agent systems,” *Proceedings - 2017 2nd International Conference on Recent Trends and Challenges in*

Computational Models, ICRTCCM 2017, pp. 363–368, 2017, DOI: 10.1109/ICRTCCM.2017.21.

[78] F. Z. Harmouch, A. F. Ebrahim, M. M. Esfahani, N. Krami, N. Hmina, and O. A. Mohammed, “An optimal energy management system for real-time operation of multiagent-based microgrids using a T-cell algorithm,” *Energies (Basel)*, vol. 14, no. 15, 2019, DOI: 10.3390/en12153004.

[79] E. Rokrok, M. Shafie-Khah, P. Siano, and J. P. S. Catalão, “A decentralized multi-agent-based approach for low voltage microgrid restoration,” *Energies (Basel)*, vol. 10, no. 10, 2017, doi: 10.3390/en10101491.

[80] X. Fang, J. Wang, C. Yin, Y. Han, and Q. Zhao, “Multiagent Reinforcement Learning with Learning Automata for Microgrid Energy Management and Decision Optimization,” *Proceedings of the 32nd Chinese Control and Decision Conference, CCDC 2020*, pp. 779–784, 2020, DOI: 10.1109/CCDC49329.2020.9164742.

[81] M. Manbachi and M. Ordonez, “Intelligent Agent-Based Energy Management System for Islanded AC-DC Microgrids,” *IEEE Trans Industr Inform*, vol. 16, no. 7, pp. 4603–4614, 2020, DOI: 10.1109/TII.2019.2945371.

[82] M. W. Khan, J. Wang, and L. Xiong, “Optimal energy scheduling strategy for multi-energy generation grid using multi-agent systems,” *International Journal of Electrical Power and Energy Systems*, vol. 124, no. October 2019, 2021, doi: 10.1016/j.ijepes.2020.106400.

[83] M. Afrasiabi, M. Mohammadi, M. Rastegar, and A. Kargarian, “Multi-agent microgrid energy management based on deep learning forecaster,” *Energy*, vol. 186, 2019, DOI: 10.1016/j.energy.2019.115873.

[84] B. Papari, C. S. Edrington, T. V. Vu, and F. Diaz-Franco, “A heuristic method for optimal energy management of DC microgrid,” *2017 IEEE 2nd International Conference on Direct Current Microgrids, ICDCM 2017*, pp. 337–343, 2017, DOI: 10.1109/ICDCM.2017.8001066.

[85] A. C. Luna, L. Meng, N. L. Diaz, M. Graells, J. C. Vasquez, and J. M. Guerrero, “Online Energy Management Systems for Microgrids: Experimental Validation and Assessment Framework,” *IEEE Trans Power Electron*, vol. 33, no. 3, pp. 2201–2215, 2018, DOI: 10.1109/TPEL.2017.2700083.

[86] J. Wasilewski, “Optimisation of multicarrier microgrid layout using selected metaheuristics,” *International Journal of Electrical Power and Energy Systems*, vol. 99, no. 504, pp. 246–260, 2018, doi: 10.1016/j.ijepes.2018.01.022.

[87] S. Chalise, J. Sternhagen, T. M. Hansen, and R. Tonkoski, “Energy management of remote microgrids considering battery lifetime,” *Electricity Journal*, vol. 29, no. 6, pp. 1–10, 2016, DOI: 10.1016/j.tej.2016.07.003.

[88] M. Marzband, F. Azarinejadian, M. Savaghebi, and J. M. Guerrero, “An optimal energy management system for islanded microgrids based on multiperiod artificial bee colony combined with Markov chain,” *IEEE Systems Journal*, vol. 11, no. 3. pp. 1712–1722, 2017. doi: 10.1109/JSYST.2015.2422253.

[89] K. S. Ei-Bidairi, H. D. Nguyen, S. D. G. Jayasinghe, and T. S. Mahmoud, “Multiobjective Intelligent Energy Management Optimization for Grid-Connected Microgrids,” *Proceedings - 2018 IEEE International Conference on Environment and Electrical Engineering and 2018 IEEE Industrial and Commercial Power Systems Europe, EEEIC/I and CPS Europe 2018*, pp. 1–6, 2018, DOI: 10.1109/EEEIC.2018.8493751.

[90] B. K. Das, Y. M. Al-Abdeli, and G. Kothapalli, “Effect of load following strategies, hardware, and thermal load distribution on stand-alone hybrid CCHP systems,” *Applied Energy*, vol. 220. pp. 735–753, 2018. DOI: 10.1016/j.apenergy.2018.03.068.

[91] M. Abedini, M. H. Moradi, and S. M. Hosseinian, “Optimal management of microgrids including renewable energy sources using GPSO-GM algorithm,” *Renew Energy*, vol. 90, pp. 430–439, 2016, DOI: 10.1016/j.renene.2016.01.014.

[92] F. Zhao, J. Yuan, and N. Wang, “Dynamic economic dispatch model of microgrid containing energy storage components based on a variant of NSGA-II algorithm,” *Energies (Basel)*, vol. 12, no. 5, 2019, DOI: 10.3390/en12050871.

[93] Y. Wang, Y. Huang, Y. Wang, H. Yu, R. Li, and S. Song, “Energy management for smart multi-energy complementary micro-grid in the presence of demand response,” *Energies (Basel)*, vol. 11, no. 4, 2018, DOI: 10.3390/en11040974.

[94] B. Dey and B. Bhattacharyya, “Hybrid Intelligence Techniques for Unit Commitment of Microgrids,” *2019 20th International Conference on Intelligent System Application to Power Systems, ISAP 2019*, pp. 5–10, 2019, DOI: 10.1109/ISAP48318.2019.9065950.

[95] D. Dabhi and K. Pandya, “Enhanced Velocity Differential Evolutionary Particle Swarm Optimization for Optimal Scheduling of a Distributed Energy Resources with Uncertain Scenarios,” *IEEE Access*, vol. 8, pp. 27001–27017, 2020, DOI: 10.1109/ACCESS.2020.2970236.

[96] M. Gharibi and A. Askarzadeh, “Size optimization of an off-grid hybrid system composed of photovoltaic and diesel generator subject to load variation factor,” *J*

Energy Storage, vol. 25, no. September 2018, pp. 310–320, 2019, DOI: 10.1016/j.est.2019.100814.

[97] J. Wasilewski, “Electrical Power and Energy Systems Optimisation of multicarrier microgrid layout using selected,” *Electrical Power and Energy Systems*, vol. 99, no. 504, pp. 246–260, 2018.

[98] H. J. Kim and M. K. Kim, “Multi-objective based optimal energy management of grid-connected microgrid considering advanced demand response,” *Energies (Basel)*, vol. 12, no. 21, 2019, DOI: 10.3390/en12214142.

[99] M. Rouholamini and M. Mohammadian, “Heuristic-based power management of a grid-connected hybrid energy system combined with hydrogen storage,” *Renew Energy*, vol. 96, pp. 354–365, 2016, DOI: 10.1016/j.renene.2016.04.085.

[100] N. A. Luu and Q. T. Tran, “Optimal energy management for grid connected microgrid by using dynamic programming method,” *IEEE Power and Energy Society General Meeting*, vol. 2015-Septe, no. 1, pp. 1–6, 2015, DOI: 10.1109/PESGM.2015.7286094.

[101] H. Shuai, J. Fang, X. Ai, J. Wen, and H. He, “Optimal Real-Time Operation Strategy for Microgrid: An ADP-Based Stochastic Nonlinear Optimization Approach,” *IEEE Trans Sustain Energy*, vol. 10, no. 2, pp. 931–942, 2019, DOI: 10.1109/TSTE.2018.2855039.

[102] A. Merabet, K. T. Ahmed, H. Ibrahim, R. Beguenane, and A. M. Y. M. Ghias, “Laboratory Scale Microgrid Based Wind-PV-Battery,” *IEEE Trans Sustain Energy*, vol. 8, no. 1, pp. 145–154, 2017.

[103] N. Wu and H. Wang, “Deep learning adaptive dynamic programming for real-time energy management and control strategy of micro-grid,” *J Clean Prod*, vol. 204, pp. 1169–1177, 2018, DOI: 10.1016/j.jclepro.2018.09.052.

[104] J. B. Almada, R. P. S. Leão, R. F. Sampaio, and G. C. Barroso, “A centralized and heuristic approach for energy management of an AC microgrid,” *Renewable and Sustainable Energy Reviews*, vol. 60, pp. 1396–1404, 2016, DOI: 10.1016/j.rser.2016.03.002.

[105] A. Choudar, D. Boukhetala, S. Barkat, and J. M. Brucker, “A local energy management of a hybrid PV-storage based distributed generation for microgrids,” *Energy Convers Manag*, vol. 90, pp. 21–33, 2015, DOI: 10.1016/j.enconman.2014.10.067.

[106] L. K. Panwar, S. R. Konda, A. Verma, B. K. Panigrahi, and R. Kumar, “Operation window constrained strategic energy management of microgrid with electric

vehicle and distributed resources," *IET Generation, Transmission and Distribution*, vol. 11, no. 3, pp. 615–626, 2017, doi: 10.1049/iet-gtd.2016.0654.

[107] H. Babazadeh, W. Gao, Z. Wu, and Y. Li, "Optimal energy management of wind power generation system in islanded microgrid system," *45th North American Power Symposium, NAPS 2013*, pp. 3–7, 2013, DOI: 10.1109/NAPS.2013.6666871.

[108] M. Střelec and J. Berka, "Microgrid energy management based on approximate dynamic programming," *2013 4th IEEE/PES Innovative Smart Grid Technologies Europe, ISGT Europe 2013*, pp. 1–5, 2013, DOI: 10.1109/ISGTEurope.2013.6695439.

[109] J. M. Lujano-Rojas, C. Monteiro, R. Dufo-López, and J. L. Bernal-Agustín, "Optimum load management strategy for wind/diesel/battery hybrid power systems," *Renew Energy*, vol. 44, pp. 288–295, 2012, DOI: 10.1016/j.renene.2012.01.097.

[110] N. Rezaei and M. Kalantar, "Stochastic frequency-security constrained energy and reserve management of an inverter interfaced islanded microgrid considering demand response programs," *International Journal of Electrical Power and Energy Systems*, vol. 69, pp. 273–286, 2015, DOI: 10.1016/j.ijepes.2015.01.023.

[111] Y. Xiang, J. Liu, and Y. Liu, "Robust Energy Management of Microgrid with Uncertain Renewable Generation and Load," *IEEE Trans Smart Grid*, vol. 7, no. 2, pp. 1034–1043, 2016, DOI: 10.1109/TSG.2014.2385801.

[112] C. Battistelli, Y. P. Agalgaonkar, and B. C. Pal, "Probabilistic Dispatch of Remote Hybrid Microgrids Including Battery Storage and Load Management," *IEEE Trans Smart Grid*, vol. 8, no. 3, pp. 1305–1317, 2017, DOI: 10.1109/TSG.2016.2606560.

[113] T. Lu, Q. Ai, and Z. Wang, "Interactive game vector: A stochastic operation-based pricing mechanism for smart energy systems with coupled-microgrids," *Appl Energy*, vol. 212, no. September 2017, pp. 1462–1475, 2018, DOI: 10.1016/j.apenergy.2017.12.096.

[114] W. Hu, P. Wang, and H. B. Gooi, "Towards optimal energy management of microgrids with a realistic model," *19th Power Systems Computation Conference, PSCC 2016*, 2016, DOI: 10.1109/PSCC.2016.7540954.

[115] J. Liu, S. Member, H. Chen, W. Zhang, B. Yurkovich, and G. Rizzoni, "for Grid-Connected Microgrids : A Chance Constrained Programming Approach," vol. 8, no. 6, pp. 2585–2596, 2017.

[116] W. Su, J. Wang, and J. Roh, “Stochastic energy scheduling in microgrids with intermittent renewable energy resources,” *IEEE Trans Smart Grid*, vol. 5, no. 4, pp. 1876–1883, 2014, DOI: 10.1109/TSG.2013.2280645.

[117] M. Zachar and P. Daoutidis, “Energy management and load shaping for commercial microgrids coupled with flexible building environment control,” *J Energy Storage*, vol. 16, pp. 61–75, 2018, DOI: 10.1016/j.est.2017.12.017.

[118] J. Shen, C. Jiang, Y. Liu, and X. Wang, “A Microgrid Energy Management System and Risk Management under an Electricity Market Environment,” *IEEE Access*, vol. 4, pp. 2349–2356, 2016, DOI: 10.1109/ACCESS.2016.2555926.

[119] H. Farzin, M. Fotuhi-Firuzabad, and M. Moeini-Aghtaie, “Stochastic Energy Management of Microgrids during Unscheduled Islanding Period,” *IEEE Trans Industr Inform*, vol. 13, no. 3, pp. 1079–1087, 2017, DOI: 10.1109/TII.2016.2646721.

[120] E. Kuznetsova, Y. F. Li, C. Ruiz, and E. Zio, “An integrated framework of agent-based modelling and robust optimization for microgrid energy management,” *Appl Energy*, vol. 129, pp. 70–88, 2014, DOI: 10.1016/j.apenergy.2014.04.024.

[121] E. L. S. Barrett, “Autonomous HVAC control, a reinforcement learning approach,” in *Machine Learning and Knowledge Discovery in Databases*, 2015.

[122] K. Mason and S. Grijalva, “A review of reinforcement learning for autonomous building energy management,” *Computers and Electrical Engineering*, vol. 78, pp. 300–312, 2019, DOI: 10.1016/j.compeleceng.2019.07.019.

[123] CHRISTOPHER J.C.H. WATKINS; PETER DAYAN, “Technical Note Q-Learning,” *2010 International Conference on Computer Information Systems and Industrial Management Applications, CISIM 2010*, vol. 292, pp. 228–232, 2010, DOI: 10.1109/CISIM.2010.5643660.

[124] A. T. D. Perera and P. Kamalaruban, “Applications of reinforcement learning in energy systems,” *Renewable and Sustainable Energy Reviews*, vol. 137, no. May 2020, 2021, DOI: 10.1016/j.rser.2020.110618.

[125] B. v. Mbuwir, F. Ruelens, F. Spiessens, and G. Deconinck, “Battery energy management in a microgrid using batch reinforcement learning,” *Energies (Basel)*, vol. 10, no. 11, pp. 1–19, 2017, doi: 10.3390/en10111846.

[126] M. Modeling *et al.*, “Mixed-Integer-Linear-Programming-Based Energy Management System for Hybrid PV-Wind-Battery Experimental Verification,” *IEEE Trans Power Electron*, vol. 32, no. 4, pp. 2769–2783, 2017, DOI: 10.1109/TPEL.2016.2581021.

[127] C. Li, F. De Bosio, F. Chen, S. K. Chaudhary, J. C. Vasquez, and J. M. Guerrero, “Economic Dispatch for Operating Cost Minimization under Real-Time Pricing in Droop-Controlled DC Microgrid,” *IEEE J Emerg Sel Top Power Electron*, vol. 5, no. 1, pp. 587–595, 2017, DOI: 10.1109/JESTPE.2016.2634026.

[128] G. Oriti, A. L. Julian, and N. J. Peck, “Power-Electronics-Based Energy Management System With Storage,” *IEEE Trans Power Electron*, vol. 31, no. 1, pp. 452–460, 2016, DOI: 10.1109/TPEL.2015.2407693.

[129] G. Byeon, T. Yoon, S. Member, and S. Oh, “Energy Management Strategy of the DC Distribution System in Buildings Using the EV Service Model,” *IEEE Trans Power Electron*, vol. 28, no. 4, pp. 1544–1554, 2013, DOI: 10.1109/TPEL.2012.2210911.

[130] P. Malysz, S. Sirouspour, and A. Emadi, “An optimal energy storage control strategy for grid-connected microgrids,” *IEEE Trans Smart Grid*, vol. 5, no. 4, pp. 1785–1796, 2014, DOI: 10.1109/TSG.2014.2302396.

[131] M. P. Marietta, M. Graells, and J. M. Guerrero, “A Rolling Horizon Rescheduling Strategy for Flexible Energy in a Microgrid,” *2014 IEEE International Energy Conference (ENERGYCON)*, pp. 1297–1303, 2014, DOI: 10.1109/ENERGYCON.2014.6850590.

[132] A. Chaouachi, R. M. Kamel, R. Andoulsi, and K. Nagasaka, “Multiobjective intelligent energy management for a microgrid,” *IEEE Transactions on Industrial Electronics*, vol. 60, no. 4, pp. 1688–1699, 2013, DOI: 10.1109/TIE.2012.2188873.

[133] C. Delgado and J. A. Dominguez-Navarro, “Optimal design of a hybrid renewable energy system,” *2014 9th International Conference on Ecological Vehicles and Renewable Energies, EVER 2014*, pp. 1–8, 2014, DOI: 10.1109/EVER.2014.6844008.

[134] C. A. Correa, G. Marulanda, and A. Garces, “Optimal microgrid management in the Colombian energy market with demand response and energy storage,” *IEEE Power and Energy Society General Meeting*, vol. 2016-Novem, pp. 1–5, 2016, DOI: 10.1109/PESGM.2016.7741905.

[135] G. Cardoso, T. Brouhard, N. DeForest, D. Wang, M. Heleno, and L. Kotzur, “Battery ageing in multi-energy microgrid design using mixed integer linear programming,” *Appl Energy*, vol. 231, no. September, pp. 1059–1069, 2018, DOI: 10.1016/j.apenergy.2018.09.185.

[136] S. Sukumar, H. Mokhlis, S. Mekhilef, K. Naidu, and M. Karimi, “Mix-mode energy management strategy and battery sizing for economic operation of grid-tied

microgrid," *Energy*, vol. 118, pp. 1322–1333, 2017, DOI: 10.1016/j.energy.2016.11.018.

[137] S. A. Helal, M. O. Hanna, R. J. Najee, M. F. Shaaban, A. H. Osman, and M. S. Hassan, "Energy Management System for Smart Hybrid AC/DC Microgrids in Remote Communities," *Electric Power Components and Systems*, vol. 47, no. 11–12, pp. 1012–1024, 2019, DOI: 10.1080/15325008.2019.1629512.

[138] E. C. Umeozor and M. Trifkovic, "Energy management of a microgrid via parametric programming," *IFAC-PapersOnLine*, vol. 49, no. 7, pp. 272–277, 2016, DOI: 10.1016/j.ifacol.2016.07.278.

[139] M. S. Behzadi and M. Niasati, "Comparative performance analysis of a hybrid PV/FC/battery stand-alone system using different power management strategies and sizing approaches," *Int J Hydrogen Energy*, vol. 40, no. 1, pp. 538–548, 2015, DOI: 10.1016/j.ijhydene.2014.10.097.

[140] P. P. Vergara, J. C. López, L. C. P. da Silva, and M. J. Rider, "Security-constrained optimal energy management system for three-phase residential microgrids," *Electric Power Systems Research*, vol. 146, pp. 371–382, 2017, DOI: 10.1016/j.epsr.2017.02.012.

[141] S. Sukumar, H. Mokhlis, S. Mekhilef, K. Naidu, and M. Karimi, "Mix-mode energy management strategy and battery sizing for economic operation of grid-tied microgrid," *Energy*, vol. 118, pp. 1322–1333, 2017, DOI: 10.1016/j.energy.2016.11.018.

[142] V. V. S. N. Murty and A. Kumar, "Multi-objective energy management in microgrids with hybrid energy sources and battery energy storage systems," *Protection and Control of Modern Power Systems*, vol. 5, no. 1, pp. 1–20, 2020, DOI: 10.1186/s41601-019-0147-z.

[143] M. H. Amrollahi and S. M. T. Bathaee, "Techno-economic optimization of hybrid photovoltaic/wind generation together with energy storage system in a stand-alone micro-grid subjected to demand response," *Appl Energy*, vol. 202, pp. 66–77, 2017, DOI: 10.1016/j.apenergy.2017.05.116.

[144] N. Anglani, G. Oriti, and M. Colombini, "Optimized energy management system to reduce fuel consumption in remote military microgrids," *IEEE Trans Ind Appl*, vol. 53, no. 6, pp. 5777–5785, 2017, DOI: 10.1109/TIA.2017.2734045.

[145] A. G. Tsikalakis and N. D. Hatziargyriou, "Centralized control for optimizing microgrids operation," *IEEE Power and Energy Society General Meeting*, vol. 23, no. 1, pp. 241–248, 2011, DOI: 10.1109/PES.2011.6039737.

[146] M. Abunku and W. J. C. Melis, “Modelling of a CHP system with electrical and thermal storage,” *Proceedings of the Universities Power Engineering Conference*, vol. 2015-Novem, 2015, DOI: 10.1109/UPEC.2015.7339926.

[147] T. Sun, J. Lu, Z. Li, D. L. Lubkeman, and N. Lu, “Modeling Combined Heat and Power Systems for Microgrid Applications,” *IEEE Trans Smart Grid*, vol. 9, no. 5, pp. 4172–4180, 2018, DOI: 10.1109/TSG.2017.2652723.

[148] R. Smith, “Directive 2008/104/EC of the European Parliament and of the Council of 19 November 2008,” *Core EU Legislation*, pp. 426–429, 2015, DOI: 10.1007/978-1-137-54482-7_45.

[149] E. and I. S. Department for Business, “Combined heat and power – Technologies. A detailed guide for CHP developers – Part 2,” 2021.

[150] S. Quoilin, M. van den Broek, S. Declaye, P. Dewallef, and V. Lemort, “Techno-economic survey of organic rankine cycle (ORC) systems,” *Renewable and Sustainable Energy Reviews*, vol. 22, pp. 168–186, 2013, DOI: 10.1016/j.rser.2013.01.028.

[151] S. Kelly and M. Pollitt, “An assessment of the present and future opportunities for combined heat and power with district heating (CHP-DH) in the United Kingdom,” *Energy Policy*, vol. 38, no. 11, pp. 6936–6945, 2010, doi: 10.1016/j.enpol.2010.07.010.

[152] A. Fragaki, A. N. Andersen, and D. Toke, “Exploration of economical sizing of gas engine and thermal store for combined heat and power plants in the UK,” *Energy*, vol. 33, no. 11, pp. 1659–1670, 2008, DOI: 10.1016/j.energy.2008.05.011.

[153] A. Mustayen, X. Wang, M. G. Rasul, J. M. Hamilton, and M. Negnevitsky, “Theoretical Investigation of Combustion and Performance Analysis of Diesel Engine under Low Load Conditions,” *IOP Conf Ser Earth Environ Sci*, vol. 838, no. 1, 2021, DOI: 10.1088/1755-1315/838/1/012013.

[154] J. B. Heywood, *Internal Combustion Engine Fundamentals*, 2nd ed. New York: McGraw-Hill Education, 2018. [Online]. Available: https://www.accessengineeringlibrary.com/content/book/9781260116106

[155] M. A. G. Chapa and J. R. V. Galaz, “An economic dispatch algorithm for cogeneration systems,” *2004 IEEE Power Engineering Society General Meeting*, vol. 1, pp. 989–993, 2004, DOI: 10.1109/pes.2004.1372985.

[156] A. Rotimi, A. Bahadori-Jahromi, A. Mylona, P. Godfrey, and D. Cook, “Optimum size selection of CHP retrofitting in existing UK hotel building,” *Sustainability (Switzerland)*, vol. 10, no. 6, pp. 1–17, 2018, DOI: 10.3390/su10062044.

[157] A. Maleki, H. Hafeznia, M. A. Rosen, and F. Pourfayaz, “Optimization of a grid-connected hybrid solar-wind-hydrogen CHP system for residential applications by efficient metaheuristic approaches,” *Appl Therm Eng*, vol. 123, pp. 1263–1277, 2017, DOI: 10.1016/j.applthermaleng.2017.05.100.

[158] D. Xie, A. Chen, C. Gu, and J. Tai, “Time-domain modelling of grid-connected CHP for its interaction with the power grid,” *IEEE Transactions on Power Systems*, vol. 33, no. 6, pp. 6430–6440, 2018, DOI: 10.1109/TPWRS.2018.2839584.

[159] L. Ma, N. Liu, J. Zhang, W. Tushar, and C. Yuen, “Energy Management for Joint Operation of CHP and PV Prosumers Inside a Grid-Connected Microgrid: A Game Theoretic Approach,” *IEEE Trans Industr Inform*, vol. 12, no. 5, pp. 1930–1942, 2016, DOI: 10.1109/TII.2016.2578184.

[160] M. Nazari-Heris, S. Abapour, and B. Mohammadi-Ivatloo, “Optimal economic dispatch of FC-CHP based heat and power micro-grids,” *Appl Therm Eng*, vol. 114, pp. 756–769, 2017, DOI: 10.1016/j.applthermaleng.2016.12.016.

[161] D. Metz, “Economic Evaluation of Energy Storage Systems and their Impact on Electricity Markets in a Smart-grid Context,” 2016.

[162] M. B. Sigalo, A. C. Pillai, S. Das, and M. Abusara, “An energy management system for the control of battery storage in a grid-connected microgrid using mixed integer linear programming,” *Energies (Basel)*, vol. 14, no. 19, 2021, DOI: 10.3390/en14196212.

[163] Z. Chen, L. Wu, and Y. Fu, “Real-time price-based demand response management for residential appliances via stochastic optimization and robust optimization,” *IEEE Trans Smart Grid*, vol. 3, no. 4, pp. 1822–1831, 2012, DOI: 10.1109/TSG.2012.2212729.

[164] J. Hardwick, H. C. M. Smith, O. Fitch-Roy, P. M. Connor, and S. Sundaram, “ICE report T1.1.1: An overview of renewable energy supply potential,” p. 43 pp, 2018, [Online]. Available: https://769a8af4-bc75-441e-9fda-c56e237f98fc.filesusr.com/ugd/fa3d30_d43861dbb8f0404588ddec47a563d438.pdf

[165] N. Halpern-Wight, M. Konstantinou, A. G. Charalambides, and A. Reinders, “Training and testing of a single-layer LSTM network for near-future solar forecasting,” *Applied Sciences (Switzerland)*, vol. 10, no. 17, pp. 1–9, 2020, DOI: 10.3390/app10175873.

[166] A. G. Kumar, M. R. Sindhu, and S. S. Kumar, “Deep Neural Network Based Hierarchical Control of Residential Microgrid Using LSTM,” in *IEEE Region 10*

Annual International Conference, Proceedings/TENCON, 2019, vol. 2019-Octob, pp. 2129–2134. doi: 10.1109/TENCON.2019.8929525.

[167] F. Yaprakdal, M. B. Yilmaz, M. Baysal, and A. Anvari-Moghaddam, “A deep neural network-assisted approach to enhance short-term optimal operational scheduling of a microgrid,” *Sustainability (Switzerland)*, vol. 12, no. 4, 2020, DOI: 10.3390/su12041653.

[168] M. B. Milam, R. Franz, J. E. Hauser, and R. M. Murray, “Receding horizon control of vectored thrust flight experiment,” *IEE Proceedings: Control Theory and Applications*, vol. 152, no. 3, pp. 340–348, 2005, DOI: 10.1049/ip-cta:20059031.

[169] A. Hooshmand, J. Mohammadpour, H. Malk, and H. Danesh, “Power system dynamic scheduling with high integration of renewable sources,” *Integrated Systems: Innovations and Applications*, pp. 227–242, 2015, DOI: 10.1007/978-3-319-15898-3_14.

[170] H. Shareef, M. S. Ahmed, A. Mohamed, and E. al Hassan, “Review on Home Energy Management System Considering Demand Responses, Smart Technologies, and Intelligent Controllers,” *IEEE Access*, vol. 6, pp. 24498–24509, 2018, DOI: 10.1109/ACCESS.2018.2831917.

[171] A. Shirsat and W. Tang, “Sensitivity analysis of time-of-use rates on operations of home energy management systems,” *IEEE Power and Energy Society General Meeting*, vol. 2020-Augus, no. January 2020, DOI: 10.1109/PESGM41954.2020.9282147.

[172] I. Javeed, R. Khezri, A. Mahmoudi, A. Yazdani, and G. M. Shafiullah, “Optimal sizing of rooftop PV and battery storage for grid-connected houses considering flat and time-of-use electricity rates,” *Energies (Basel)*, vol. 14, no. 12, pp. 1–19, 2021, DOI: 10.3390/en14123520.

[173] X. Pan, R. Khezri, A. Mahmoudi, and S. M. Muyeen, “Optimal planning of solar PV and battery storage with energy management systems for Time-of-Use and flat electricity tariffs,” *IET Renewable Power Generation*, vol. 16, no. 6, pp. 1206–1219, 2022, DOI: 10.1049/rpg2.12433.

[174] A. M. Soomar, A. Hakeem, M. Messaoudi, P. Musznicki, A. Iqbal, and S. Czapp, “Solar Photovoltaic Energy Optimization and Challenges,” *Front Energy Res*, vol. 10, no. May, pp. 1–18, 2022, DOI: 10.3389/fenrg.2022.879985.

[175] R. Hledik, W. Gorman, M. Fell, M. Nicolson, and G. Huebner, “The Value of TOU Tariffs in Great Britain: Insights for Decision-makers Volume I: Final Report PREPARED FOR PREPARED BY,” 2017.

[176] Usepa, “Guidance on the development, evaluation, and application of environmental models,” *USEPA Publication*, vol. EPA/100/K-, no. March, p. 90, 2009, [Online]. Available: papers2://publication/uuid/06FC4BA9-AC3B-4E49-A54F-950F3200B970

[177] J. Yu, L. Tian, C. Yang, X. Xu, and J. Wang, “Sensitivity analysis of energy performance for high-rise residential envelope in hot summer and cold winter zone of China,” *Energy Build*, vol. 64, pp. 264–274, 2013, DOI: 10.1016/j.enbuild.2013.05.018.

[178] M. Ginocchi, F. Ponci, and A. Monti, “Sensitivity analysis and power systems: Can we bridge the gap? a review and a guide to getting started,” *Energies (Basel)*, vol. 14, no. 24, 2021, DOI: 10.3390/en14248274.

[179] J. C. Lam and S. C. M. Hui, “Sensitivity analysis of energy performance of office buildings,” *Build Environ*, vol. 31, no. 1, pp. 27–39, 1996, DOI: 10.1016/0360-1323(95)00031-3.

[180] W. Tian and P. de Wilde, “Uncertainty and sensitivity analysis of building performance using probabilistic climate projections: A UK case study,” *Autom Constr*, vol. 20, no. 8, pp. 1096–1109, 2011, DOI: 10.1016/j.autcon.2011.04.011.

[181] R. Khezri, A. Mahmoudi, and H. Aki, “Multi-objective optimization of solar PV and battery storage system for a grid-connected household,” *9th IEEE International Conference on Power Electronics, Drives and Energy Systems, PEDES 2020*, 2020, DOI: 10.1109/PEDES49360.2020.9379481.

[182] R. Khezri, A. Mahmoudi, and M. H. Haque, “Optimal Capacity of Solar PV and Battery Storage for Australian Grid-Connected Households,” *IEEE Trans Ind Appl*, vol. 56, no. 5, pp. 5319–5329, 2020, DOI: 10.1109/TIA.2020.2998668.

[183] G. Simons, S. Barsun, G. Simons, and S. Barsun, “Chapter 23 : Combined Heat and Power Evaluation Protocol The Uniform Methods Project : Methods for Chapter 23 : Combined Heat and Power Evaluation Protocol The Uniform Methods Project : Methods for Determining Energy Efficiency Savings for,” no. October, 2017.

[184] S. B. Module, “GXC250-NG GXC250-NG.”

[185] M. Shahidehpour, C. Liu, H. Zhang, Q. Zhou, and T. Ding, “A Two-layer Model for Microgrid Real-time Scheduling using Approximate Future Cost Function,” *IEEE Transactions on Power Systems*, vol. 8950, no. c, pp. 1–1, 2021, DOI: 10.1109/tpwrs.2021.3099336.